COOPERATIVE BASE STATION PROCESSING IN MULTIDIMENSIONAL INTERFERENCE

by

Sara Bavarian
Master of Applied Sciences, Simon Fraser University 2004
Bachelor of Engineering, Sharif University of Technology 2001

THESIS SUBMITTED IN PARTIAL FULFILLMENT OF
THE REQUIREMENTS FOR THE DEGREE OF

DOCTOR OF PHILOSOPHY

In the
School of Engineering Science

SIMON FRASER UNIVERSITY

Summer 2009

APPROVAL

Name: **Sara Bavarian**

Degree: **Doctor of Philosophy**

Title of Thesis: **Cooperative Base Station Processing in Multidimensional Interference**

Examining Committee:

Chair: **Dr. Kamal K. Gupta**
Professor, School of Engineering Science

_____

Dr. James K. Cavers
Senior Supervisor
Professor, School of Engineering Science

_____

Dr. Paul Ho
Supervisor
Professor, School of Engineering Science

_____

Dr. Rodney Vaughan
Supervisor
Professor, School of Engineering Science

_____

Dr. Sami (Hakam) Muhaidat
Internal Examiner
Assistant Professor, School of Engineering Science

_____

Dr. Stephen V. Hanly
External Examiner
Associate Professor,
Department of Electrical and Electronic Engineering,
The University of Melbourne, Victoria, Australia

Date Defended/Approved: April 23, 2009

Declaration of
Partial Copyright Licence

ABSTRACT

Cooperative base station (CBS) processing takes advantage of the entire infrastructure fabric in system-wide multiuser detection (MUD) of each and all mobile stations (MSs). It is a promising paradigm for increasing the efficiency of future wireless communications systems, benefiting from increased dimensionality through macrodiversity as well as increasing the capacity largely through the achievement of full frequency reuse. Managing the high levels of interference occurred in this scheme is the main dilemma discouraging the practical implementation. In this thesis, we introduce innovative methods to handle and reduce co-channel interference in the uplink of CBS systems.

Based on the groupwise iterative multiuser detection (IMUD), we come up with a new way to reduce the complexity of belief propagation (BP) algorithm. The resulting reduced complexity BP (RCBP) algorithm is a flexible, efficient technique that can be used for joint detection in a variety of high interference situations.

We apply RCBP for distributed MUD in CBS uplink and show that its performance is close to that of the BP algorithm at lower computational cost in the simplified channel model and it has excellent performance in joint decoding and detection using the low-density parity-check (LDPC) codes. We also examine CBS processing in a realistic

wireless network model, and illustrate how system-wide RCBP MUD can successfully detect the co-channel signals originating from the MSs in the neighbouring cells, included in the detection set. However, the system performance in such system is limited by the unmodeled interference from the MSs outside the detection set.

We apply the RCBP algorithm for MUD in frequency selective multiple-input, multiple-output (MIMO) channels. Our study proves that the RCBP is an efficient equalizer dealing with inter-symbol interference in high interference situations and in iterative joint detection and decoding.

In order to reduce the unmodeled interference in CBS networks, we propose a novel power control policy for CBS uplink allowing the MSs to control according to the total received power in their detection set. We investigate the performance of this method and show that it reduces the intercell interference, saves power and improves the BER performance.

ACKNOWLEDGEMENTS

They say, “It takes a village to raise a child.” In my case, this work was not possible but for the constant support and encouragements, I received throughout this journey. First, I have to thank my senior supervisor Dr. Jim Cavers for being a great teacher, mentor and a role model. Jim introduced me to this problem when I started my graduate studies and gave me the freedom to explore different aspects of it, while giving me the guidance and support when I needed it. I have to thank my supervisory committee Dr. Rodney Vaughan and Dr. Paul Ho for teaching me the fundamentals of wireless communications in their classes or over cups of coffee. I also have to thank my examiner Dr. Muhaidat and Dr. Hanly for reading this work and giving their comments.

An extensive list of previous or relevant research is included in the reference section. In particular, I was inspired by the work by Dr. Hanly and his colleague on the adoption of the belief propagation (BP) algorithm in distributed base station (BS) processing. The BP has a key role in my work and I want thank Dr. Judea Pearl for his work on this topic. I was also deeply moved when I found out that he is the father of the late journalist Daniel Pearl and about his contributions to peace in Daniel Pearl foundation.

I am grateful for the help and support of the faculty, staff, and graduate students of the department of Engineering Science, Simon Fraser University. I have to thank my

colleagues in wireless communications lab for their support, understanding and friendship, in particular Dr. Brad Zarikoff, and Shirin Karimifar. I would like to thank the Natural Sciences and Engineering Research Council of Canada (NSERC) for providing the financial support of this work.

This work would have not been possible without the constant support of my friends and family and I appreciate them all for being there for me. No matter where in the world, we have been, all my girlfriends especially Dr. Parastoo Nikaeen and Tara Rohani have always been there to listen to me and encourage me through the challenges and for that, I am always grateful to them. I would like to thank my siblings Maryam, Mona and Mohammad as well as my in-laws Lorna and John Truscott. My parents Dr. Fatemeh Baradaran and Dr. Behrouz Bavarian have been my biggest supporters and role models in perseverance and hard work. I would like to thank my stepson Lawson for his kind heart and for being a constant joy in my life. Last but not the least; I do not have enough words to thank my husband Lawrence Cofield for being my best friend, partner, and for believing in me every step of the way.

TABLE OF CONTENTS

LIST OF FIGURES

LIST OF TABLES

GLOSSARY

3G	Third Generation Cellular Standards
4G	Fourth Generation Cellular Standards
apP	*a priori* Probability
APP	*a posteriori* Probability
AWGN	Additive White Gaussian Noise
BCJR	Bahl, Cocke, Jelinek and Raviv
BER	Bit Error Rate
BP	Belief Propagation
BPSK	Binary Phase-Shift Keying
BS	Base Station
BSC	Base Station Controller
BTS	Base Transceiver Station
CBS	Cooperative Base Stations
CDMA	Code Division Multiple Access
CMM	Conditional Metric Merge
CSI	Channel State Information

DFE	Decision Feedback Equalizer
DFT	Discrete Fourier Transform
DSSS	Direct Sequence Spread Spectrum
FDMA	Frequency Division Multiple Access
FG	Factor Graph
FHSS	Frequency Hopping Spread Spectrum
FIR	Finite Impulse Response
FSM	Finite State Machine
GSM	Global Systems for Mobile Communications
i.i.d.	Independent Identically Distributed
IEEE	Institute of Electrical and Electronics Engineers
IMUD	Iterative Multiuser Detection
ISI	Intersymbol Interference
LDPC	Low Density Parity Check
LLR	Log Likelihood Ratio
LTE	Long Term Evolution
MAP	Maximum *a posteriori*
MDM	Multiply Detected Macrodiversity
MIMO	Multiple Input Multiple Output
ML	Maximum Likelihood
MMSE	Minimum Mean Square Error
MS	Mobile Station

MUD	Multiuser Detection
MUI	Multiuser Interference
NP	Non Polynomial
OFDM	Orthogonal Frequency Division Multiplexing
OJM	Optimal Joint Marginalization
PDA	Probability Data Association
pdf	Probability Density Function
PER	Packet Error Rate
QoS	Quality of Service
RCBP	Reduced Complexity Belief Propagation
SD	Sphere Decoder
SDR	Semidefinite Relaxation
SINR	Signal to Interference plus Noise Ratio
SIR	Signal to Interference Ratio
SiSo	Single Input Single Output
SISO	Soft Input Soft Output
SNR	Signal to Noise Ratio
SSD	Soft Sphere Decoder
TDMA	Time Division Multiple Access
W-CDMA	Wideband CDMA
WiMax	Worldwide Interoperability for Microwave Access
ZF	Zero Forcing

CHAPTER 1

INTRODUCTION

1.1 General Comments

Wireless communications has revolutionized our day-to-day lives and it is the fastest growing section of the communications industry. The wireless industry has demonstrated an amazing capability to meet the ever-growing consumers' needs from hardware and infrastructure to design and web applications. Despite the harsh restrictions of wireless medium, this match of needs and services is sustained by continuous hard work and innovative research. This dissertation accounts for our contributions to this endeavour.

Multiple different and sometimes conflicting concerns make it challenging to design or expand wireless communication systems. Primarily, frequency spectrum is a scarce resource, shared among many different users and applications. Signal attenuation is highly volatile and the received signal not only suffers from the thermal noise but it is also distorted by interference caused by echoes of multipath channel, intersymbol interference (ISI) or the signals from other co-channel users, multiuser interference

(MUI). Quality of service (QoS) and efficient power consumption are some of the other issues that have to be addressed.

Conventional wireless systems are designed based on a layered and mostly non-cooperative approach that has simplified the complexities of implementation and interoperation. However, the existing structures generally lack the flexibility to increase the capacity or to improve the efficiency of consuming power and spectrum resources. In order to cross these barriers, a trend towards cognitive, cross-layer, and cooperative techniques has recently emerged in literature [1]. This movement has stimulated a major paradigm shift from the non-cooperative classic system design, opening a vast unchartered area for exploration.

This thesis focuses on studying the cooperative base stations (CBSs) uplink. We consider a cellular system where the base stations (BSs) cooperate to share the information about the signals they receive. With such CBSs, the spillover of the signals from the intercell co-channel mobile stations (MSs) represents additional dimensionality rather than interference and the entire infrastructure fabric can be employed in a system-wide detection of all MSs. This approach leads to a new view of cellular system layout and the role of cells themselves and results in significant capacity increase mostly through the achievement of full frequency reuse in all the cells.

Interference management is a key dilemma in the practical implementation of CBS schemes. We study multiple aspects of this problem in detail and provide viable solutions based on two main principles. The first is to deal with strong interference through an advanced multiuser detection (MUD) technique and the second is to reduce the

unmodelled interference by applying a new power control policy for CBS systems. We confirm that both methods bear successful results in dealing with interference.

1.2 Novel Contributions

This thesis presents several novel contributions to the promising field of cooperative base stations. We offer a number of solutions to handle and mitigate interference in the uplink of CBS systems, outlined as follows

- the development of the reduced complexity belief propagation (RCBP) algorithm as an efficient technique to handle multidimensional interference.
- proposing a new CBS processing framework based on the distributed RCBP receivers at the BSs.
- examination of CBS performance in a realistic propagation environment that allows interference among all cells.
- formulation and performance of iterative decoding and CBS processing.
- providing a new solution for handling combined coding, ISI and MUI through RCBP equalization.
- the development of a new power control policy for CBS systems to reduce MUI interference.

We initially introduce the RCBP algorithm (first published in [2]). The RCBP algorithm is powerful, sophisticated framework for joint detection of large number of interfering symbols and it is based on the well-known belief propagation (BP) algorithm [3]. RCBP inherits the flexibility and near-optimal performance of BP, and it reduces the

BP computational complexity by employing an iterative groupwise strategy inspired by the iterative multiuser detection (IMUD) algorithm [4].

The IMUD algorithm is designed to provide an efficient solution for multiuser detection (MUD) in overloaded multiple-input, multiple-output (MIMO) problems where the number of receive antennas is less than the number of transmit antennas. The original IMUD, developed by Zarikoff *et al.* [5], divides the interfering symbols into non-overlapping groups and detects the groups iteratively and in succession using optimal joint marginalization (OJM) at its core. We improve IMUD with a novel method to reduce its computational load by replacing the OJM core with more efficient quasi-optimal methods such as the soft sphere decoder (SSD) [6] algorithm [4].

We propose a new CBS processing framework by applying distributed RCBP receivers at the BSs [7, 8]. We compare the system-wide performance of the RCBP with the previously studied distributed BP detection [9, 10] in a simplified system model that limits the co-channel interference sources to immediately adjacent cells [7]. We confirm that RCBP has the ability to reduce the computational load of distributed CBS processors without significant performance loss.

There was some concern, however, if the suboptimal RCBP maintains the close to optimal performance in coded schemes and if it is practical in realistic propagation channel models, where any co-channel MSs in the system contributes to the interference. We study these issues through simulations [8], and demonstrate the success of RCBP in iterative decoding schemes. As for realistic propagation models, we observe that RCBP is able to handle the interfering signals when they are included in joint detection, and the

receiver has access to their channel state information (CSI). The unmodelled interferers, however, are treated as noise, limiting the performance with an error floor.

The distributed CBS processing based on RCBP provides an efficient structure to deal with MUI. In real systems, however, the ISI issue has to be addressed as the signals from different MSs arrive at the BSs asynchronously and with delay spread. We extend the application of RCBP approach to ISI, as well as MUI through multiuser MIMO equalization [11] at the BSs. We examine the performance of the proposed RCBP equalizer in different channel models, in iterative decoding schemes, and note that it achieves excellent performance in dealing with high levels of interference even in overloaded situations where the channel matrix is rank-deficient. We note that the RCBP equalizer is the generalization of our earlier work in soft decision equalization in frequency selective MIMO channels [12].

In order to reduce the co-channel interference in CBS systems, we introduce the total power control policy [13]. The new method reduces the average power of unmodelled interference in CBS systems. It also saves transmit power particularly in the MSs located in the cell boundaries. We demonstrate that this new power control policy has the ability to improve the BER performance of CBS processing in both coded and uncoded scenarios.

1.3 List of Publications

Ph.D. research contributions and results have been published (or are accepted to appear) in the following refereed journals and conference proceedings.

- **S. Bavarian** and J.K. Cavers, "Total Power Control for Cooperative Base Stations Uplink," accepted for presentation in *IEEE Vehicular Technology Conference Spring 2009 (VTC-spring09)*, 2009.
- **S. Bavarian** and J.K. Cavers, "A new framework for soft decision equalization in frequency selective MIMO channels," *Communications, IEEE Transactions on*, vol. 57, pp. 415-422, 2009.
- **S. Bavarian** and J.K. Cavers, "Reduced-Complexity Belief Propagation for System-Wide MUD in the Uplink of Cellular Networks," *Selected Areas in Communications, IEEE Journal on*, vol. 26, pp. 541-549, 2008.
- B.W. Zarikoff, J.K. Cavers and **S. Bavarian**, "An iterative groupwise multiuser detector for overloaded MIMO applications," *Wireless Communications, IEEE Transactions on*, vol. 6, pp. 443-447, 2007.
- **S. Bavarian** and J.K. Cavers, "Reduced Complexity Distributed Base Station Processing in the Uplink of Cellular Networks," *Global Telecommunications Conference, IEEE (GLOBECOM '07)*, pp. 4500-4504, 2007.
- **S. Bavarian** and J.K. Cavers, "Reduced Complexity Belief Propagation Algorithm Based on Iterative Groupwise Multiuser Detection," *Electrical and Computer Engineering, Canadian Conference on (CCECE 2007)*, pp. 466-468, 2007 **(winner of a best student paper award)**.

1.4 Thesis Structure

Chapter 2 provides the background information about some of the challenges in wireless design and outlines a number of existing solutions. Chapter 3 reviews the background literature on capacity results and detection techniques for CBS processing, outlining the challenges and identifying the motivations for our research. In Chapter 4, we review the BP algorithm, go over the principles of IMUD, and introduce the RCBP framework by employing the groupwise IMUD to reduce the complexity of the BP algorithm. Chapter 5 investigates the application of RCBP receivers for system-wide MUD in the uplink of cellular networks. We compare the performance of proposed method to BP based distributed decoding and show that it can reduce the computational burden without significant performance loss. Chapter 6 studies the capability of the RCBP algorithm in dealing with ISI and Chapter 7 presents a total power control policy for the uplink of cellular networks. We express our views about some of the open problems in CBS processing and finish with some concluding remarks in Chapter 8.

CHAPTER 2

GENERAL BACKGROUND

As mentioned earlier, the wireless radio channel is a harsh medium, impeding reliable, high-speed communications. The core objectives of wireless research are better understanding the characteristics of the channel through physical analysis as well as experiment, facilitating new investigations through analytical modelling, and finding innovative solutions to improve the efficiency of wireless link. This chapter provides the background information on the challenges of wireless design and outlines some of the existing solutions. On each subject, we mainly point out the issues that are related to or motivate CBS processing, denote the models used in later chapters, and offer references for more information.

2.1 Challenges

The two major challenges faced in designing reliable wireless links are unpredictable and rapidly changing attenuation and interference. MUI is caused by multiple users sharing the same channel while the premise behind ISI and variable channel gains is the multipath channel as depicted in Figure 2.1.

according to their phase of arrival. Therefore, the multipath fading is also referred to as *small-scale propagation effect*.

The signals also experience *large-scale propagation effects* of *path loss* and *shadowing*. Path loss models the effect of power dissipation over the distance, and shadowing represents the random variations of the signal power at a given distance due to the obstacles between the transmitter and the receiver. Shadowing is also caused by changes in reflecting surfaces and scattering objects. The exact characteristics and location of these obstructing objects or scatterers are generally unknown, so statistical models are used to portray the shadowing effect.

Various propagation models based on complicated analytical methods or extensive empirical measurements have been proposed to estimate the statistical characteristics of wireless signals. The detailed investigation of these signal propagation models can be found in [14-16] (as well as references therein). Because of the complexity of wireless channel, it is hard to find a single model that yields accurate descriptions of different environments. For general wireless design and analysis, a simple model representing the basic features of signal propagation is sometimes preferable. Here, we briefly mention a widely accepted simplified model [15] that we used in our simulations.

2.1.1 Propagation Model

The received signal power P_r can be modelled using the simplified equation (2.1).

$$P_r(\text{dB}) = P_t(\text{dB}) - \text{PL}(\text{dB}) - 10\log\left(\frac{d}{d_0}\right)^{\gamma\psi_{\text{dB}}} \qquad (2.1)$$

where P_t denotes the signal transmit power and γ is the path loss exponent, ranging normally between 2-6 (the signal power typically falls off sharper than the inverse square model, representing free space propagation). The shadowing effect is commonly considered to have log-normal distribution [14-16], and in logarithmic domain, ψ_{dB} is modelled as a Gaussian random variable with zero mean and variance $\sigma^2_{\psi_{\mathrm{dB}}}$. For outdoor channels, the standard deviation $\sigma_{\psi_{dB}}$ is empirically estimated to be between 4-13 dB. The unshadowed path loss at reference distance d_0 (1-10m indoors and 10-100m outdoors), K, can be easily calculated knowing the signal wavelength λ, assuming omnidirectional antennas

$$K\ \mathrm{dB}=20\log_{10}\frac{\lambda}{4\pi d_0} \quad . \tag{2.2}$$

Figure 2.2 illustrates the effect of path loss, shadowing and fading on P_r/P_t versus the distance between the transmitter and receiver d, according to this simplified statistical model. We should note that this model is generally valid only for transmission distances $d > d_0$. The average received power becomes 10γ dB weaker as the distance increases a decade. This sharp power fall off confines the wireless signal mostly in a local area outside which the received power is negligible, which is the idealized model underlying cellular system layouts.

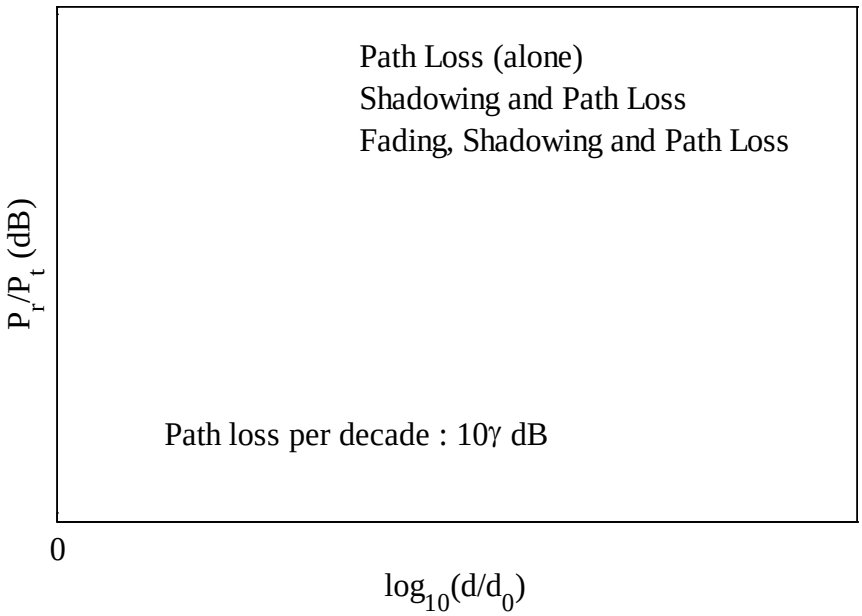

Figure 2.2: Path loss, shadowing and multipath versus distance.

Throughout this thesis, we consider a discrete-time, baseband equivalent of a wireless channel. In the flat fading channel

$$\frac{P_r}{P_t} = E\left[|h|^2\right], \tag{2.3}$$

where h is the single-input, single-output (SiSo) channel gain. As we discussed, the channel gain is the sum of multiple independent path gains and in the absence of a dominant or line of sight path, it can be approximated by a normal distribution according to the central limit theorem. We assume the channel gain h to be a zero mean complex Gaussian random variable with variance $P_t P_r$. As a result, $|h|$ has a Rayleigh distribution and this model is referred to as Rayleigh fading.

The channel gain in frequency selective channel is commonly modelled as a linear finite impulse response (FIR) filter with L symbol-spaced taps $\mathbf{h} = [h_0 h_1 \cdots h_{L-1}]$.

$$\frac{P_r}{P_t} = \sum_{l=0}^{L-1} E\left[|h_l|^2\right], \tag{2.4}$$

where h_l is assumed to be a zero mean Gaussian random variable. The power delay profile of a channel represents the distribution of scatterers (density of power) in the delay time domain τ. In the discrete model, power delay profile characterizes the power distribution in the filter taps. Most empirical studies for outdoor channels suggest an exponential power delay profile [14], but equal power delay taps are also frequently used in the literature as a benchmark.

2.2 Existing Solutions

In this Section, we outline the available methods to deal with the propagation, and interference issues. Most of them are already used in current wireless systems and some are proposed for the future standards.

2.2.1 Multiple Access Techniques

The purpose of multiple access techniques is to avoid MUI through allocating orthogonal or quasi-orthogonal signal dimensions to multiple users. Frequency division multiple access (FDMA), and time division multiple access (TDMA), assign different frequency bands or time-slots to different users. However, code division multiple access (CDMA) spectrally spreads the signals using orthogonal or pseudo-random (quasi-orthogonal) codes in direct sequence spread spectrum (DSSS) and pseudo-random carrier frequency in frequency hopping spread spectrum (FHSS).

FDMA requires guard bands between the channels to compensate for adjacent channel interference produced by imperfect filters, oscillator frequency errors and Doppler spreading. FDMA also makes it hard to assign more than one channel to a user to increase the data rate as such a scheme generally requires receivers that are more complex. However, FDMA is the most common multiple access technique in analog communications systems. In addition, if the channels are sufficiently narrow, the frequency response will be almost flat over the bandwidth and FDMA users will not experience frequency selective fading.

TDMA channels, on the other hand, occupy the whole system bandwidth, which is generally wideband. As explained in 2.1 , wideband schemes usually experience frequency selective fading and need some form of ISI mitigation as a result. TDMA systems also require synchronization among different users and higher transmit power. To avoid interference from adjacent time slots, TDMA channels often have guard intervals. One benefit of TDMA systems is that it is easy to assign multiple channels to one user in order to accommodate higher data rates. GSM and IS-136 digital cellular phone standards use TDMA.

CDMA signals occupy the same time and bandwidth and they are separated by the spreading architecture as the spreading sequences generally have small cross correlation (zero in orthogonal spreading). CDMA signals occupy a much wider bandwidth compared to FDMA and TDMA signals with the same data rates. However, CDMA does not require guard bands or intervals and allows a soft limit on the number of users through non-orthogonal spreading. It is also easy to allocate multiple channels to one user by assigning multiple codes. Because of these qualities, CDMA became very popular

with third generation systems and it is used in IS-95, W-CDMA and CDMA2000 digital cellular standards. CDMA performance and capacity is limited by interference since the spreading codes are not perfectly orthogonal. Near-far effect is one of CDMA's drawbacks, meaning that the near strong users might swamp the signal from far weaker users, and hence, there is need for stricter power control than in FDMA or TDMA. CDMA also suffers from poor spectral efficiency and as a result, it is abandoned for the proposed 4G standards.

2.2.2 Cellular Systems

In cellular systems, the spatial area is divided into non-overlapping cells and each cell has a BS that provides access to a backbone wired network for the MSs inside the cell. The communication link from MSs to the BS is called uplink or reverse link, and the link from the BS to MSs is referred to as downlink or forward link. The premise behind the conventional cellular systems is that signals from BSs or MSs are largely confined to the cell occupied by the transmitters. The sharp power decay of the signals with distance is the reason for this localization.

Spillover of the signals to other cells is considered an interference problem, to be dealt with by spatial separation of co-channel cells in case of narrowband FDMA/TDMA, or by spectral spreading in the case of CDMA. In narrowband systems, each cell is assigned a channel set C_n , and these sets are reused in geographically separated locations. The number of unique channel sets is called cluster size. Figure 2.3 shows a hexagonal cellular system with cluster size 7. CDMA systems, however, enjoy full frequency reuse, meaning that the wider bandwidth caused by spreading the signals is

used by all the cells in the system. As we mentioned, capacity and performance in CDMA systems are limited by the intercell and interacell interference.

When a mobile moves from one cell to another, its call must be handed off to the new BS. In narrowband networks, this change of control was abrupt (*hard handoff*) and caused some connection problems for the MSs located in cell boundaries. Because of the full frequency reuse in CDMA networks, MSs are allowed to be connected to more than one BS during the handoff process (*soft handoff*) as shown in Figure 2.4. Soft handoff improved the connection quality by exploiting selection diversity (as we explain in 2.2.4) however, only one BS contributed to the detection of a MS signal at a time.

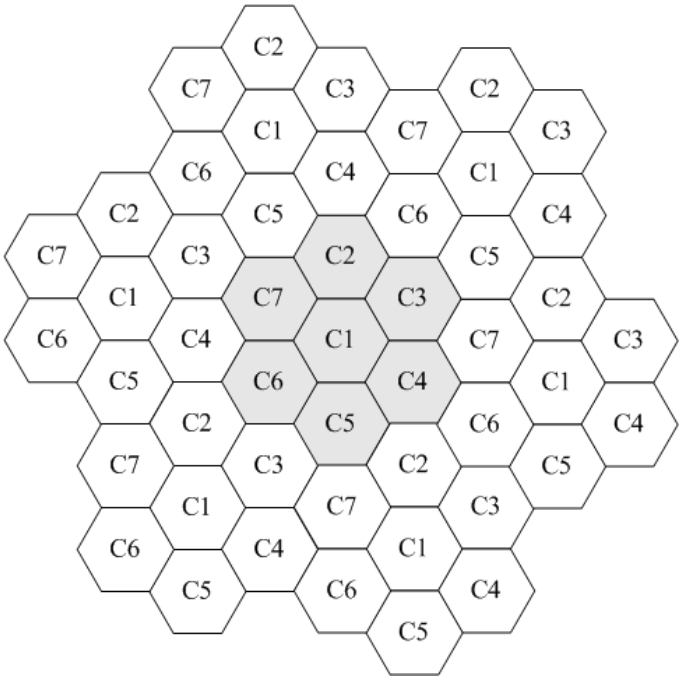

Figure 2.3: Cellular system with cluster size 7.

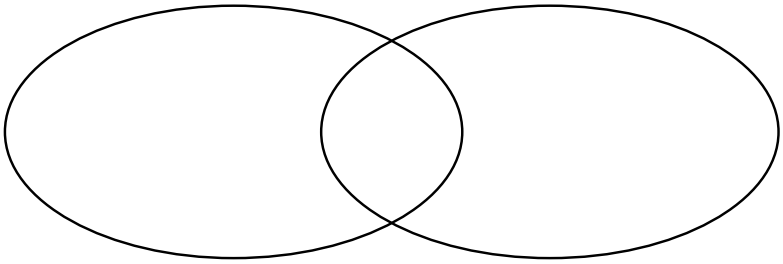

without considering their power, or equal gain combining. The optimal maximum likelihood (ML) method is called maximal-ratio combining (MRC), adding the weighted sums of phase aligned signals.

Diversity can be achieved through sending multiple instances of the signal in different times or frequencies, which means spending our scarce spectrum resource for performance improvement. However, an increasingly popular form of diversity is spatial diversity, gained through applying multiple antennas at the transmitter or the receiver at the expense of increased hardware and processing costs. Figure 2.5 illustrates the advantages of reception diversity in a system with one transmit and N_r receive antennas, BPSK modulation and Rayleigh fading channel. The bit error rate (BER) versus signal to noise ratio (SNR) for additive white Gaussian noise (AWGN) noise channel is included for comparison. The antenna array at the receiver improves the BER performance by increasing the total received SNR, array gain as well as the diversity gain.

Most of the studies in diversity techniques consider point-to-point transmission or the case where all antennas are located at one base station in the cell (microdiversity). Microdiversity as pointed out is a powerful tool in dealing with small-scale fading. However, diversity can also be used to deal with the effects of shadowing as well as fading if the antennas are far enough from each other or in different cells (macrodiversity). Macrodiversity requires global or cooperative BS processing, so it has been deemed impractical by most researchers. However, this issue is the focus of our thesis, and we demonstrated that the achievable performance may justify the increased system complexity. In Chapter 3, we review the literature on macrodiversity as starting point towards CBS research.

Multiple-input, multiple-output (MIMO) systems employ multiple antennas at both the receiver and the transmitter. They utilize the multipath scattering and promise capacity increase linear to the channel dimension [17, 18]. MIMO technology created substantial excitement in wireless industry and it is provisioned in the next generation Wi-Fi and cellular standards. Detailed information about MIMO techniques and their limits can be found in [16]. Dealing with increased interference is one of the major challenges facing the efficient implementation of MIMO systems. Chapter 6 provides a solution for equalization in frequency selective MIMO channels.

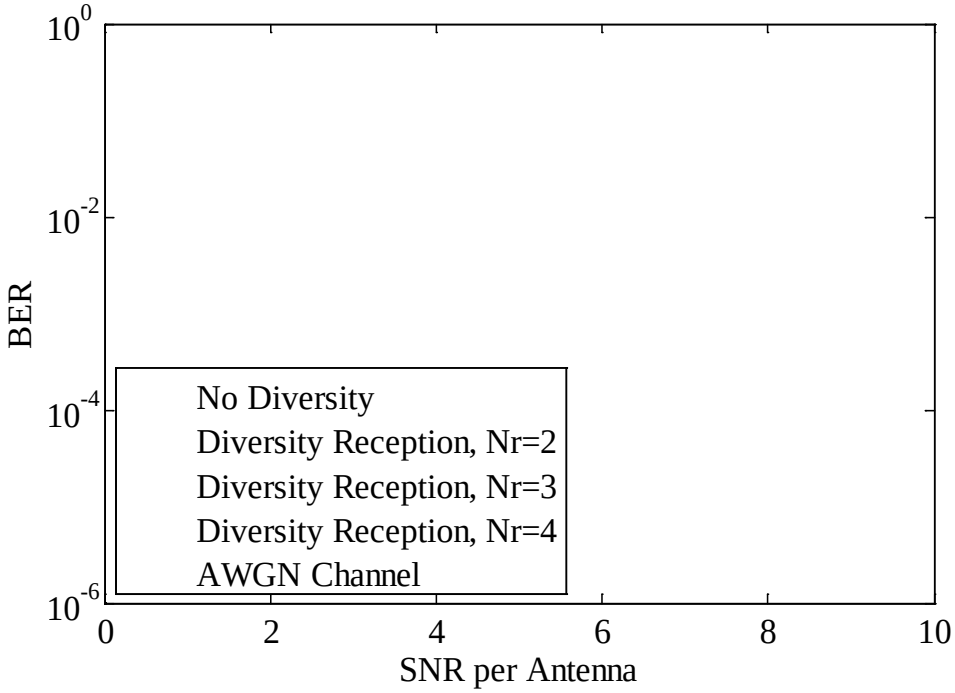

Figure 2.5: Diversity Reception, BPSK modulation.

2.2.5 Multiuser Detection and Equalization

One approach in solving interference issues, both ISI and MUI, is to eliminate them by using an interference suppression technique such as directional antennas, beam forming, decision feedback equalization (DFE), *etc.* In contrast, multiuser detection (MUD) and MUD-based equalization techniques are based on joint detection of all the interfering signals (MUI in case of MUD and ISI in case of equalization) and improving the performance through the increased dimensionality. There is debate in different scenarios whether interference suppression or detection produces better results. The answer usually varies in different situations. All the same, detection techniques that cope with interference are an essential part of wireless systems design.

Optimal joint detection involves solving an integer least squares problem, which is in general non-polynomial (NP) hard. The maximum *a posteriori* (MAP) Bahl, Cocke, Jelinek and Raviv (BCJR) algorithm [19] and the Viterbi algorithm model the channel as a finite state machine (FSM) (illustrated by a trellis) and find the optimal solution. Their computational complexity grows exponentially with the number of bits that interfere in each measurement. Consequently, situations with several interferers or high order signal constellations may make optimal joint detection impractical. An alternative is to use suboptimum methods like linear zero-forcing (ZF) and minimum mean square error (MMSE) detectors or nonlinear DFE. These techniques cause performance loss due to noise enhancement or error propagation (in DFE). Moreover, they sacrifice the dimensions that could be used for diversity. In consequence, they cannot handle overloaded situations efficiently, where the channel matrix is rank deficient *e.g.* in a cellular system uplink.

Extensive research has been undertaken in order to improve the efficiency of the above-mentioned algorithms. Some are based on reducing the number of states by delayed decision feedback [20] or set-partitioning [21] or pre-filtering [22]. Other methods keep only a limited number of paths through the trellis [23, 24] . Soft decision techniques provide the probabilities of different results rather than the final answer (hard decision). Better performance is also realized by incorporation of soft-decision and iterative decoding schemes [25]. Yet achieving close to optimal performance at low computational complexity becomes increasingly challenging as the constellation of the symbols or the number of interferers grows.

New prospects for solving complex detection problems have emerged in recent years. Quasi-optimal detection algorithms such as sphere decoding (SD) [26, 27], probabilistic data association (PDA) [28], semidefinite relaxation (SDR) [29], and belief propagation (BP) [3, 30], introduced initially in mathematics, target tracking, convex optimization and artificial intelligence, respectively, are now successfully applied in solving various communications problems. Under specific conditions, these algorithms are able to achieve optimal or near-optimal performance with computational costs comparable to the standard sub-optimal methods. BP is most competent in sparse problems, however, SD, SDR and PDA are most efficient when SNR is high enough and problem is not rank-deficient.

The common downside of these quasi-optimal methods is that they lack the flexibility to work efficiently outside their particular areas of competence. In order to address this problem, hybrid solutions are needed to improve detection efficiency with more flexibility. Dividing the interfering signals into smaller groups and applying iterative

techniques to detect those groups successively, is an example of such hybrid solutions. Smaller numbers of interfering bits presents the possibility of more efficient detection within each group and offer opportunities for improved overall efficiency. The iterative MUD (IMUD) [4] provides a flexible MUD framework involving Gaussian forcing, SD and soft interference cancellation in iterative groupwise detection. Inspired by IMUD, in Chapter 4, we introduce the reduced-complexity BP (RCBP) algorithm as flexible technique to deal with multidimensional interference and explain its characteristics.

2.2.6 Coding

Coding techniques allow the transmission errors to be detected or corrected by a decoder at the receiver. Because of the unreliability of the channel, coding is an essential element of a wireless system. Different varieties of convolutional and linear block codes along with an interleaver have long been the standard design and adaptive coding techniques provided a way to improve the performance of conventional systems. A major boost came with the introduction of iterative Turbo codes and rediscovery of low-density parity check (LDPC) codes. These iterative codes are capable of providing the capacity very close to the ones predicted by Shannon theory [31].

Both LDPC and Turbo decoders receive soft information as the input and produce soft decisions at the output. These soft-input, soft-output (SISO) decoders are then able to improve their decisions through iterative processing. Iterative soft decoders opened the possibility for further improvement by iterative joint detection and decoding and Turbo equalization [25]. These schemes require the design of efficient SISO detectors. We examine the performance of our proposed structures in both coded and uncoded scenarios.

First discovered by Gallager in 1960s [32], LDPC codes were mostly forgotten until rediscovered three decades later [33]. They became very popular for their near-Shannon limit performance, and a vast amount of research has studied them in recent years. LDPC codes are positioned to become a standard in the developing highly efficient data transmission methods. Because the LDPC decoders are based on the BP algorithm and have similar structure to our proposed BP-based detection scheme, we consider LDPC codes in iterative detection and decoding design in Chapter 5 and Chapter 6.

2.2.7 Cooperation

Cooperation is a widespread phenomenon in nature and it has been the subject of intensive studies in many different fields from natural and social sciences to mathematics and artificial intelligence. Wireless communications is another area where cooperation can be studied to bear results, if right structures and methods are designed and implemented. Cooperative techniques can be applied across the layers of a communications system and across different networks.

Implicit cooperation has been an integral part of wireless protocols, as the users had to share common resources. In contrast, explicit cooperative designs such as cross layer optimization, cognitive radio, cooperative coding, virtual antenna arrays and wireless sensor networks have been recently gaining grounds. A paradigm shift is happening in wireless and mobile communications as we consistently observe that cooperation pays off. A broad-spectrum account of cooperative wireless research can be found in [1].

The general objective for these cooperative techniques is to improve the efficiency of wireless networks through more complex behaviours or policies. There is need to design

smarter components and to maintain adequate communications between these components despite the restrictions imposed by the wireless channel. The scope of cooperative research, as a result, is vast and highly specific. Cooperation between the BSs in the uplink of wireless cellular networks is the focus of this thesis. We next outline the background information for CBSs research.

CHAPTER 3

COOPERATIVE BASE STATIONS UPLINK

Combining MUD and inter-BS communications in the uplink of cellular networks in order to form a CBS system opens up many questions of performance and cost. The potential capacity gain is the strongest motive for CBS networks. Another driving factor is taking advantage of macrodiversity in dealing with propagation effects as discussed in 2.2.4 . CBS systems are also expected to allow smooth handoff procedures and power saving policies especially for MSs located at cell boundaries. On the other hand, there are many challenges facing the implementation of CBS systems, such as the need for a high-capacity backbone for inter-BS traffic and high levels of co-channel interference.

Many questions also arise about the downlink of CBSs, such as efficient beam forming techniques, and methods to deal with the asynchronous nature of multi-access broadcast. Exploring all these issues is a vast undertaking and it is out of the scope of this thesis. Our investigation exclusively focuses on interference handling and mitigation in the uplink of CBSs. This chapter provides background information related to this subject. We first review the existing results on the capacity of cellular multiple access systems.

These investigations use simplified models for theoretical analysis, seeking much-needed insight into the benefits of BSs cooperation. Achieving these prospective gains, however, requires addressing a whole range of inter-related issues from feasible system architecture to efficient algorithms and practical policies. We go over the existing solutions addressing these concerns and point out the shortcomings that motivated our research.

3.1 Capacity of Cellular Multiple Access Systems

The widespread success and the need for expansion of cellular systems sparked many questions on the optimality of the designs and practices. What is the Shannon-theoretic limit on the capacity of cellular multiple access networks? How should the frequency spectrum be allocated to intercell and interacell users? What is the effect of reception diversity on system capacity? The complex nature of wireless multi-access channel with random mobility, interference, and propagation effects impedes finding accurate analytical answers to the above-mentioned questions.

In an early paper [34], the authors explore the information-theoretic capacity of multi-receiver networks and prove that an efficient network structure cannot be built on reuse partitioning. As a result, they advocate CDMA networks to allow for full frequency reuse. In [35], Wyner considers a very simple model for the uplink of cellular network with K MSs in each cell. The received signal at a BS is the sum of the signals transmitted from within that cell plus a factor $\alpha(0 \le \alpha \le 1)$ times the sum of the signals transmitted from adjacent cells plus random Gaussian noise. The analysis verifies that intercell orthogonal channel separation in time or frequency (partial frequency reuse) results in capacity loss compared to unit frequency reuse and a global optimal receiver.

This conceptual and analytical approach provided considerable insight that continues to motivate new work. However, the interference model is simplistic, allowing interference only between immediately adjacent cells, assuming all signals to have equal received power and omitting propagation models of fading, path loss and shadowing. Consequently, the specific conclusions regarding performance bear limited resemblance to outcomes in a real system.

In [36], the authors extend Wyner's results to flat fading channels and show that a system with unit frequency reuse maintains a superior capacity compared to intercell TDMA (partial frequency reuse) under all fading conditions. There are still many open problems in capacity analysis of CBS networks. One point is clear, though, that joint processing techniques have the potential to improve the spectral efficiency of future wireless networks, largely by avoiding partial frequency reuse. Capacity, however, simply illustrates the theoretical limits of network throughput; practical aspects such as channel estimation, unmodelled interference, and backbone traffic pose a variety of challenges and options in system design.

3.2 Backbone Architecture and Traffic

Cooperative behaviour necessitates exchange of information between the cooperating entities. Cellular systems are infrastructure-based networks meaning that there is a wired backbone connecting the BSs and accommodating the control data traffic. The backbone also provides the link to BSs serving the MSs in other cells as well as subscribers or data from other communications networks, such as cellular networks, wired landline phones or internet. Employing the CBS concept in cellular networks clearly increases the demand on infrastructure backbone. On the other hand, backbone architecture shapes the

nature of communication between the BSs. In this Section, we look at three potential structures for CBS systems, and briefly discuss some traffic issues.

In his original paper [35], Wyner proposed a joint global receiver that has access to all the received signals and detects them all optimally. Figure 3.1 illustrates this central processing model, where each BS acts as an antenna for the global receiver that performs optimal multiuser decoding. This global receiver is desirable because it allows for full cooperation between the BSs and optimal performance; however, its implementation is practically challenging. The BSs are geographically separated over a large area and collecting all of their signals at one central place might not be possible. This central global architecture may also be less flexible for future upgrades or expansions.

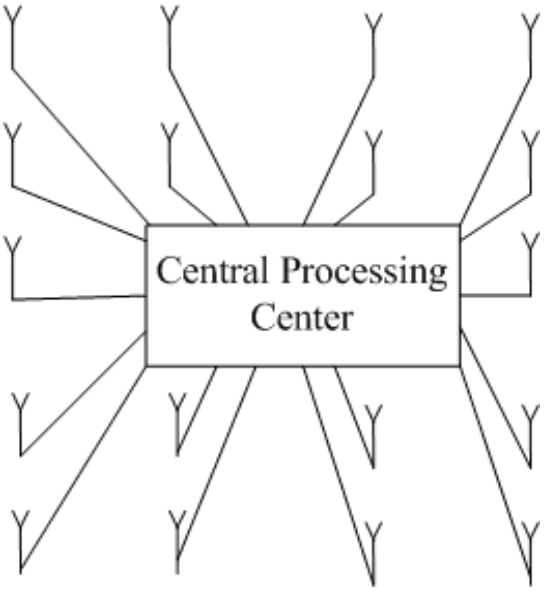

Figure 3.1: Global receiver structure.

Along with the global receiver, [35] proposes a global optimal or suboptimal MUD. The complexity of optimal global MUD grows exponentially with networks size, and even using a global suboptimal detector such as linear MMSE or ZF results in non-linear growth in computational complexity. Therefore, it is better to use distributed or partially distributed suboptimal detectors even in the presence of global receiver topology.

Another possible structure for backbone architecture is the distributed model shown in Figure 3.2. Each BS is connected to the neighbouring BSs instead of a central receiver forming a distributed network of receivers cooperating locally through the backbone. As mentioned in Section 2.2.2 , propagation effects confine the interference from MSs mostly to the nearby BSs. In consequence, this architecture for local cooperation can attain most of the potential gain from a global central receiver. Implementing smaller local receivers is more practical and network design is more flexible to change and easier to expand. However, cooperative MUD of MSs in distributed topology requires iterative communications between neighboring BSs and increases the demand on backbone traffic compared to the central topology.

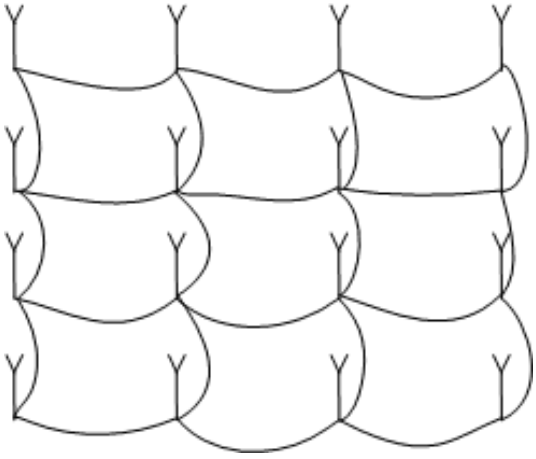

Figure 3.2: Distributed network.

A hybrid solution is to design a network connecting groups of neighbouring BSs into clusters in a quasi-central fashion and then connecting these clusters by a distributed backbone as we see in Figure 3.3. This clustered network design has been practical in prior cellular standards such as GSM. It reduces the local traffic and is easy to implement. The CBS processing framework, we propose in this work mostly focuses on the distributed architecture, however, we later show that it can easily be adapted for clustered design in Section 5.4.2 . The distributed algorithms can also be implemented physically in a global receiver as their complexity generally grows only linearly with network size.

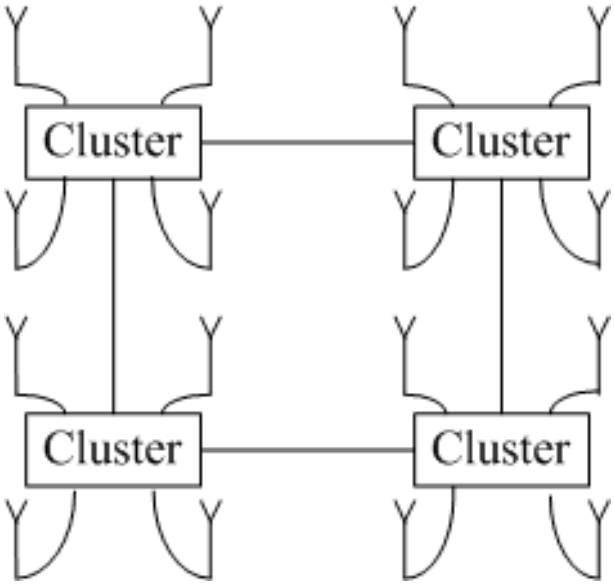

Figure 3.3: Hierarchical network.

Traffic related issues are an additional cause of concern in CBS networks. In a recent paper [37], the effect of limited capacity backhaul between the BSs is explored. The authors show that even when the capacity of the backbone is limited, cooperation between BSs improves the overall network capacity. As discussed above, the traffic requirements depend on the network structure. It is interesting to study the communication patterns in each scheme, analyse the capacity needs and find efficient methods to reduce the traffic in real-time systems. Quantization and source coding techniques are valuable tools in this quest. Another option is to devise innovative policies for limiting the information exchange merely to the situations that need it most, or bear the most results. Some examples of such policies are allowing cooperative detection for MSs in the boundary areas to enjoy diversity reception, or in congested cells to increase the spectral efficiency.

Investigating these issues is out of the scope of our present work. One reason for this choice is that assuming a high capacity backbone such as optical fibre alleviates most of the potential traffic concern, leaving interference as the main dilemma in practical implementations of CBS systems. Therefore, in this thesis, we concentrate on solutions for the interference problem.

3.3 MUD in CBS Networks

As we discussed in Chapter 2, cellular systems conventionally cope with co-channel interference through frequency reuse or power control. Joint detection of interfering signals through MUD is usually considered in the context of interacell CDMA where it exhibits excellent performance [38]. Combining MUD and macrodiversity to form

cooperative networks is a relatively new concept. Here, we provide a review of macrodiversity MUD literature as well as the more recent CBS material.

Early research studied the effect macrodiversity in narrowband systems where MS signals were received by several spatially separated BSs. The BS with the strongest channel makes the decision (selection diversity) [39]. In [40], each BS made hard decisions and sent them back to a central node. The central node accepts any of them that satisfy the error check. If none of them satisfies the check, the bit-by-bit decision is made based on the majority rule (post detection equal gain combining).

Macrodiversity concept was also practically applied in CDMA networks in the form of *soft handoff*. As a MS enters the cell boundaries in CDMA systems, it does not change its frequency band because of the unit frequency reuse; instead, it adds the neighbouring BS into its active set. The BSs in the active set of a MS independently decode its signal, if there is any difference the BS receiving the highest quality of signal, makes the decision [41]. Hence, soft handoff procedure offers selection-based macrodiversity in dealing with shadowing and fading.

In [42], a narrowband post-detection combining scheme called the multiply detected macrodiversity (MDM) is developed. MDM detects the received signals at each BS based on the maximum likelihood (ML) criterion. Then it combines the individual hard decisions from the BSs with a measure of the link's quality to form a final decision. The authors compare MDM with selection diversity and show its ability to reduce the systems BER significantly. In [43], the uplink of a macrodiversity CDMA system with geographically separated antennas is considered. MUD is not applied, yet all the antennas

contribute to the detection of all users. The author develops a power control algorithm based on a carrier-to-interference ratio for such system.

As we mentioned before, Wyner considered a global receiver performing optimal joint MUD in the uplink of cellular networks [35], but the computational complexity of this scheme grows exponentially with network size. As an alternative, he proposed a global suboptimal linear MMSE receiver to reduce the computational costs. Nevertheless, even the suboptimal global receiver is not practical because its complexity increases non-linearly as the network size grows (a polynomial of third degree in case of MMSE). One good but suboptimal way to deal with this problem is to apply joint detection to clusters of BSs rather than the whole network with little communication between the clusters.

Another way is to take advantage of the fact that MSs generate significant interference only in a few BSs, and design joint MUD schemes based on the locality or signal strength. In [44], authors address the system-wide ML-MUD, in which all BS measurements are sent to a central decision point, and introduce the conditional metric merge (CMM) algorithm. The CMM algorithm is a reduced complexity, spatio-temporal Viterbi-like method based on dynamic programming and exploits the fact that, in most cases, only subsets of symbols are significantly present at each BS. Although it still suffers from exponential growth of computation load, the ratio of CMM's load to that of the brute force version of ML-MUD decreases to zero exponentially as the network size increases.

The Viterbi-based CMM algorithm provides hard decision ML results and is not suitable for iterative schemes. The authors of [45] present a soft-decision iterative detection procedure based on the BCJR algorithm [19]. A soft-input, soft-output (SISO)

MUD processor is located at each BS, and neighbouring BSs share the soft information about the MSs they detect. The combined soft decisions then go through a SISO decoder and this process continues iteratively according to the Turbo principles. The soft decision combining proposed in this scheme is a basic instance of BP principles [3]. It is interesting to note that the asynchronous reception that is natural to systems-wide MUD is handled by the BCJR equalizer as a temporal interference.

Distributed BS processing based on the BP algorithm has recently been proposed in [9, 10, 46]. This scheme achieves system-wide MUD through local actions, exchanging information only between immediately adjacent BSs. Pearl's BP algorithm is an iterative message passing technique for calculating the *a posteriori* probabilities (APP) of random variable in a graphical model through the knowledge of some evidentiary variables. BP has been proven optimal in graphical models without cycles [3, 30], yet, it maintains near-optimal performance even in presence of loops [47]. We provide a more detailed discussion about the characteristics of the BP algorithm in Section 4.1 .

In [46], Shental *et al.* considered the application of a more complex generalized BP algorithm in the Wyner model. They state that the BP detectors show very poor convergence when there are a large number of short cycles, and provide a generalized version for clustered cells to solve the convergence problem. This claim seems to contradict our research [7, 8] and [9, 10] as they (both our work and Aktas *et al.*) show near optimal performance even without clustering. In [10], authors blame this different observation on the fixed channel model used in [46] as opposed to random fading model.

In [9, 10], Aktas *et al.* considered an extension of Wyner model to include random fading and apply BP detection at each BS of this model. They have reported bit error rate

(BER) performance near the single-user limit, which suggests that we can rival the efficiency of a global receiver using a distributed system. In [10], they also offer an iterative two-dimensional version of BCJR and compare it with the BP approach. They extend the rectangular model to the more familiar hexagonal structure and observe similar results, noting that the BCJR method is harder to implement in this case.

However, the applicability of this conclusion is limited, since it depends on interference being restricted to contributions only from the immediately adjacent cells in an extended version of the Wyner model with fading. As for computation, the use of local processing allows the complexity of all these methods to grow exponentially only with the number of interfering symbols at each base station. Although this load is far less than that of [44], and vastly smaller than that of brute force system-wide MUD, it is still a significant burden, particularly in systems that allow more than one co-channel user per cell or experience significant interference energy from several nearby cells.

In Chapter 4, we offer a solution to these problems by introducing the reduced complexity BP (RCBP) algorithm, an efficient MUD framework to deal with the multidimensional interference. We then apply it in high interference CBS networks in Chapter 5. We show that it reduces the computational load, while its performance is close to that of optimal BP. RCBP system-wide MUD can handle a realistic channel model and works well in iterative joint decoding and detection. Throughout our investigation, we assume perfect channel state information (CSI) and high capacity backhaul.

CHAPTER 4

REDUCED COMPLEXITY BELIEF PROPAGATION ALGORITHM

As we have discussed, CBS processing requires advanced multiuser detection procedures to be able to provide close to optimal performance in high interference scenarios efficiently. Inspired by the groupwise IMUD, here, we present the reduced complexity belief propagation (RCBP) algorithm (also appears in [2]). Throughout this work, we demonstrate RCBP's exceptional flexibility and capability in handling multidimensional interference.

4.1 Belief Propagation

The belief propagation (BP) algorithm was originally introduced in the 1980's by Pearl in the context of artificial intelligence [3]. BP is an iterative method for updating marginal distributions of variables in a graphical model. In the last decade, the BP algorithm has been successfully applied in communications and information theory. It was rediscovered in iterative decoding of LDPC decoders [30, 33] in the form of Gallager's sum-product algorithm [32]. It was also used in the interpretation of Turbo

codes [48] and in equalization [47]. Even the Viterbi and BCJR algorithms can be viewed as examples of the BP algorithm, with exchange of information on trellis models. Probabilistic reasoning and the BP principles offer much needed insight into iterative methods and facilitate the development of new detection, decoding and estimation techniques.

Let $x_1, x_2, \ldots, x_n$ be a collection of random variables with a finite domain A_i for each i. Associated with the variables are m marginal functions $y_j(X_j)$, where X_j is a subset of variables that y_j depends on. In the problems dealt with in this thesis, y_j can be vector values; typically, it represents a few noisy samples from different times, frequencies, or antennas. A factor graph (FG) is a bipartite graphical model used to represent conditional dependencies among function and variable nodes. In factor graphs, a cycle is a loop starting and ending on the same node. Figure 4.1 and Figure 4.2 show examples of FGs with or without cycles, respectively. BP is based on iteratively exchanging information on the edges of the FG between variable and function nodes and is proved optimal in cycle free FGs [3].

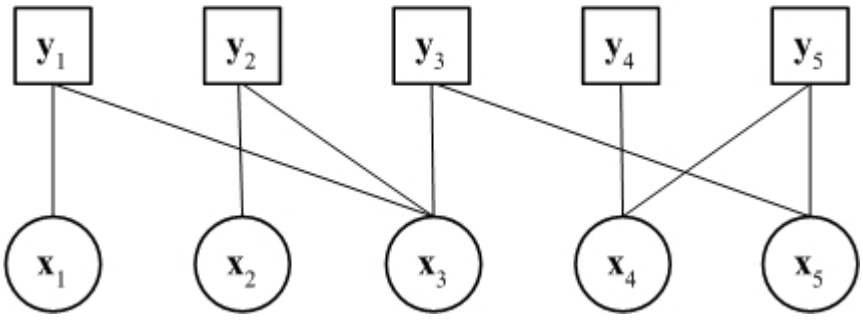

Figure 4.1: A factor graph without cycles.

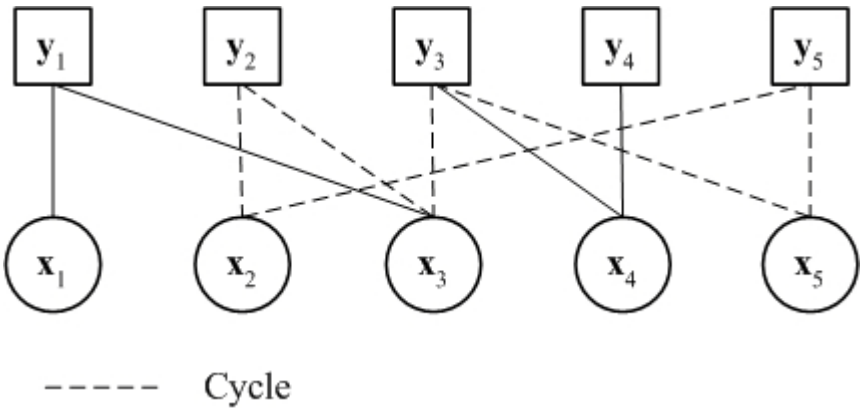

Figure 4.2: A factor graph with a 6-edge cycle.

Each function node is an independent processing unit that receives the a *priori* probabilities (apPs) of the dependent variables $p(x)_i$ via the edges connecting them. It computes the *a posteriori* probabilities (APP) $p(x|y)_{ij}$ of the symbols through probabilistic reasoning. Optimal joint marginalization (OJM) of the random variables in the function nodes involves calculating the probabilities over all possible conditional outcomes and because of that, its computational complexity grows exponentially with number of edges connected to that function node. If x_i and y_j nodes are connected, the messages exchanged on the edge connecting them is calculated according to the following expressions [30, 47]

$$M_{x_i \to y_j} = \prod_{y_{ki} \text{ connected to } k \neq j} , \tag{4.1}$$

$$M_{y_j \to x_i} = \sum_{\sim\{x_i\}} \left[\right] (|)_{jj} \prod_{x_{kj} \in k \neq i} \tag{4.2}$$

The notation $\sum_{\sim\{x_i\}}$ stands for summing over all possible values for x_j excluding x_i values. The messages sent to an edge do not depend on the message previously received on the same edge, i.e. only *extrinsic information* is exchanged. The above messages can also be computed in logarithmic domain

$$\bar{M}_{x_{ij}\to y_{ij}} = \sum_{y_{ki} \text{ connected to } k\neq j} \bar{M}_{y_{ki}\to x_{ij}}, \tag{4.3}$$

$$\bar{M}_{y_{ij}\to x_{ij}} = -\ln\left(\sum_{\sim\{x_{ij}\}} \exp\left[\sum_{k\neq i} \bar{M}_{x_{kj}\to y_{ij}}\right]\right). \tag{4.4}$$

These messages can be interpreted as conditional probabilities or likelihoods in Bayesian networks without loops. The marginal distributions of the random variables are then can be calculated as follows:

$$M_{x_{ij}} = \prod_{y_{ki} \text{ connected to}} M_{y_{ki}\to x_{ij}}, \tag{4.5}$$

$$\bar{M}_{x_{ij}} = \sum_{y_{ki} \text{ connected to}} \bar{M}_{y_{ki}\to x_{ij}}. \tag{4.6}$$

The information is exchanged iteratively on the edges and the messaged can be calculated at the same time (parallel processing) or in succession (serial processing). The results are proven to converge to optimal values in a finite number of iterations in cycle-free graphs [3]. We discuss the detailed expressions for calculating BP messages, later in Chapter 5 and Chapter 6 in the case of CBS processing, as well as in MIMO equalization. Here, we discuss the performance and characteristics of the BP algorithm

and explain how its complexity can be reduced by adapting the principles of the groupwise IMUD algorithm.

As we mentioned, the BP algorithm has been proven optimal in cycle-free graphs [3]. The convergence is not guaranteed in the presence of cycles; however, simulations have shown that in many cases, BP maintains near-optimal performance. In [47], the authors model the ISI channel with a FG and study the BP equalizer. Their results show near-optimal performance when the cycles have six or more edges. In the presence of 4-edged cycles, they propose a *stretching* technique that allows the equivalent of 6-edged cycles. Similarly, as mentioned in 3.3 , Shental *et al.* applied the BP detectors in the Wyner model and reported very poor convergence in the presence of a large number of short cycles. They provided a more complex generalized BP for clustered cells to solve the convergence [46]. Both these studies assume static channel gains in their simulations.

Assuming fading channel model, however, Aktas *et al.* observed near-optimal performance in the presence of 4-edged cycles even without clustering [9, 10]. Although the convergence is not guaranteed in loopy graphs, as we see in Chapter 5 and Chapter 6, our research confirms these near-optimal results after a finite number of iterations. One reason for this phenomenon lies in the random nature of fading channels characterising the links in the FGs of many wireless problems. Deep fades can effectively break many of the short-cycle loops in the model maintaining near-optimal BP performance even with the presence of many 4-edge cycles in the factor graph [10].

BP has a more flexible structure compared to the optimal trellis-based Viterbi or BCJR algorithm. It allows for parallel as well as the traditional serial data processing. Parallel structure is advantageous for high-speed hardware implementation.

Unfortunately, the computational complexity of exact BP grows exponentially with the number of edges arriving at a function node. The OJM in the function nodes is the reason for BP high computational complexity. This high computational load restricts the applications of the BP algorithm to the sparse problems where the number of edges arriving at a function node is limited.

The best way to reduce the computational costs is to replace the OJM by a suboptimal method. However, this problem is generally rank-deficient meaning that the function's dimension is less than the number of variables the function depends on. Most well known sub-optimal and quasi-optimal algorithms cannot handle rank-deficient problems effectively. Linear algorithms like MMSE or ZF have poor performance in overloaded conditions and are inappropriate for joint marginalization in BP function nodes. The soft SD (SSD) [6] will have close to optimal performance but its computation complexity grows exponentially with the degree of rank deficiency. The PDA algorithm [28] does not fail, but experiences increasing performance loss as the degree of rank deficiency increases. The iterative groupwise multiuser detection (IMUD) algorithm [4], however, is designed to handle overloaded detections efficiently, and appears to be a good option to replace brute-force marginalization in the BP algorithm.

4.2 IMUD

IMUD is an iterative groupwise SISO multiuser detection algorithm. It divides the interfering symbols into non-overlapping groups that are detected separately and in succession. To detect a group, IMUD first removes what is known about all other groups by soft cancellation. Then the results go through an optimal joint marginalizer, which provides soft decisions for the symbols in the selected group. The soft decisions are in

turn used in the soft cancellation of that group's symbols when detecting the subsequent groups. After all the groups are detected, we repeat the process and iterate until all the APPs converge, which usually happens in two or three iterations [4].

As mentioned above, the IMUD algorithm has a joint marginalizer in its core that processes the signals and the apPs of the symbols in the group to provide the extrinsic probabilities of these symbols at the output. The complexity of the OJM grows exponentially with the group size. To further decrease the IMUD computational complexity, we could replace the OJM with near optimal, low complexity algorithms like the SSD or PDA.

The SD algorithm [26] finds maximum likelihood solutions with lower computational costs than OJM, if the SNR is high enough and the system is not overloaded. SD reduces the computational complexity by restricting the search to the signal points inside a sphere centered on the received vector. The original SD provided only hard output, but soft output variations have been proposed ([6] and references therein). PDA, on the other hand, is an iterative algorithm based on Gaussian forcing (assuming the unknown part of the signal to be a Gaussian random variable) and soft interference cancellation. It was originally designed for target tracking in the 1970s and applied to multiuser detection in [28]. PDA provides soft decisions, and in [49] a soft-input soft-output version of the algorithm (SISO-PDA) was proposed for turbo equalization. It has polynomial computational complexity and near optimal performance. The option of choosing SSD and SISO-PDA cores offers another level of design flexibility in IMUD framework.

IMUD has been designed to handle rank-deficient problems and has a flexible structure, as it allows for different group sizes and ordering schedules (the method used

in dividing interferers into non-overlapping groups) in addition to the choice of different algorithms for the core joint marginalizer. This flexibility enables us to adjust IMUD for a specific problem's structure, computational power and performance requirements. These qualities make the IMUD detector a perfect option for replacing the OJM in the functions nodes of BP algorithm to form the reduced complexity BP (RCBP) algorithm.

4.3 RCBP

Our proposed RCBP keeps the flexible BP framework, yet replaces the OJM in function nodes with the groupwise IMUD. Therefore, it reduces the computations with relatively small degradation in performance. RCBP offers the flexibility to trade off performance and complexity by choosing the group size as well as the IMUD core marginalization method. IMUD's sorting and grouping strategies can also be modified to adapt to specific structure of a problem. RCBP also allows for more advanced hybrid core selection as we show in 5.4.2 .

We illustrate how we have adapted RCBP algorithm for CBS processing and MIMO equalization in Chapter 5 and Chapter 6 respectively. We demonstrate RCBP's capability in dealing with these high interference problems. While the original IMUD uses the error variance minimization (EVM) method in the first iteration and random selection for the second iteration, the same policy does not produce the best results in the problems we considered. We adapt RCBP grouping and selection strategy in CBS processing and MIMO equalization. RCBP application is not limited to those discussed in this work and in 8.1 , we outline a few other potential applications for RCBP. The capability to deal with multidimensional interference and flexible structure makes the RCBP algorithm a promising option for the future wireless systems.

CHAPTER 5

DISTRIBUTED MUD IN CBS SYSTEMS

In this chapter, we apply the RCBP algorithm to system-wide distributed MUD in the uplink of CBS systems. We show that its performance is close to, or identical to, that of BP in the simplified network model. We also observe excellent performance by iterative multiuser detection and decoding of LDPC. Furthermore, we examine RCBP performance in a more realistic wireless network model, with path loss, shadowing, fading and power control. These results, though poorer than those of the simplified network, show that system-wide MUD with cooperating BSs provides great improvement compared with conventional systems. The contents of this Chapter are also published in [7, 8][*] .

5.1 Introduction

As we discussed in Section 3.3 , distributed detection is a more viable option for the uplink of CBS-based cellular networks compared to the global system-wide receiver.

[*] ©2007 and ©2008 IEEE. Reprinted, with permission, from [7, 8].

Distributed MUD of local MSs (located in neighboring cells) and sharing the information among local BSs is natural to the cell system structure, as a user causes significant interference, primarily in nearby cells. We mentioned the recent publications proposing distributed BP receivers [9, 10] or the more complex generalized BP [46], with information exchange only between immediately adjacent BSs. These schemes are applied in Wyner-based models where the interference is restricted to contributions only from the immediately adjacent cells. Therefore, their conclusions have limited relevance in real systems, which experience interference from many cells not just those immediately adjacent.

Computational complexity grows linearly with the network size in the distributed BP detection compared to the exponential growth in global receiver. Nevertheless, computational burden is still a source of concern, since the computational complexity of the local receivers grow exponentially with the number of interfering symbols at each BS. In this chapter, we extend the application of BP-based methods to system-wide MUD in the uplink of CBS systems, and address three major practical issues: the computation load, the performance in coded systems, and the performance in more realistic propagation conditions.

Regarding computation load, we propose a sub-optimal RCBP receiver. The main advantage of this method is that its computational complexity does not grow exponentially with the number of interfering users at each base station. It is also very flexible in the sense that we can control the performance and complexity by changing the group sizes. We believe that the RCBP receiver is a practical method for CBS processing in future cellular communication networks.

Regarding the performance in a coded system, we investigate combined iterative multiuser detection and LDPC decoding, using the RCBP algorithm to reduce complexity. LDPC codes are chosen for this investigation as they use the BP algorithm in their own decoder. We show that the performance of this scheme, after only a few iterations, is very close to that of a coded single user with no interference.

Regarding the last issue, the performance in realistic propagation conditions, we show that RCBP continues to function well in the noise-limited region, but has an error floor in high SNR conditions because of the residual interference from cells beyond those directly involved in the BP calculations. We also quantify the performance improvement attributable to the cooperation of BSs, compared with individual operation, which is another new result.

5.2 Simplified Network Model

In the first part of our investigations, we adopt and extend the simplified propagation model of Aktas *et al.* [9, 10], which is in turn an extension of the Wyner model [35]. The original Wyner model does not include fading, shadowing or path loss, and interference comes only from MSs in the immediately adjacent cells; further, the path gains of all such interfering MSs have the same, fixed value. The model in [9, 10] extends [35] to include fading, although the variances of the path gains are the same and fixed. On the other hand, it restricts [35] by considering a square cell layout with interference only from the side-adjacent cells.

The simplified model is valuable since it permits some degree of analysis for the ideal performance and it highlights key interactions in the complex problem of BS

cooperation. Our main goal is to show that applying RCBP in distributed base station processing can reduce the computational load efficiently. Using this simple model helps us explain the principles of this process more clearly and compare performance with exact BP results of [9, 10]. However, conclusions regarding performance do not necessarily apply to real CBS cellular networks, as we show in Section 5.6 .

We assume that the cells are located on a rectangular $N \times N$ grid and there are K co-channel users within the cell. Each user has only one antenna and each base station has N_r omnidirectional antennas. We slightly extend the model of [9, 10] by allowing more than one user per cell and more than one antenna in the BSs. For simplicity, we assume BPSK modulation. The BS in the cell (i,j) receives the signals from users within the cell $b_{ijk} \in \{-1, 1\}, k = 1 \ldots K$ and interference from users in the four side-adjacent cells, such as $b_{i-1,jk}, k = 1 \ldots K$ from cell $(i-1, j)$. Extending the results to the more familiar hexagonal model and higher modulation schemes is conceptually straightforward.

Channel gains from user k, located in the cell (m,n), to the base station (i,j) are denoted by the length-N_r vector $\mathbf{h}_{ijk(m,n)} = [h_{ijk(m,n)}^{(1)} \ldots h_{ijk(m,n)}^{(N_r)}]^T$, $(m,n) \in \mathrm{N}$, where the *neighbour set* $\mathrm{N} = \{(0,0),(1,0),(0,1),(-1,0),(0,-1)\}$. The received signal $\mathbf{y}_{ij}$ at cell (i,j) is equal to

$$\mathbf{y}_{ij} = \sum_{k=1}^{K} \mathbf{h}_{ijk(0,0)} b_{ijk} + \sum_{k=1}^{K} \mathbf{h}_{i-1,jk(1,0)} b_{i-1,jk} + \sum_{k=1}^{K} \mathbf{h}_{i+1,jk(-1,0)} b_{i+1,jk} + \sum_{k=1}^{K} \mathbf{h}_{ij-1k(0,1)} b_{ij-1k} + \sum_{k=1}^{K} \mathbf{h}_{ij+1k(0,-1)} b_{ij+1k} + \mathbf{n}_{ij}, \tag{5.1}$$

where $\mathbf{n}_{ij}$ is the additive white Gaussian noise. Without lack of generality, we can assume that the power of noise is equal to 1. In a flat Rayleigh fading channels, the

components of $\mathbf{h}_{ijk}(m,n)$ are complex Gaussian random variables with zero mean and variance equal to Γ if $m=n=0$ and $\alpha^2\Gamma$ otherwise, where Γ is the SNR per antenna of the users received in their current cell and α is a ratio controlling the power of interference from neighboring cells. The signal to interference ratio (SIR) seen at any single BS in this model is quite poor, at $\left(\alpha^2(|\mathcal{N}|-1)\right)^{-1}$.

By defining the $N_r K \times$ matrix $\mathbf{H}_{ij}(m,n) = \left[\mathbf{h}_{ij1}(m,n) \cdots \right.$ and the $K \times 1$ vector $\mathbf{b}_{ij}(m,n) = \left[b_{ij1}(m,n) \cdots \right]^T$, (5.1) can be written more concisely as

$$\mathbf{y}_{ij}(m,n) = \mathbf{H}_{ij}(m,n)\mathbf{b}_{ij}(m,n) + \sum_{(m',n') \in \mathcal{N}} \mathbf{H}_{ij}(m',n')\mathbf{b}_{ij}(m',n') + \mathbf{n}_{ij}(m,n), \quad (5.2)$$

where the array $\mathbf{H}_{ij} = \left[\mathbf{H}_{ij}(m',n') \cdots\right]$ $\mathcal{N}$ is $N_r K \times |\mathcal{N}|$ and the vector $\mathbf{b}_{ij} = \left[\cdots \mathbf{b}_{ij}(m',n') \cdots\right]^T$ is $|\mathcal{N}|K \times 1$. A simplifying assumption is perfect CSI; that is, each BS has access to the values of the channel gain arrays that affect its measurement (5.2). Except in Section 5.5, we deal only with uncoded transmission.

The goal is to use all the received signals in the network $\mathbf{Y} = \{\mathbf{y}_{ij}\}$ to calculate the users' APPs $p(b_{ijk}|\mathbf{Y})$ by marginalizing over the data symbols. With N^2K users in the system, the order of computational complexity of optimal global calculation of the APPs is $O(2^{N^2K})$. CBS processing based on BP approximates this calculation task with less complexity, at $O\left(N^2 2^{|\mathcal{N}|K}\right)$ per iteration. As we show later, RCBP receiver can further reduce computational requirements without causing substantial performance loss.

5.3 RCBP in CBS Networks

The interference environment described in 5.2 can be represented by the bipartite factor graph of Figure 5.1, for a 44 network. The variable nodes are the unobserved values , whose APPs are to be estimated, and the function nodes are the evidentiary variables (the received signals) . The edges show the dependencies between the function and variable nodes. In the BP algorithm, messages and are exchanged iteratively between function and variable nodes to calculate the marginal probabilities, i.e. the APPs. These messages are computed according to the principles, discussed in Section 4.1 , for (with appropriate modifications for exterior cells of the network that have fewer neighbours).

For simplicity, we have written them as log-likelihood ratios (LLRs) for a binary alphabet, although other representations are more appropriate for larger signal constellations. A function node needs to calculate the APPs by marginalizing extrinsic probabilities as

$$p(b_{ijimjnk}=\pm 1) = \sum_{\mathbf{b}_{ij}:\, b_{imjnk}=\pm 1} \frac{p(\mathbf{y}_{ij}\mid \mathbf{b}_{ijij})}{p(b_{imjnk}=\pm 1)}, \tag{5.3}$$

where

$$p(\mathbf{y}_{ij}\mid \mathbf{b}_{ijij}) \propto \exp\left(-\frac{1}{2\sigma^2}\left\|\mathbf{y}_{ij}-\mathbf{H}\mathbf{b}_{ijij}\right\|^2\right). \tag{5.4}$$

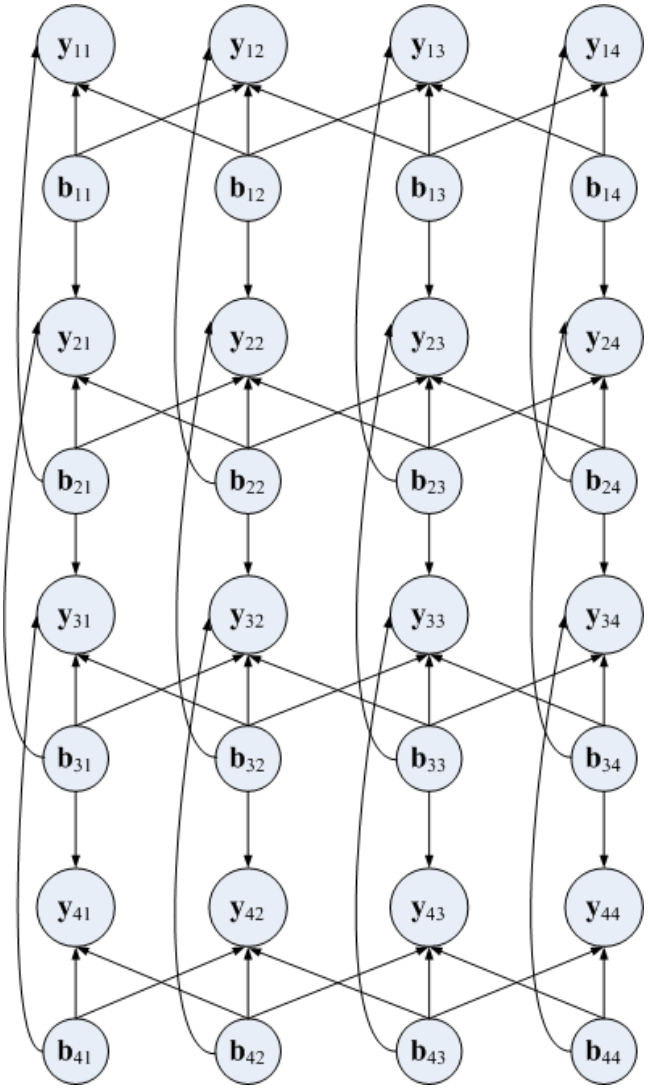

Figure 5.1: Factor graph for the simplified network model. To save space, b_{ij} here represents $b_{ij}(0,0)$.

The calculation is performed when the function node has received apPs from all the variable nodes to which it is connected. Initially, those messages (the LLRs) are set to zero. The function node then computes the messages for each of the K users in the variable nodes to which it is connected, as follows:

$$M_{\mathbf{y}_{ij} \to b_{imjnk}} = \underbrace{\log \frac{p(b_{imjnk}=+1 \mid \mathbf{y}_{ij})}{p(b_{imjnk}=-1 \mid \mathbf{y}_{ij})}}_{\text{a posteriori information}} \underbrace{\qquad}_{\text{a priori information}}$$
$$= \underbrace{\log \frac{p(\mathbf{y}_{ij} \mid b_{imjnk}=+1)}{p(\mathbf{y}_{ij} \mid b_{imjnk}=-1)}}_{\text{extrinsic information}}. \tag{5.5}$$

When a variable node has received messages from all the function nodes to which it is connected, it replies with messages containing its updated partial apPs to each of those function nodes as follows:

$$M_{b_{imjnk} \to \mathbf{y}_{imjn}} = \underbrace{\log \frac{p(b_{ij}=+1)}{p(b_{ij}=-1)}}_{\text{a priori information}} + \sum_{(\tilde{m},\tilde{n}) \in \mathcal{N}(i,j) \setminus (m,n)} M_{\mathbf{y}_{i\tilde{m}j\tilde{n}} \to b_{ij}} + \underbrace{\tilde{\quad}}_{\substack{\text{a priori information} \\ \text{from other sources}}}. \tag{5.6}$$

The last term in (5.6) might represent additional extrinsic information received from, say, a turbo decoder or LDPC decoder, as we see in Section 5.5 . This exchange of messages between variable nodes and function nodes continues iteratively until the APPs converge. As mentioned in Chapter 4, convergence is not guaranteed in FGs with loops, however, the BP algorithm maintains near optimal performance even in the presence of loops in many problems. In this work, we have investigated the performance after a fixed number of iterations. Individual symbol decisions are then made by selecting the value with the greatest APP.

Physically, function node computations are performed in parallel (in all the BSs at once) at the BS (ij) where y_{ij} is measured. Variable node computations for data symbols b_{ijk} are performed at the BS of the cell (ij) where the MS (ijk) is located. The backbone network is then required only for transmission between adjacent BSs of K LLRs in each direction for each iteration. Other organizations are possible, such as for the irregular and more extensive interference patterns produced by path loss and shadowing in realistic wireless networks as we discuss in Section 5.6 .

Though suboptimal in graphs with loops, BP has several advantages: data flows are local, rather than to a central decision point; it allows parallel computation; and its delays in making decisions are much smaller than those of the trellis-based approaches (Viterbi-based CMM [44] or two-dimensional BCJR [10]) for networks of two and higher dimensions. Unfortunately, the marginalization in (5.3) causes the computational complexity of BP to grow exponentially with the number of edges arriving at a function node. Since the number of edges equals the number $K|\mathbb{N}|$ of interfering symbols at each BS, the complexity grows as $O\left(2^{K|\mathbb{N}|}\right)$, or $O\left(2^{5K}\right)$ per iteration for the rectangular Wyner model. This high computational load restricts the applications of the BP algorithm.

We adapt the RCBP structure to cooperative base station processing in the uplink of cellular networks. Figure 5.2 shows a function node in RCBP processing. The apps of the interfering symbols arrive from the variable nodes via the connecting edges. The symbols are divided into non-overlapping groups and the APPs are calculated using the IMUD algorithm. The messages to variable nodes are then calculated and sent back to the nodes.

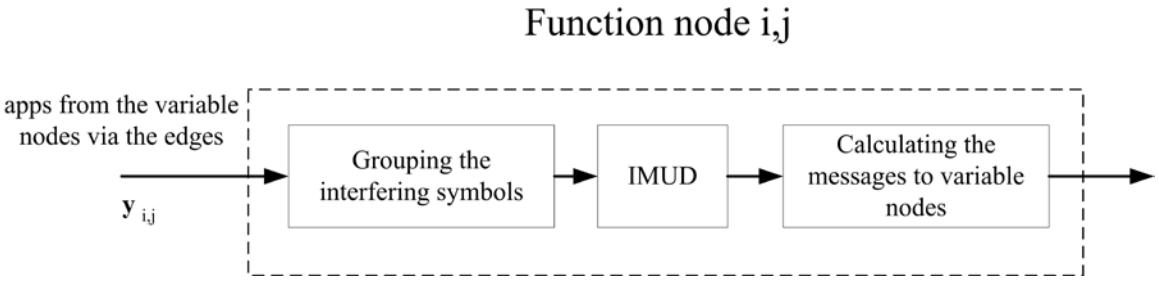

Figure 5.2: A function node in RCBP processing.

As we discussed in Chapter 4, the main advantage of this approach is that its computational complexity does not grow exponentially with the number of interfering users at each base station. It is also very flexible in the sense that we can control the performance and complexity by changing the group sizes. With the symbols split into N_G non-overlapping groups of size G_i, we rewrite the received signal (5.1) at an arbitrary BS as

$$\mathbf{y} = \sum_{i=1}^{N_G} \mathbf{H}_i \mathbf{b}_i + \mathbf{n} \tag{5.7}$$

Groups of interfering users are detected in sequence to obtain the APPs of their symbols $b_{i,m}$, $m = 1, \ldots, G_i$ as $\pi_{i,m}(b) = \Pr[b_{i,m} = b]$. Then $b_{i,m}$, $\mu_{i,m} = \pi_{i,m}(+1) - \pi_{i,m}(-1)$, and the *a posteriori* means $\mu_{i,m} = \pi_{i,m}(+1) - \pi_{i,m}(-1)$ are formed into the vector $\mathbf{b}_i$. We adopt Gaussian forcing and suppose that $e_{i,m}$, zero mean Gaussian random noise, and *a posteriori* variances $\sigma^2_{e_{i,m}} = 1 - \mu^2_{i,m}$ are formed into the array $\mathbf{E}_i = diag\left[\sigma^2_{e_{i,1}}, \ldots, \sigma^2_{e_{i,G_i}}\right]$, which assumes independence of the estimates.

Figure 5.3 illustrates the structure of IMUD in RCBP distributed detectors. Soft cancellation of a group is performed by subtracting its *a posteriori* means from the measurements and adding the covariance to the noise:

$$\tilde{\mathbf{y}} = \mathbf{y} - \sum_{i=1}^{N_G} \quad (5.8)$$

$$\mathbf{R}_{\tilde{\mathbf{y}}\tilde{\mathbf{y}}} = \mathbf{H}\mathbf{E}[\quad]\mathbf{H}^{\dagger} + \sum_{k=1}^{N_G} \quad (5.9)$$

Introducing these intermediate variables reduces the number of computations needed at each IMUD step. To detect group i, we add the soft information of this group to the intermediate variables

$$\tilde{\mathbf{y}}_{im} = \tilde{\mathbf{y}} + \quad . \quad (5.10)$$

$$\mathbf{R}_{im} = \mathbf{H}\mathbf{E}[\quad]\mathbf{H}^{\dagger}. \quad (5.11)$$

The basis of marginalization to estimate $\mathbf{b}_i$ is the Gaussian assumption, giving the joint probability density function (pdf) of

$$p(\tilde{\mathbf{y}}_{im}, \mathbf{b}_i) = \left(\quad \right)^{\dagger} \quad ^{-1} \left(\quad \right) \prod_{m=1}^{G_i} \left(\quad , \quad \right) \quad (5.12)$$

where the apP of $\mathbf{b}_i$ is expressed as the product of probabilities of its components.

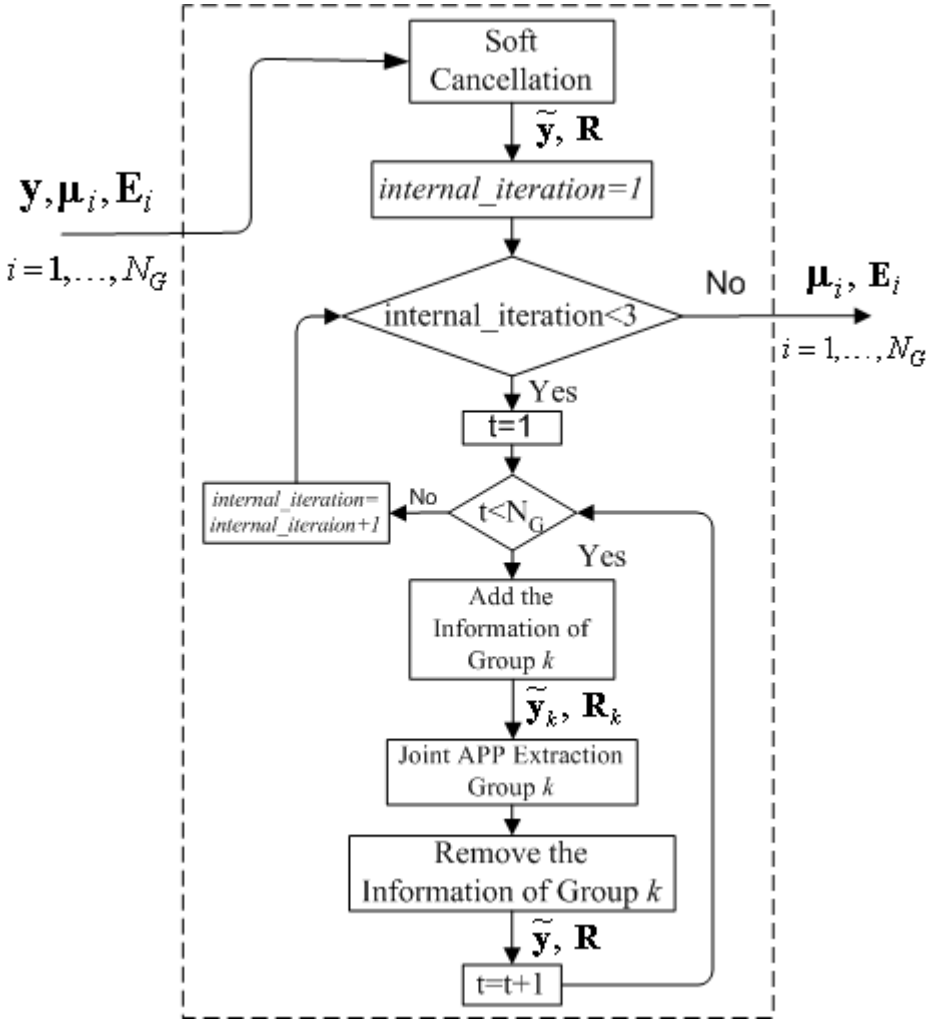

Figure 5.3: IMUD structure in RCBP detectors.

As mentioned in Chapter 4, IMUD allows for further reduction of the computation through the choice of core detector. Basic IMUD's computational complexity grows exponentially with the group size G_i , rather than with the total number $K|N|$ of interfering symbols. The larger the group size, the closer the detection performance will be to that of the BP, and with a single group of size $K|N|$, RCBP and BP are the same. If the group size is equal to one, IMUD reduces to the PDA algorithm [50]. By selection of the group size, IMUD gives us the opportunity to trade off performance and complexity. We can also modify the detection order of the groups in order to improve the performance. After all the groups are detected, the membership of the groups is randomized (not shown in Figure 5.3), and the whole process repeats until all the APPs converge, which usually happens in two iterations, the value we used in our simulations.

The RCBP detector calculates the APPs of the users in the network the same way as the distributed BP receiver. The only difference is that RCBP computes the messages using IMUD instead of OJM so it is doubly iterative, with external BP iterations as well as internal IMUD iterations. As just mentioned, grouping strategies in IMUD can be modified to trade off performance and complexity, and RCBP inherits this quality. In using RCBP we will clarify the method by mentioning the group sizes in parentheses; for example, RCBP (3,2) means that we have two groups, the first of three users and the second of two. Similarly, RCBP (4,4,4) means that we have three groups of 4 users.

Geographical location of the users does not affect RCBP's grouping strategy. Unless otherwise specified, we sort the users initially in order of decreasing mean SNR at the function node before dividing them into the specified groups (i.e., best SNR first). From simulations, not shown here, we found that this ordering was almost as effective in RCBP

as the much more computationally expensive minimum error variance sorting of the original IMUD algorithm [4]. Because of the variable signal strengths caused by fading, a group may contain users from different cells. For all the results in this work, we run the simulations at least 100,000 times or until at least 200 errors occur.

5.4 RCBP Performance in Simplified Model

5.4.1 Distributed Network

In this section, we address performance and complexity of RCBP for CBS processing in the distributed simplified network model of Figure 3.2. Each BS (i,j) performs the computation for its function node $\mathbf{y}_{ij}$ and for all variable nodes in $\mathbf{b}_{ij}$ $(0,0)$ (i.e., the MSs within the same cell). Figure 5.4 compares the performance of several algorithms on a 9×9 network of BSs, each with a single antenna $N_r = 1$ and a moderate interference level $a = 0.5$. The results shown in this figure are for 6 parallel BP iterations for $K = 1$ users per cell, and 10 parallel BP iterations for $K = 2$. The curves do not include the users in the exterior cells of the network; their performance is significantly worse than that of users inside the grid because, even though they have less interference, they experience less diversity. We have also illustrated the performance of a single user in the network (no multiuser interference) as a limit.

Table 5.1 presents the normalized processing time per user for various algorithms, obtained directly from measurements of the simulation code. Although they depend on details of the simulation package and, to some extent, on the skill of the programmer, they include the “housekeeping” details usually omitted from the asymptotic order of complexity.

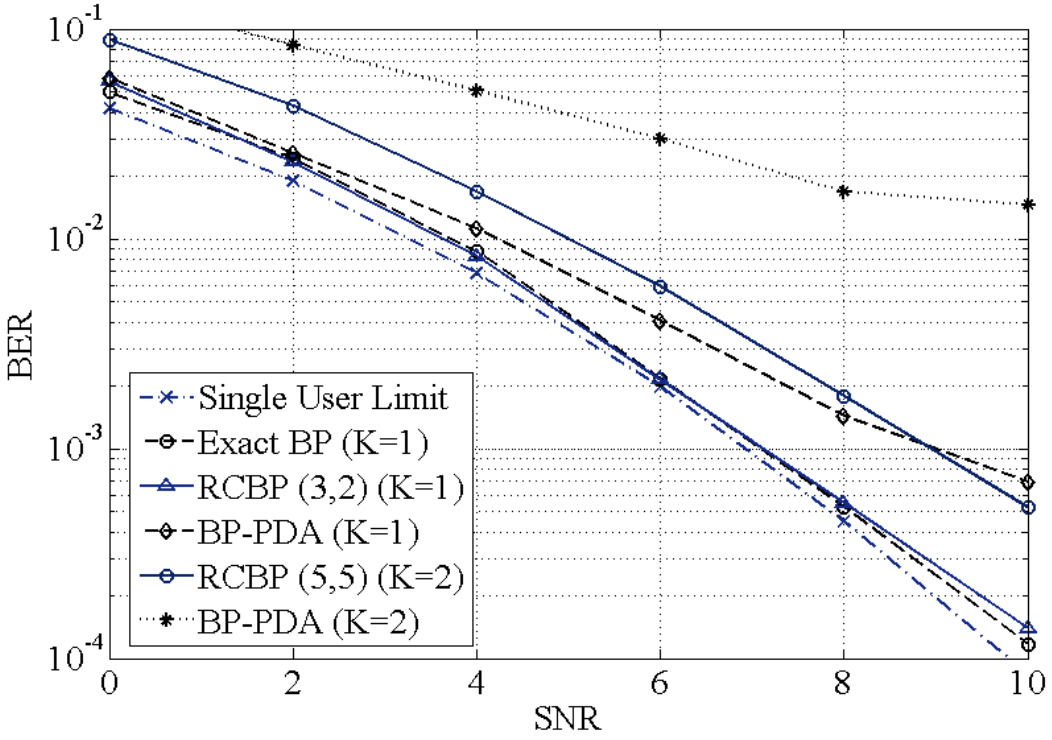

Figure 5.4: RCBP BER performance in a 9x9 simplified network model, $a = 0.5$ **and** $Nr = 1$ **.**

Table 5.1: Processing Time Ratios Decomposed RCBP

Method	Normalized Processing Time
BP (K=1)	1
RCBP (2,3) (K=1)	0.485
BP-PDA (K=1)	0.061
RCBP (5,5) (K=2)	2.06

We first observe that, for $K=1$ user per cell, RCBP (3,2) provides virtually the same performance as exact BP out to $\Gamma = 8\,\mathrm{dB}$, and is about 0.4 dB poorer by 10 dB. They are both close to the performance of a single user, as was previously shown in [9, 10]. As for computation, RCBP (3,2) is more than 50% faster than exact BP on these curves. Moving up to $K=2$ users per cell, *so that 10 MS signals interfere at each single-antenna BS*, we adopt RCBP (5,5), with two groups of 5 users. The SNR penalty, relative to a single user per cell, is 2 dB, and the two curves run almost parallel at high SNR. The processing time per user is about twice that of the $K=1$ case, for a total of four times as much processing as for $K=1$. In contrast, for exact BP, doubling the number of users per cell increases the computation load by a factor of 32, since its complexity is $O\left(2^{5K}\right)$. For this reason, its performance is not shown in Figure 5.4. Aside from the greatly improved computational load, it is encouraging to see such good performance in an significantly rank-deficient environment with a very low SIR signal-to-interference ratio (-4.8 dB for $a=0.5$). It is clear that CBS processing provides additional signal energy through macrodiversity as well as additional dimensionality to assist the MUD in each cell.

As for the BP-PDA algorithm with $K=1$, it is extremely fast, with 8 times less computational load than RCBP (and 16 times less than exact BP). However, it suffers from significant performance loss and divergence from exact BP. In simulations not included in Figure 5.4, we examined the performance of BP-PDA up to SNR=30 dB and noticed a floor of $5*10^{-4}$ in BER. With a second user per cell ($K=2$), the rank deficiency is acute and its performance is no longer near-optimal.

5.4.2 Clustered Network

In clustered networks Figure 3.3, nearby base stations are grouped together, and are considered as a single function node. Figure 5.5 shows an 8×8 network clustered into 2×2 groups. This scheme is natural for the structure of some real communications systems; for example, in GSM networks several neighboring base transceiver stations (BTSs) are controlled by one base station controller (BSC), as we discussed in Section 3.2 . The function nodes in this model have more dimensionality, which gives more room for modifying the RCBP algorithm. Moreover, clustering reduces the number of 4-edge loops in the system and decreases the network traffic compared to the decomposed model.

As we see in Figure 5.5, each cluster receives interference from the four immediately adjacent clusters and the interference originates only from the users in the two nearest cells of each of those neighboring clusters (in the assumed Wyner model) so the total number of interfering users in each cluster is $8K$ while there are $4K$ users inside the cluster. Compare this system with the previously discussed distributed scheme, where each base station receives $4K$ interferers from outside the cell, and K users inside. A base station in the distributed system or a base station controller in the clustered scheme have to communicate the information about all the interfering users per iteration, therefore, the number of messages for two iterations, per user is $2 \times 4K = 8K$ in the clustered model; that is, only half of the $2 \times 8K = 16K$ messages needed in the distributed model.

We compared the BER performance and processing time of several RCBP schemes in the clustered model shown in Figure 5.5 to that of the decomposed exact BP algorithm

via simulations. The results are illustrated in Figure 5.6 and Table 5.2. RCBP (4, 4, 4) divides the 12 interfering users into three groups of four users. Other than the reduced traffic, this method is not very interesting because performance loss is as much as 1dB and processing time saving is not significant. BP-PDA, however, is very fast because of its one-user “groups”, and its performance is closer to exact BP in moderate SNRs than it is in the decomposed model. We also apply a hybrid RCBP approach that divides the 12 interfering users into two groups: 4 users within the cluster and 8 users out of the cluster. The dimension of each cluster node has rank 4 so we use a soft SD algorithm to detect the group of 4 but because the group of 8 is sparse and rank deficient we use PDA to decode that. Hybrid-RCBP (4,8) is even faster than BP-PDA and gives better performance than BP-PDA in moderate to high SNRs, making it an excellent choice for this simplified network.

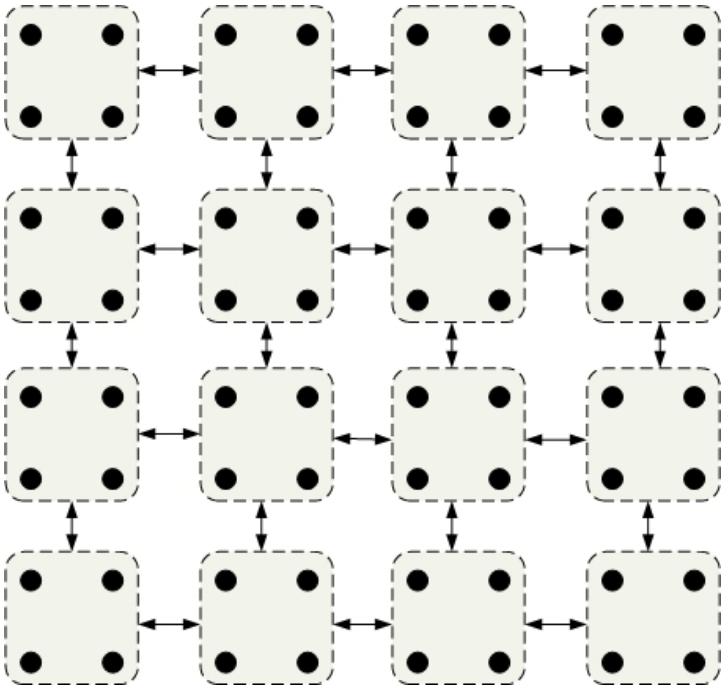

Figure 5.5: An 8x8 cellular graph clustered into 2x2 groups.

Table 5.2: Processing Time Ratios Clustered RCBP

Method	Normalized Processing Time
BP (K=1)	1
Clustered RCBP (4,4,4) (K=1)	0.971
Clustered BP-PDA (K=1)	0.118
Clustered Hybrid RCBP (4,8) (K=1)	0.087

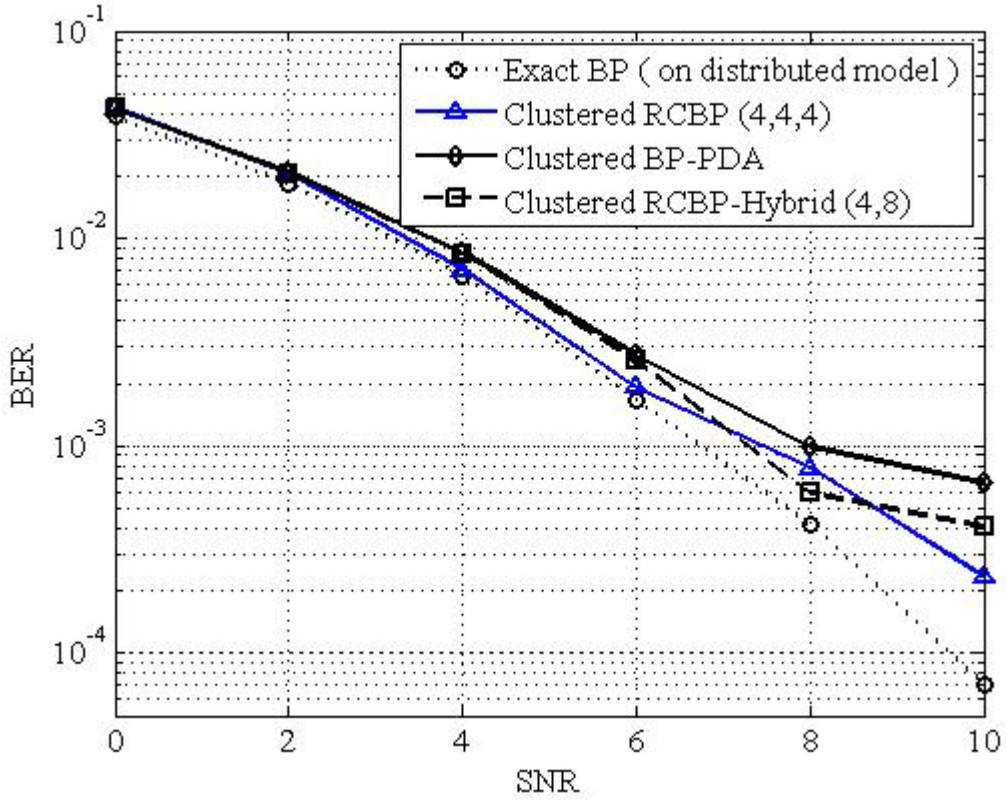

Figure 5.6: RCBP BER performance in clustered model, $a = 0.5$ **.**

5.5 Coded Systems

In this section, we look at the performance of RCBP in an iterative detection and decoding system. Any codes can be applied in such scheme. We have chosen to consider LDPC codes because their decoders are based on BP as well. The joint detection and decoding then involves three levels of iteration: the internal IMUD iterations, the external BP iteration between the BSs, and the BP decoder iterations. We do each decoding and detection iteration in two steps. The first step includes parallel RCBP detection in each BS separately, followed by decoding the main user in each cell. The second step includes sharing the extrinsic information between the BSs, followed by another round of decoding.

Figure 5.7 shows the performance of such an iterative detection and decoding system in a 21x21 cell grid with the propagation model of Section 5.2 . As in the last simulation, we do not include the users in the outer cells. We have used randomly generated LDPC codes with rate $R_c = 1/2$, length $(M,N) = (128,256)$, and $(w_c,w_r) = (3,6)$, where M is the number of parity checks, N is the block length, w_c and w_r are the number of ones per column and rows of parity check matrix respectively. In step 1 of each iteration, we applied a parallel iteration of RCBP (3,2) with two internal IMUD iterations, and both steps 1 and 2 employed 10 internal iterations of the BP LDPC decoder. We assume slow fading, so the channel gain is static through the whole block and changes randomly in the next block. As in other graphs, the horizontal axis is the SNR of information bits at each antenna; *i.e.* it is the SNR of coded bits divided by the code rate R_c .

We perform two iterations and compare the results with the single user performance. The single user detection follows the above-mentioned steps of detection and decoding as well. We have also approximated the decoder performance of the single user analytically, using the macrodiversity distribution of SNR according to one strong and 4 weak antennas, and a code SNR threshold of 1.5 dB. This threshold is estimated from the BER performance of the code in AWGN channel via simulation (not included here). After only two iterations, the packet (codeword) error rate (PER) performance of our iterative method in the presence of multiuser interference is very close to both the analytical and simulated results for a single user.

A great advantage of using LDPC codes is that we can exit the iterative process once the parity-check matrix is satisfied (not applied in our simulations). This property can save much computation, especially in high SNRs. It would be interesting to apply this method and quantify its potential computational savings. Further attractive research is to find optimal coding methods for CBS systems when the blocks are longer or the fading is fast. It would also be fruitful to consider adaptive channel estimation along with iterative decoding and detection.

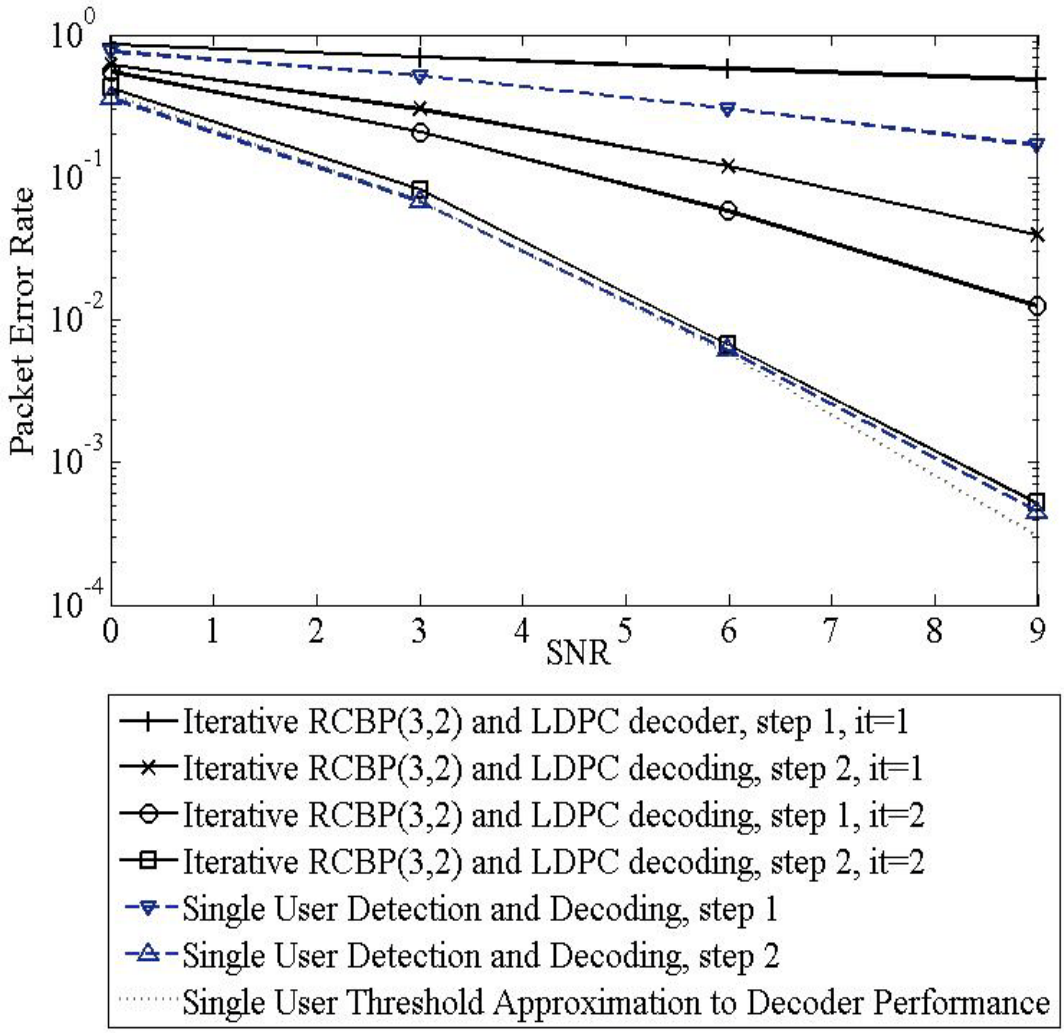

Figure 5.7: Packet (codeword) error rate of iterative RCBP MUD and LDPC code $(N,M)=(128,256)$ **,** $(w_c,w_r)=(3,6)$ **, simplified 21x21** $a=0.5$ **,** $N_r=1$ **,** $K=1$ **.**

5.6 Wireless Network Model

As noted earlier, the simplicity of the Wyner model helps us understand some aspects of BS cooperation, but conclusions based on the model do not necessary apply in real wireless systems. In this section, we adopt a more realistic model for the wireless environment and demonstrate different behaviour and a host of interesting research issues. The principal change as we move to the wireless network model is that the average signal power from a MS is received at the BSs of all cells, at levels determined by path loss, shadowing and power control. This is in contrast to the simplified network model, in which MS signals were received at a fixed average level and only in-cell and in side-adjacent cells. Multipath fading is present in both network models.

As discussed in 2.1.1 , we model loss (formally, path gain) as an inverse γ^{th} power of the distance between an MS and a BS, where γ is typically 3 to 4, so that it depends on the location of MS within its cell. Shadowing power gain, caused by relatively large obstacles in the path, is modelled as a multiplicative log-normal variation with standard deviation typically in the range 4 dB to 8 dB.

We employ a simple power control model: the MS adjusts its transmit power in response to commands from a controlling BS in order to keep its received SNR at that BS constant at a target value Γ in the face of varying path loss and shadowing changes as the MS changes position. Power control does not attempt to track fading, and no account is taken of the additional signal energy from adjacent BSs through cooperation. The controlling BS is the one that receives the MS signal with greatest strength (averaged over fading), and is not necessarily the BS in the same cell as the MS. The average SNR

at BS (i,j,m) of the signal received from mobile k of cell (i,j) that is power controlled by BS (i,j,k) is then

$$\Gamma_{ijk,ijk,ijk}^{mn} = \left(\frac{d_{ijk}^{ij'}}{d_{ijk}^{mn}} \right)^{\gamma} \exp\left(0.1 \ln(10)\left(\psi_{ijk} - \psi_{ij'k}\right)\right) \tag{5.13}$$

where d is the appropriate distance and ψ is the appropriate shadowing exponent, which is Gaussian with standard deviation σ_ψ dB. To allow comparison with the results for simplified network model, we keep the rectangular grid. We have also kept the assumption of perfect CSI.

In principle, therefore, a BS receives interference from all MSs in the system; conversely, energy from an MS signal is received at all BSs in the system. In practice, path loss causes both effects to be limited approximately to nearby cells, although the pattern of gains is very irregular because of shadowing and MS location in its cell. To distinguish the various effects, we define four sets: the interference set at a BS is the set of user symbols that affect the measurement $\mathbf{y}_{ij}$ (i.e., up to all MSs in the system); the macrodiversity set at a MS is the set of BSs whose measurements are used in the *a priori* update (i.e., up to all BSs in the system); the detection set at a BS is the set of user symbols over which marginalization is performed; and the connection set at a BS (cell) is the set of nearby BSs (cells) to which it has a direct backbone connection, including itself.

If computational resources put a limit on the detection set size, then the residual interference from interference set symbols not in the detection set results in an error rate floor as the SNR Γ becomes large. The fact that the simplified network model exhibited

no such floor resulted from the detection set being equal to the interference set. If computation resources or network delays limit the macrodiversity set size, the asymptotic order of diversity is reduced. If the connection set does not include the BSs hosting the interference set and the macrodiversity set, and no communication is allowed between these BSs, then SNR degradation, loss of diversity and an error floor can all result. This *unmodelled interference* has been ignored in the simulations of the simplified network model.

For simulation investigations, we restrict the connection set at a BS to the 8 surrounding BSs and the BS itself, for a total of 9. The detection set at a BS consists of the $9K$ MSs in the connection set (so if we use BP, rather than RCBP, the computational burden is $O(2^{9K})$ at each BS). The corresponding factor graph is shown in Figure 5.8. The macrodiversity set of a MS is limited to the 9 BSs in the connection set of the BS in its own cell. The interference set remains all the MSs in the system. Power control is exercised on a MS by the BS in its macrodiversity set that receives its signal with the greatest SNR. Many variations are possible.

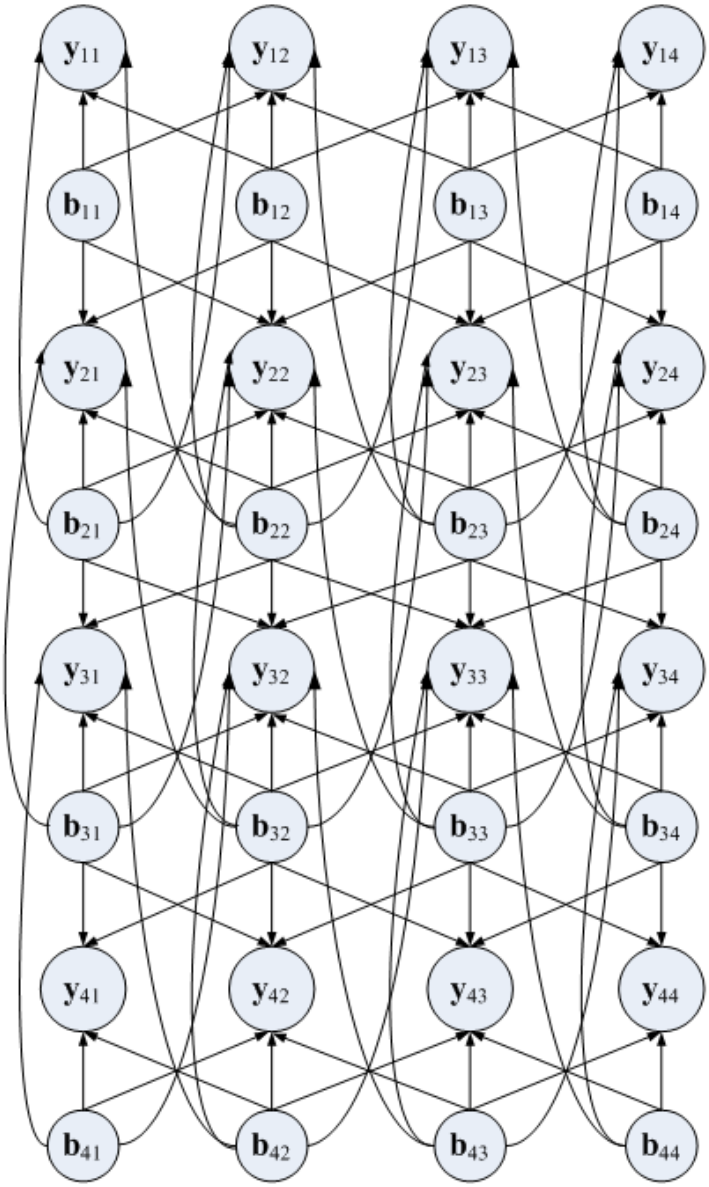

Figure 5.8: Factor graph for wireless network model with detection set confined to nine cells.

Considering all these limitations, we want to see if distributed base station processing is effective in a wireless network model. Figure 5.9 shows the results of our simulations on a 21x21 network with $\gamma = 3.5$ and $\sigma_\psi = 4\,\mathrm{dB}$. The number of BS antennas N_r is either 3 or 4; this is a large number in current practice, but was used in order to bring the performance into the same region as the more benign simplified model of Section 5.4 . There is a single randomly located user ($K = 1$) within each cell. The "Single User, Single BS" reference curve allows a single user in the system, detected without macrodiversity (i.e., microdiversity only) at the BS which exercises power control. This classical result requires no simulation.

A second reference curve ("Single BS Processing") illustrates the same single-user detector without macrodiversity when all MSs in the system are active. The "Single BS-MUD" curves show the effect of MUD at each BS in isolation (no information exchange with other BSs); from the 9-symbol detection set, only the decisions for a user in the same cell are retained. Finally, the remaining curves show cooperative BS processing using RCBP (3,3,3) with a SSD core. We did not employ exact BP, because it would have taken 15 times more computation than RCBP for our choice of simulation parameters.

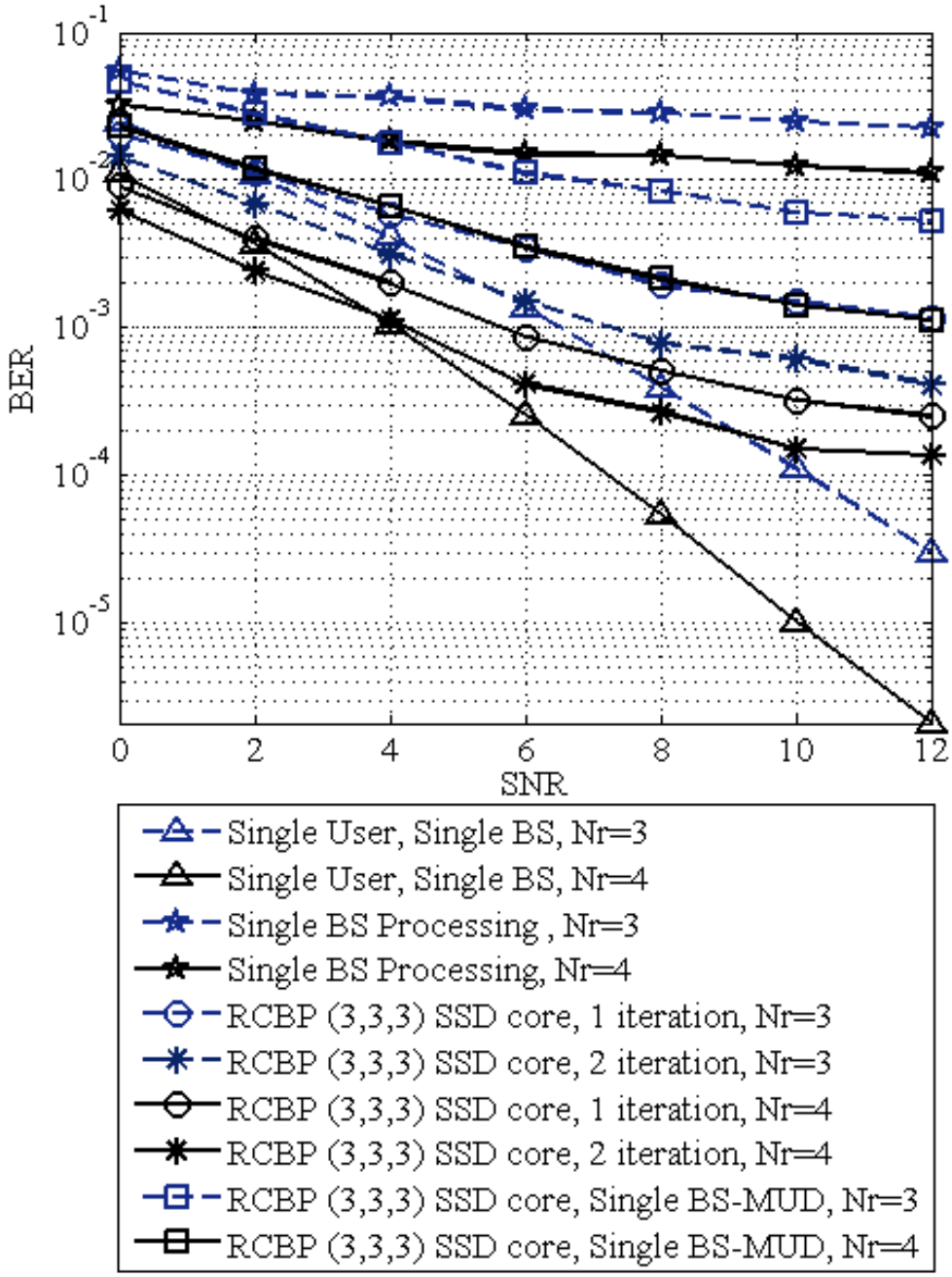

Figure 5.9: BER performance of the central user in 21x21 wireless network with $\gamma = 3.5$ and $\sigma_{\psi} = 4$ dB .

We first note that single-BS processing is ineffective, with a BER floor of 10^{-2} or greater, even for 4 antennas. This is primarily because the signal-to-interference ratio is very poor, on average 1.5 dB with full channel reuse and interference from all cells, and there is no MUD. The value of BS cooperation for system-wide MUD is shown clearly in the RCBP curves. If we allow MUD at BSs, but no inter-BS communication, the BER improves substantially, by an order of magnitude at 10 dB for 4 antennas. A floor remains, due to interferers outside the detection set.

The value of having BSs cooperate is shown in the BER improvement resulting from use of RCBP (3,3,3) with SSD core and two iterations; in the near-floor conditions at 10 dB, cooperation lowers the BER by an order of magnitude for 3 antennas, and almost an order of magnitude for 4 antennas, compared with single-BS MUD. We also see that the CBS approach using RCBP is better in the noise-limited SNR region than single-user performance. This is because the single-user curve does not enjoy the macrodiversity contributed by the exchange of LLRs between cooperating BSs. Little or no improvement in RCBP was observed after 3 iterations.

In Chapter 7, we develop a new power control scheme to reduce the levels of unmodelled interference. We examine through simulations a system with mobile users, hexagonal cells, and iterative detection and decoding and observe the effect of power control strategy on the reduction of co-channel interference and the error floors they create.

5.7 Conclusions

We have explored cooperative BS design for the uplink of multi-cell wireless networks, using local message passing based on BP in order to achieve full frequency reuse. Because the complexity of BP grows exponentially with the number of interfering users at each base station, we developed the RCBP distributed detector that still works well in the generally rank-deficient conditions at BP function nodes. We tested RCBP on both a simplified network model with very limited inter-cell propagation, and on a more realistic wireless network model, that includes system-wide interference, path loss, shadowing and power control.

In the simplified model, we found that RCBP provides the same error rate as exact BP over most of the useful BER range at a fraction of the computational cost. With approximately 2 dB degradation and four times the computation, RCBP can accommodate a second user in every cell, even with a single BS antenna. We have also observed performance close to the single user limit in the coded system. However, conclusions based on the simplified model, such as the lack of a BER floor, do not necessarily hold up in a more realistically modelled wireless network.

In the more realistic wireless network model, interference patterns are irregular because of path loss, shadowing and power control, and residual interference from users in cells outside the immediate neighbourhood produces a BER floor at high SNR. Nevertheless, the cooperative BS approach, as implemented by RCBP, shows a dramatic improvement compared with multi-user detectors implemented at BSs individually.

CHAPTER 6

BASE STATIONS WITH MULTIUSER MIMO EQUALIZATION

In Chapter 5, we saw that RCBP provides a computationally efficient method of signal detection in a system with cooperative base stations. We also explored the resulting performance in realistic propagation conditions that accounts for interference from cells outside the immediate neighbourhood. That study made the assumption of symbol-synchronous arrivals at all BSs. In a real system, however, user signals arrive asynchronously by symbol and with delay spread. These factors add intersymbol interference (ISI) to the existing MUI, forming multidimensional interference challenge to RCBP.

In this chapter, we extend the RCBP approach to ISI as well as MUI, and demonstrate very good to near-optimal performance via simulations in a variety of scenarios. We mainly concentrate on individual BSs with multiple receive antennas detecting multiple users (with equal average received power) in frequency selective channels. MIMO equalization is an excellent platform for displaying RCBP capability in handling multidimensional interference.

We apply the RCBP algorithm for soft decision equalization in frequency selective MIMO channels. The multipath channel is modelled using a factor graph (FG) where the transmitted and received signals are represented by the function and variable nodes respectively. The edges connecting the function and variable nodes illustrate the dependencies of the multipath channel and soft decisions are developed by exchanging information on these edges iteratively. The computational complexity of this RCBP equalizer grows only linearly with block size and memory length of the channel. The proposed framework has a flexible structure that allows for parallel as well as serial detection. We illustrate through simulations that the RCBP equalizer can even handle overloaded scenarios where the channel matrix is rank deficient, and it can achieve excellent performance by applying iterative equalization in combination with LDPC codes.

Although the primary focus is the organization of computation for combined ISI and MUI, the chapter also presents results for a simplified two-cell CBS system with a realistic propagation model. Extension to large multicell systems with both ISI and MUI, in which the information is exchanged between neighbouring BSs cooperatively, is seen as a fruitful area for future investigation. The contents of this chapter except for Section 6.5 are previously published in [11][*].

6.1 Introduction

MIMO systems promise to increase spectral efficiency far beyond the single-input single-output Shannon limit. In order to achieve this increased capacity, we need to

[*] ©2009 IEEE. Reprinted, with permission, from [11].

develop efficient and reliable receivers for MIMO channels. As we have seen throughout this work, the design can be challenging, especially in frequency selective channels where the transmitted signal has to be detected in the presence of noise, ISI and MUI.

Equalization of frequency-selective MIMO channels is not efficient for most quasi-optimal algorithms, as several papers have shown. The SD equalizer is studied in [6], and a soft decision equalization (SDE) algorithm based on PDA is introduced in [50]. The major drawback of SD and SDE equalizers is their block-detection processing, since the computational complexity of these algorithms grows roughly cubically with the number of symbols in the block. One way to deal with this problem is to use sliding windows to process the blocks of data [51]. This method is not always desirable because the computational complexity grows cubically with the memory size of the channel. Another way is to track the noise and ISI by Kalman filtering [52, 53]. This approach experiences a substantial performance loss because of noise and interference enhancement caused by the zero forcing (ZF) filters used in the structure.

Unlike the block-oriented methods, BP computational complexity grows only linearly with the block size. BP equalization in frequency selective MIMO channels is studied in [54, 55] and is shown to enjoy good performance and flexible structure. Unfortunately, the application of BP equalizers is commonly limited to sparse channels because its computational complexity grows exponentially with the product of number of users and number of paths in the channel. In [56], a complex framework using sliding-windows, group detection methods and MMSE filtering for ISI mitigation reduces the computational complexity of the exact BP algorithm. Inspired by the groupwise IMUD [4] and by updating APPs at each time interval, we introduced a reduced complexity

updating APP (RCUA) algorithm in [12]. The RCUA equalizer is in fact the first iteration of the serial RCBP algorithm described in this chapter.

Here, we introduce a framework based on RCBP for soft decision equalization in frequency selective MIMO channels, both single-user and multi-user. This approach is doubly iterative, with internal IMUD iterations in the function nodes as well as the external BP iterations. The RCBP equalizer enjoys the diversity of frequency dispersive channels, and it inherits the flexible structure of the BP equalizer, allowing for serial or parallel iterations. The computational complexity of RCBP algorithm grows only linearly with the number of channel paths so its application is not limited to sparse channels. We will illustrate through simulations that the RCBP equalizer can even handle overloaded scenarios (rank deficient channels) efficiently. The iterative equalization can easily be combined with decoding of LDPC codes, so that iteration takes place on three levels to provide excellent performance.

6.2 System Model

We consider a discrete-time, baseband equivalent of a MIMO system with N_t transmit and N_r receive antennas. The transmit antennas can belong to one or multiple different users. Each of the $N_t N_r$ links in this system is modelled as a linear FIR dispersive channel with L symbol-spaced taps. The gain of each tap has an independent Gaussian distribution according to the channel's power delay profile. We assume that the receiver has perfect CSI and that the transmitter has no knowledge of the channel. Our proposed framework is not block-oriented and does not require the channel to be constant over a block. However, to simplify the description and simulations, we assume that the

channel is block fading, where the overall channel impulse response is constant in a block of N symbols and changes independently to the next.

Figure 6.1 shows our MIMO system model. The channel impulse response from the j^{th} transmitter to the i^{th} receiver is denoted by $\mathbf{h}^{(ij)}=[h_0^{(ij)} h_1^{(ij)} \ldots h_{L-1}^{(ij)}]$. We assume that all subchannels have equal expected power gain, *i.e.*, $\sum_{l=0}^{L-1} E\left[\left|h_l^{(ij)}\right|^2\right] = \sigma_s^2$. The symbol sent from the j^{th} transmitter, in time interval k is denoted by $b_k^{(j)}$. In this work, we describe the BPSK case, where $b_k^{(j)} = \pm 1$, in order to simplify the formulas. Generalization of the method to an M-ary constellation with $E\left[\left|b_k^{(j)}\right|^2\right]=1$ is straightforward. At the receiver end, the signal is perturbed by independent and identically distributed (i.i.d.) additive complex Gaussian noise. We also suppose that each noise sample $v_k^{(i)}$ is a complex Gaussian random variable with unit variance $\sigma_{vk}^{2(i)}=E\left[\left|v_k^{(i)}\right|^2\right]=1$, and that they are mutually independent. The SNR per bit at each receive antenna is hence equal to $\Gamma = P_s/\sigma_v^2 \log_2(M)$ where M is the constellation size.

The signal at the i^{th} receiver antenna in time interval k can then be expressed as

$$y_k^{(i)} = \sum_{l=0}^{L-1} \sum_{j=1}^{N_t} h_l^{(ij)} b_{k-l}^{(j)} + v_k^{(i)}, \quad i = 1, \ldots, N_r \quad (6.1)$$

Equation (6.1) can be written in vector and matrix form as

$$\begin{aligned}\mathbf{y}_k &= \sum_{l=0}^{L-1}\sum_{j=1}^{N_t} \mathbf{h}_{k,l,j}\, b_{k-l,j} + \mathbf{v}_k \\ &= \sum_{l=0}^{L-1} \mathbf{H}_l \mathbf{b}_{k-l} + \mathbf{v}_k \\ &= \mathbf{H}\tilde{\mathbf{b}}_k + \mathbf{v}_k ,\end{aligned} \tag{6.2}$$

where $\mathbf{y}_k = [y_{1,k}\ y_{2,k}\ \cdots\ y_{N_r,k}]^T$, $\mathbf{v}_k = [v_{1,k}\ v_{2,k}\ \cdots\ v_{N_r,k}]^T$, $\mathbf{b}_k = [b_{1,k}\ b_{2,k}\ \cdots\ b_{N_t,k}]^T$, $\mathbf{h}_{l,k} = [h_{1,1,k}\ h_{2,1,k}\ \cdots\ h_{N_r,1,k}\ h_{1,2,k}\ \cdots\ h_{N_r,N_t,k}]^T$ and $\mathbf{H}_l = [\mathbf{h}_{l,1}\ \mathbf{h}_{l,2}\ \cdots\ \mathbf{h}_{l,N_t}]$, $\mathbf{H} = [\mathbf{H}_0\ \mathbf{H}_1\ \cdots\ \mathbf{H}_{L-1}]$, $\tilde{\mathbf{b}}_k = [\mathbf{b}_k^T\ \mathbf{b}_{k-1}^T\ \cdots\ \mathbf{b}_{k-L+1}^T]^T$. From the above equations we can observe that each length-N_r received vector, $\mathbf{y}_k$, contains information about the NL_t different symbols that affect it. It is extremely challenging to handle such a high level of interference without massive performance loss or impractical exponential complexity.

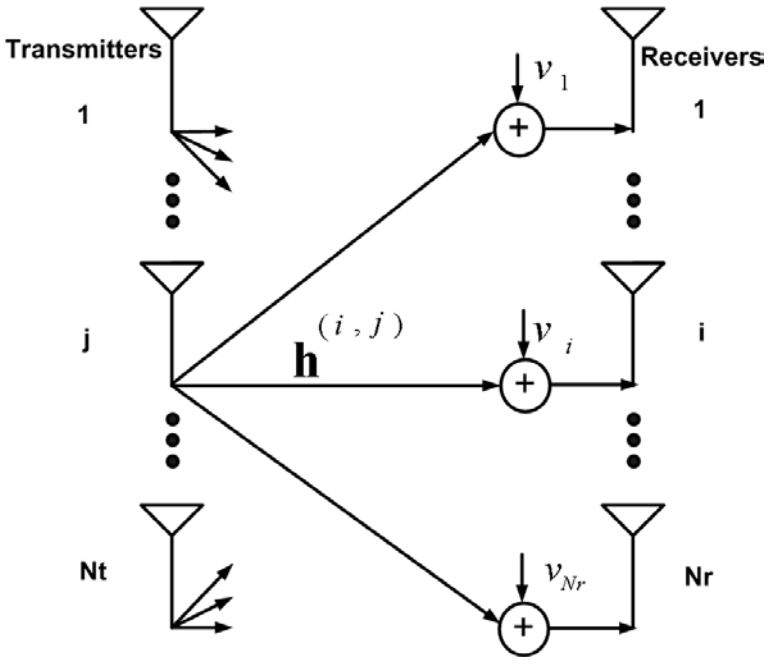

Figure 6.1: MIMO channel model.

6.3 RCBP Equalizer

Figure 6.2 shows the FG of a frequency selective MIMO channel with $L=3$. The received vectors $\mathbf{y}_k$ are the function nodes shown in the squares and the transmitted vectors $\mathbf{b}_k$ are the variable nodes shown in the circles. The edges connecting the function and variable nodes illustrate the dependencies of the multipath channel. Messages go back and forth on these edges iteratively in order to improve the *a posteriori* probabilities (APPs) of the symbols.

Each function node is an independent processing unit that receives the *a priori* probabilities (apPs) of the interfering symbols from all variable nodes to which it is connected. It then computes the APPs of the symbols and sends the extrinsic information back to the variable nodes where the new apPs are calculated. The message sent from function node $\mathbf{y}_k$ to variable node $b_i^{(j)}$, $i=k-L+1,\ldots,k+L-1$ and $j=1,\ldots,M$ is denoted by $M_{\mathbf{y}_k \to b_i^{(j)}}$ and calculated as

$$M_{\mathbf{y}_k \to b_i^{(j)}} = \underbrace{\log \frac{p(b_i^{(j)}=+1)}{p(b_i^{(j)}=-1)}}_{\text{a priori information}} \underbrace{\qquad\qquad}_{\text{extrinsic information}}$$
$$= \underbrace{\log \frac{p(\mathbf{y}_k \mid b_i^{(j)}=+1)}{p(\mathbf{y}_k \mid b_i^{(j)}=-1)}}_{\text{extrinsic information}} \tag{6.3}$$

In the same manner, $M_{b_i^{(j)} \to \mathbf{y}_k}$ is the information sent from variable node $b_i^{(j)}$ to the function node $\mathbf{y}_k$ for updating APPs. It is equal to the sum of the extrinsic information coming to the variable node from all function nodes but $\mathbf{y}_k$, plus the information from other sources, such as a decoder, as shown by

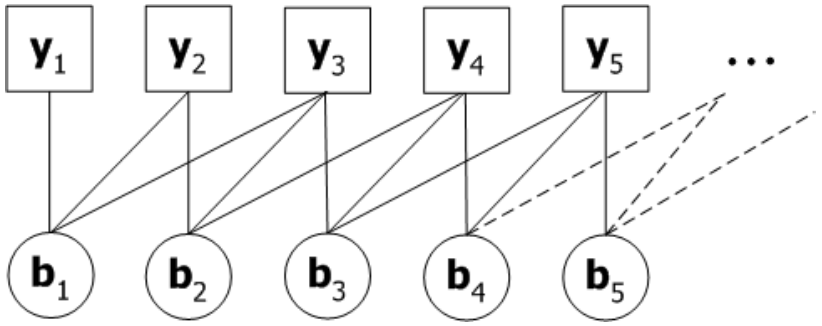

Figure 6.2: Factor graph of a frequency selective channel $L=3$.

$$M_{b_i^{(j)}\to \mathbf{y}_k} = \underbrace{\log \frac{p(b_i^{(j)}=+)}{p(b_i^{(j)}=-)}}_{\text{a priori information}} = \underbrace{+\sum_{\substack{l=1\\ l\neq k}}^{L-1} M_{\mathbf{y}_l \to b_i^{(j)}}}_{\text{a priori information from other sources}} \tag{6.4}$$

The processing units of the function nodes compute the above messages conventionally by joint marginalization of the probabilities over all the possible outcomes, as in

$$p(b_i^{(j)}=\pm) = \sum_{\substack{\text{all } \tilde{\mathbf{b}}_k \\ b_i^{(j)}=+1}} \frac{p(\mathbf{y}_k \mid \tilde{\mathbf{b}}_k)\, p(\tilde{\mathbf{b}}_k)}{p(b_i^{(j)}=\pm)} \tag{6.5}$$

The computational complexity of this OJM grows exponentially with NL which is no better than the optimal trellis-based methods like VA and BCJR algorithm in dense channels.

As we discussed in Chapter 4, the BP algorithm, however, has many other advantages over the optimal trellis-based algorithms. It is very popular in sparse channels because its computational complexity depends on the number of non-zero paths,

not the memory length of the channel. The BP equalizer is also very flexible because of its distributed structure and it allows for parallel as well as serial processing. The messaging schedule and number of iterations can be changed adaptively for the special requirements of a situation; for example, by the priority of a user or channel variations. The SISO structure of BP also facilitates high performance iterative joint detection and decoding. The RCBP equalizer makes it practical to enjoy these qualities at lower computational cost.

We adapt the IMUD grouping strategy according to the structure of the MIMO equalization problem to form the RCBP equalizer. As mentioned in Chapter 4, the original IMUD algorithm groups the users according to the EVM method in the first iteration and random selection in the second iteration. Here, we suggest a temporal grouping and ordering strategy for IMUD that is based on the natural structure of the frequency selective MIMO channels. In simulations not shown here, we observed that the proposed algorithm outperforms random or EVM grouping methods in the RCBP equalizer.

The $N_t L$ interfering symbols in the function node k, $\tilde{\mathbf{b}}_k = [\,]^T_{k-L+1} \cdots {}^T$ are divided into L groups $G_{t,k}(j) = \mathbf{b}_{\quad+1}$, $t = 1 \ldots$, of the N_t symbols comprising $\mathbf{b}_{k-1}$. Figure 6.3 shows the structure of a function node in the RCBP equalizer. The received signal y_k and messages from the dependent variable nodes $M_{b_t^{(j)} \to y_k}$ are the inputs of function node k. The first step is soft interference cancellation. Using the apPs, we can calculate the mean and variance of each symbol. For illustrative purposes, we assume binary transmission so that

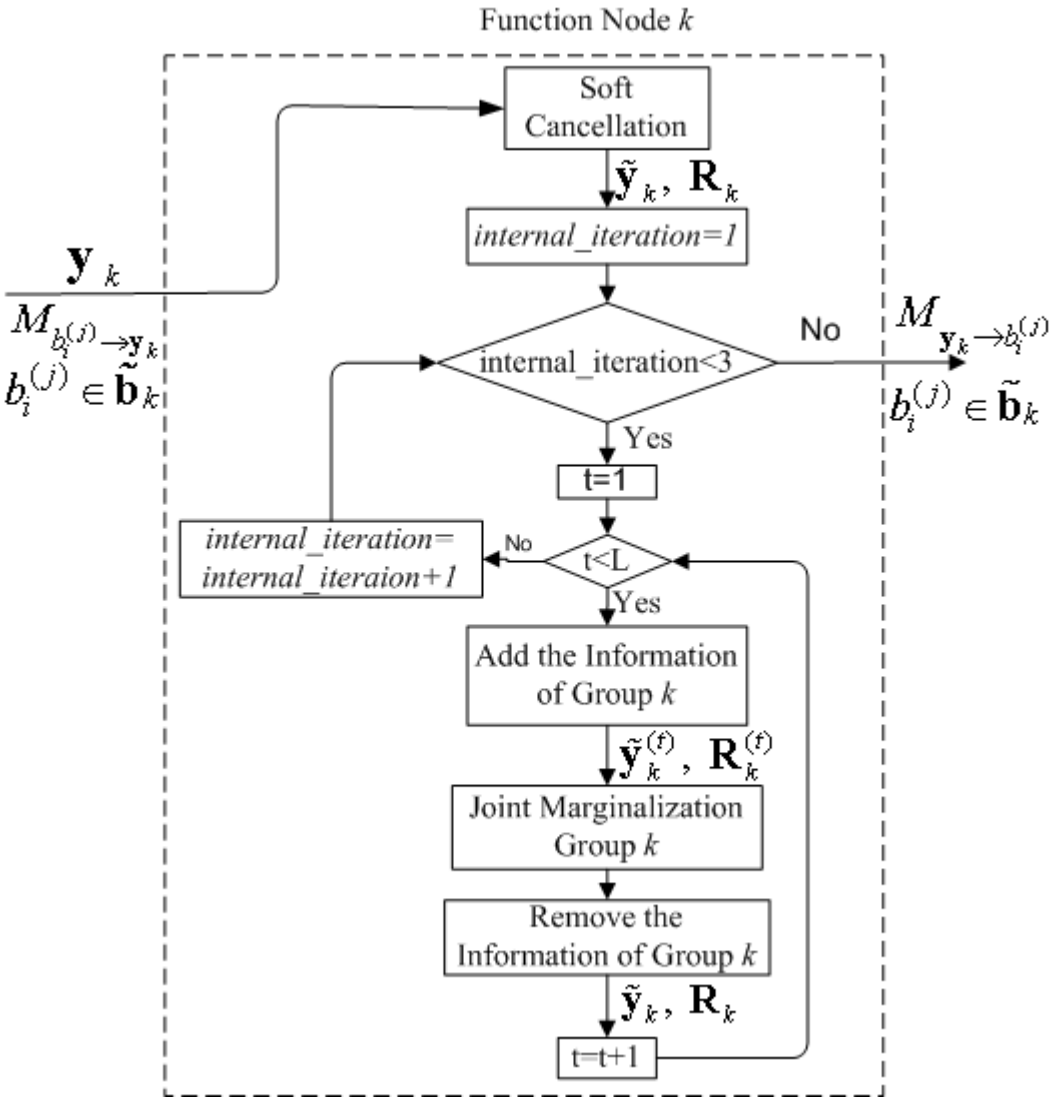

Figure 6.3: A function node of RCBP equalizer.

$$\mu_{iiii}^{(0)(0)(0)} = \Pr(1)\Pr(1)2\Pr(1)1, \tag{6.6}$$

$$\sigma_{iii}^{(0)2(0)(0)} = 4\Pr(1)(1\Pr(1)). \tag{6.7}$$

What we know about $b_i^{(0)j}$ is $\mu_i^{(0)j}$, and $\sigma_i^{(0)2}$ shows the amount of uncertainty. For soft cancellation of the effects of this symbol on the measurements, we should subtract the mean and add the variance to the covariance of noise. In other words, we adopt Gaussian forcing and suppose that what we do not know about $b_i^{(0)j}$ is a complex, zero mean Gaussian random noise with variance $\sigma_i^{(0)2}$, independent from all other symbols. The equations below show $\tilde{y}_k$ and the covariance matrix $\mathbf{R}_k$, the results of soft interference cancellation of all the symbols.

$$\tilde{y}_{kkkl} = - \sum_{lj=01}^{L-1} \sum^{N_t} {}^{(0)(0)}\mu_{-} \tag{6.8}$$

$$\mathbf{R}_{hhkkkl} = \sum_{lj=01}^{L-1} \sum^{N_t} {}^{(0)(0)}\sigma^{2(0)2}\sigma_{-} \tag{6.9}$$

Introducing these intermediate variables reduces the number of computations needed at each IMUD step. To detect $G_t()x$, we first restore the soft information about the symbols of this group alone, by

$$\tilde{y}_{kkkl}^{(0)(0)} = + = \sum_{j=1}^{N_t} \mu_{+1} \quad ,1....tL \tag{6.10}$$

$$\tilde{y}_{kkkk}^{(0)(0)(0)} = \sum_{j=1}^{N_t} b_{+1} + \quad . \tag{6.11}$$

$$\mathbf{R}_{k}^{(0)} \left(\quad \right) \quad \sum_{j=1}^{N_t} \quad \sigma \quad 1 \tag{6.12}$$

where $\mathbf{n}_k^{(0)}$ is approximated by a vector of zero mean Gaussian random variable with covariance $\mathbf{R}_k^{(0)}$. We then feed $\tilde{\mathbf{y}}_k^{(0)}$, $\mathbf{R}_k^{(0)}$ and apPs of the symbols in $G_1(k)$ to a joint marginalizer, and use the resulting LLRs to update $\tilde{\mathbf{y}}_k$ and $\mathbf{R}_k$ as we see in Figure 6.3.

Symbols in $G_1(k)$ are the most recent symbols, so in serial detection we have the least *a priori* information about them. The best strategy is to start the detection from this group because we have apPs of all other groups and can cancel them. Next, we detect the other groups in ascending order. After detecting all the groups, we go back to $G_1(k)$ and start the process again. LLRs typically converge in two or three iterations. We chose only two internal IMUD iterations in the RCBP equalizer. As throughout our simulations, we observed that more internal iterations bring about little performance improvement.

As we discussed in Chapter 4, the OJM in IMUD can be replaced with near optimal, low complexity algorithms like the SSD or PDA. The computational complexity order of the basic BP equalizer is $O(2)^{NL}$. The RCBP algorithm reduces the computational order to $O(2)^{N_t}$ by replacing the optimal detector at each function node with a OJM-cored IMUD algorithm. The computations are further reduced by using SSD or PDA in place of OJM in the IMUD core. In the case of the PDA-cored IMUD, the complexity order is $O(N)LN_t^3$, but for SSD-cored IMUD, it is $O(2)^{\alpha N_t}$. If the SNR is high enough and the system is not overloaded, then the exponent α is small enough and $2^{\alpha N_t}$

can be approximated by $p(N_t)$, a polynomial function of N_t that is of degree 4 or less [27].

6.4 Performance and Variations

In this section, we evaluate the performance and variations of RCBP equalizer through simulations. For our simulations, we have assumed a frequency selective MIMO channel as described in Section 6.2 . Unless otherwise specified, we have used an exponential power delay profile with constant decay exponent of -1 per symbol, and $L=3$: $[0.6652 \; 0.2447 \; 0.09]$. Exponential power delay profile is generally believed to be a realistic model for frequency selective fading channel. We mostly use serial detection, where function nodes are processed in a serial forward or backward direction one at a time. In our simulations, the first iteration of the serial BP or RCBP is a forward pass through the whole block of data, then the second iteration is in the backward direction and the third iteration is another forward pass. In 6.4.3 , we compare the performance of serial RCBP with parallel RCBP where the functions nodes are processed in parallel all at the same time.

6.4.1 Performance

We expect the RCBP equalizer to experience some performance loss compared to the basic BP because its IMUD core is suboptimal. It is essential to determine how significant this performance loss is. We compare the performance of RCBP algorithm with the basic BP, as well as with the optimal BCJR and with MMSE-DFE in random delay spread channels. The system has $N_t=2$, $N_r=2$, $L=3$ and we have used the block length $N=10$. Here, we used a short block length only to facilitate comparisons

with block oriented detectors that are limited to small block lengths because of their computational load. In simulations not shown here, we observed that the block length does not affect the BER performance of the RCBP equalizer and the process time grows only linearly with the increasing block length.

In Figure 6.4, we have assumed that all the delay taps have equal power, but in Figure 6.5, we have used an exponential power delay profile. With a forward then a backward iteration, basic BP performance is very close to the optimal BCJR performance. More iterations did not show any significant performance improvement (not shown in these figures). Yet, for the RCBP, an additional forward iteration gave a small improvement in performance in the case of equal power delay profile. As we see in both figures, RCBP offers massive improvements compared to MMSE-DFE and at $SNR = 10$ dB, it is only 1.5 dB worse than the basic BP in the case of equal power delay profile and only 0.6 dB worse in the more realistic exponential power delay profile.

6.4.2 Flexibility

One of the strong qualities of the RCBP algorithm is that it is flexible under different load conditions. Both Figure 6.4 and Figure 6.5 showed its performance in a critically loaded system, where $N_r = N_t$. Figure 6.6 shows the performance of the RCBP equalizer in an under-loaded system ($N_r < N_t$) and the challenging overloaded system ($N_r > N_t$). The RCBP performance is almost optimal in under-loaded system. It seems the extra information coming from more antennas helps the algorithm to feed back better estimates and improve the performance. In the overloaded case, we experience a few dB in performance loss because of the increased interference. The overloaded situation is

generally the hardest to handle in all other reported suboptimal methods. RCBP experiences some performance loss in this situation but it does not fail as MMSE-DFE and its computational complexity does not increase exponentially like SD algorithm. Because of this flexibility in handling variable load conditions, the RCBP algorithm is a good choice in cellular system uplink where the number of users can change randomly.

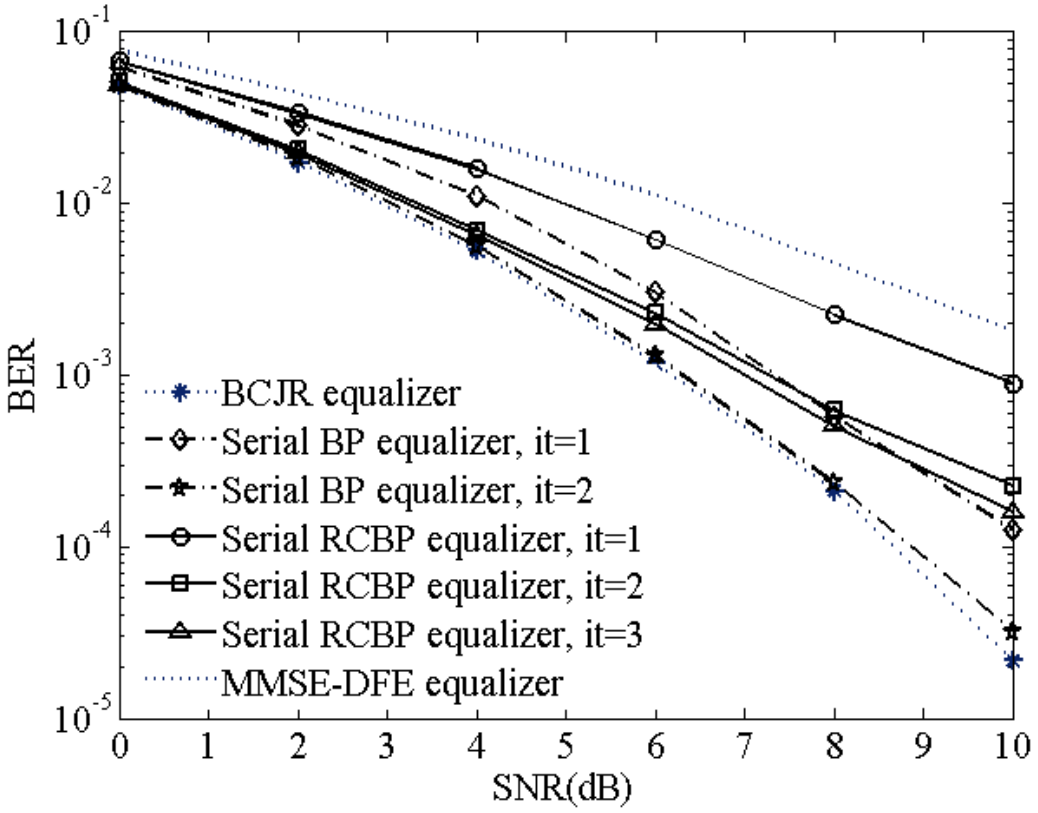

Figure 6.4: RCBP performance comparison, $N_0 = 2$, $L = 3$, $N = 10$, and uniform power delay profile.

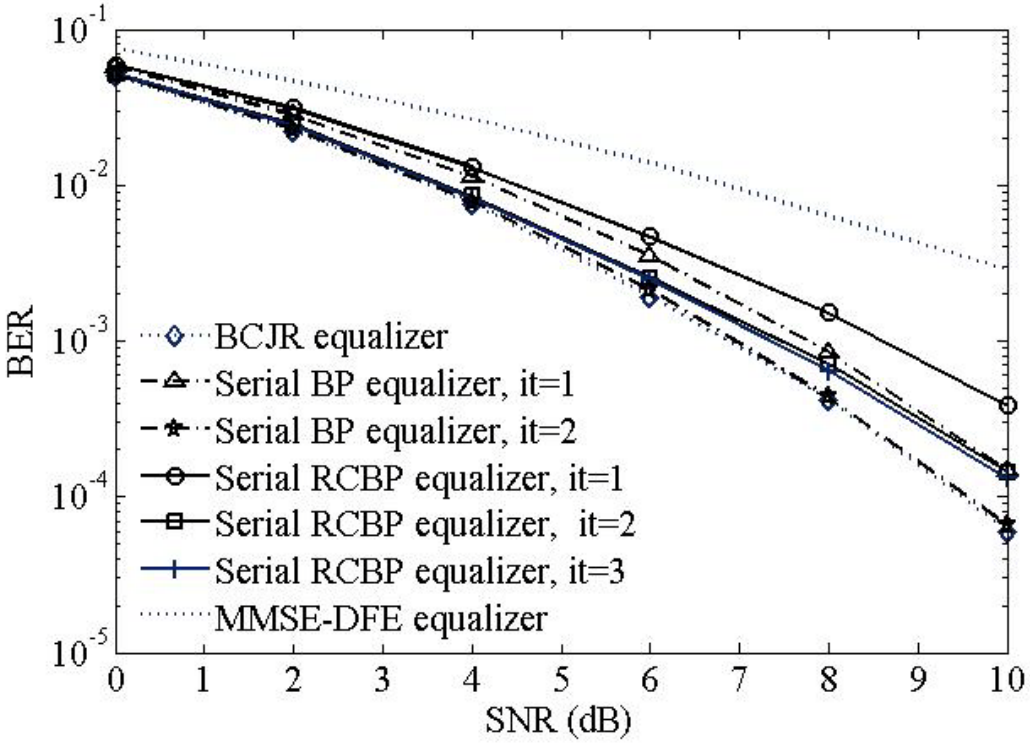

Figure 6.5: RCBP performance comparison, $N_f = 2$, $L = 3$, $N = 10$, and exponential power delay profile.

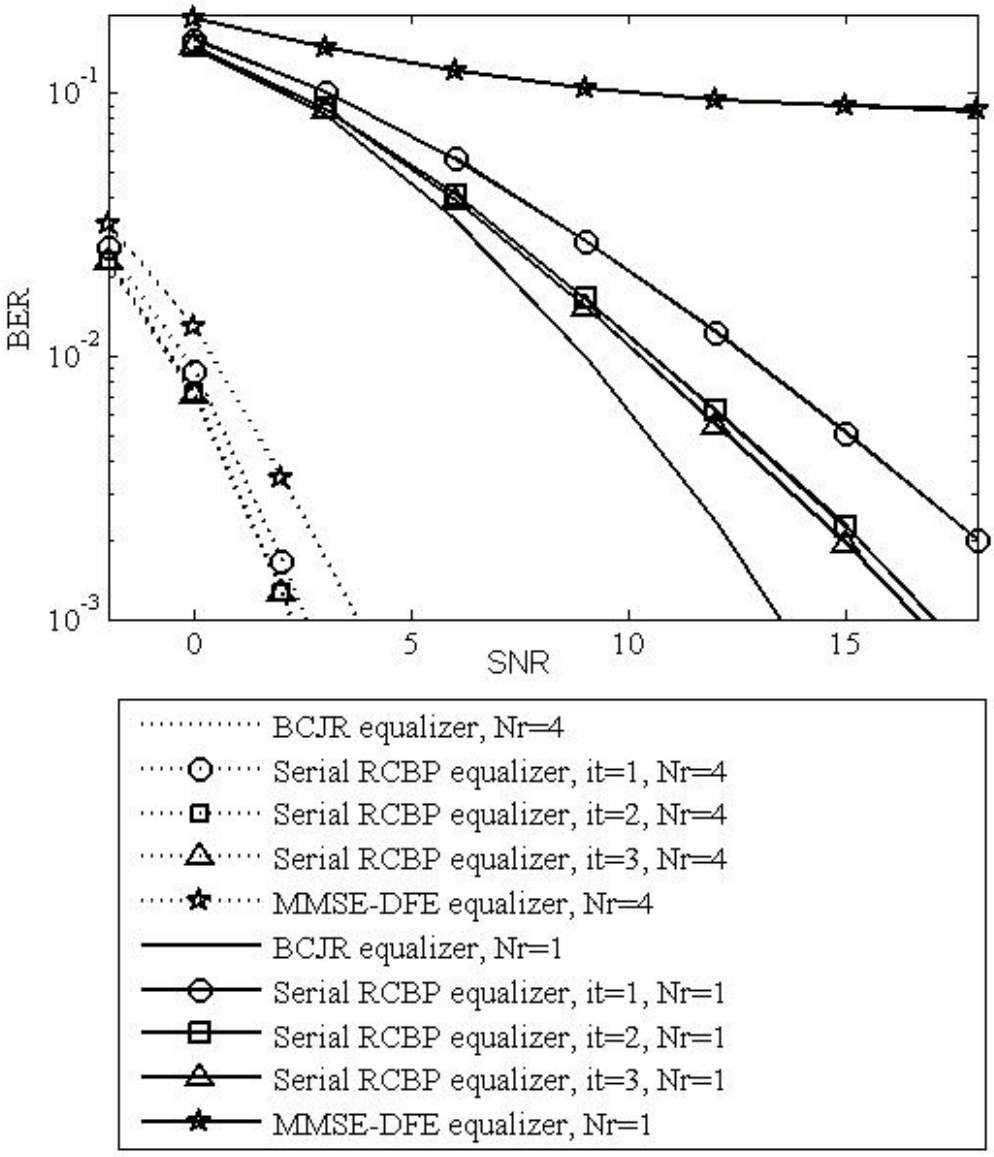

Figure 6.6: RCBP flexibility comparison, $N_t = 2$, $L = 3$, $N = 10$, and exponential power delay profile

6.4.3 Serial or Parallel Iteration

As we discussed in Chapter 4, the RCBP algorithm inherits the BP's flexibility in pattern and schedule of information flow. Depending on our needs, data processing in function and variable nodes can be parallel (at the same time) or serial (in succession), and in the case of serial processing, it can be in the forward or backward direction through the data block. Figure 6.7 compares the performance of the serial and parallel RCBP iterations. It is clear that with a few more iterations, parallel processing performance curve is very close to that of serial processing. Parallel structure is advantageous in hardware implementation of high speed iterative decoding, especially when LDPC codes, are used because they are usually decoded using the BP algorithm that has the same high-level structure as the RCBP.

6.4.4 Choice of Core Decoder

As we explained earlier, the RCBP equalizer has the choice of using different SISO detectors at its core. Figure 6.8 compares the performance of RCBP-OJM, RCBP-SSD and RCBP-PDA. We have used the algorithm proposed in [57] to implement a reduced complexity SSD for our simulations. A PDA-based RCBP algorithm offers the lowest computational complexity but suffers from the worst performance loss. This poor performance can be explained by the weakness of SISO-PDA algorithm in occasionally converging to non-optimal solutions [49]. SD, on the other hand, always finds the optimal hard solution. However, calculating the APPs in soft SD involves marginalizing the probabilities on the points in a sphere, so the results might be different from exact APPs.

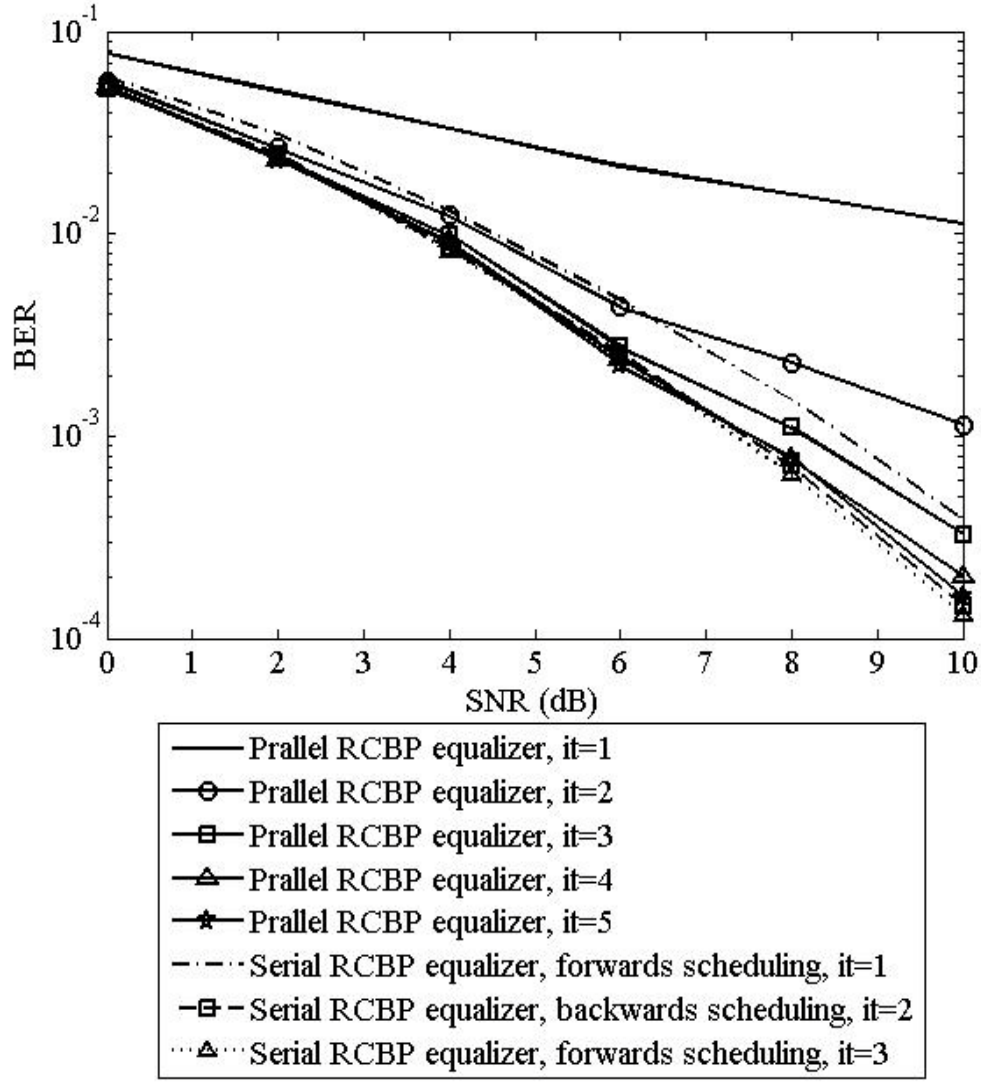

Figure 6.7: Parallel vs. serial RCBP $N_u = 2$, $L = 3$, $N = 10$, and exponential power delay profile.

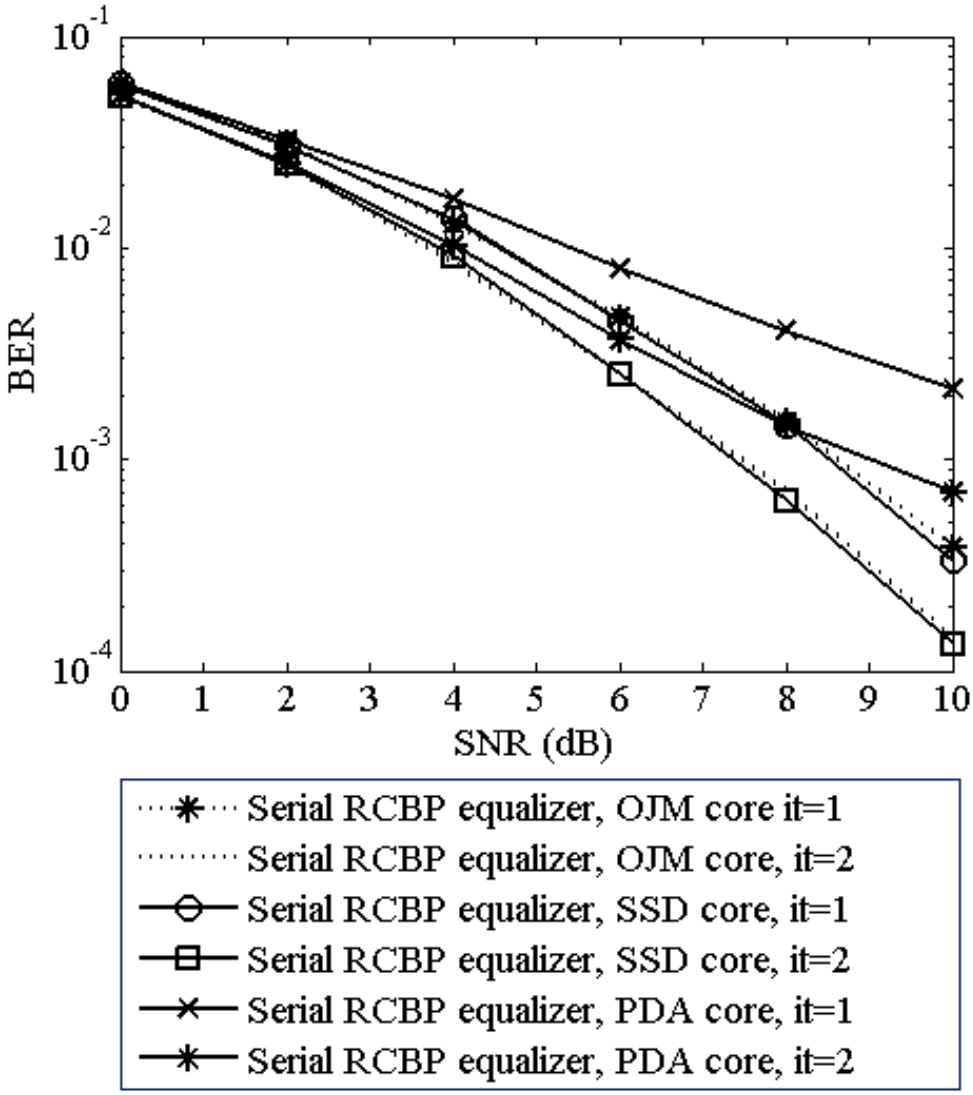

Figure 6.8: The effect of different SISO detection on the RCBP performance, $N_t = N_r = 2$, $L = 3$, $N = 10$, and exponential power delay profile.

6.4.5 Iterative Equalization and Decoding

In this section, we investigate via simulations the performance of joint equalization and decoding of LDPC codes. We use the standard iterative equalization and decoding method illustrated in Figure 6.9. The information bits are coded at the transmitter, and then they pass through the frequency selective MIMO channel. The received signal is first processed by the equalizer followed by a few iterations of the LDPC decoder. This whole process can repeat for improved performance.

Figure 6.10 shows the performance of such an iterative equalization and decoding system. We have used randomly generated LDPC codes with rate $R_c = 1/2$, length $(M,N) = (256,512)$, and $(w_c,w_r) = (3,6)$ where M is the number of parity checks, N is the block length, w_c and w_r are the number of ones per column and rows of parity check matrix respectively. As in other graphs, the horizontal axis is the SNR of information bits at each antenna; i.e. it is the SNR of coded bits divided by the code rate R_c .

We have applied a serial iteration of RCBP equalizer with two internal IMUD iterations or the optimal BCJR equalizer followed by 5 internal iterations of the BP decoder. We see the performance of BCJR and RCBP equalizers by themselves, after 1 joint iteration, and after 2 joint iterations. It is observed that after 2 joint iterations, the RCBP equalizer is less than 1 dB away from the optimal BCJR equalizer. This is a great performance improvement compared to the equalizer output and it is much closer to the optimal BCJR equalization and decoding, than the results observed for Kalman equalizer in [53].

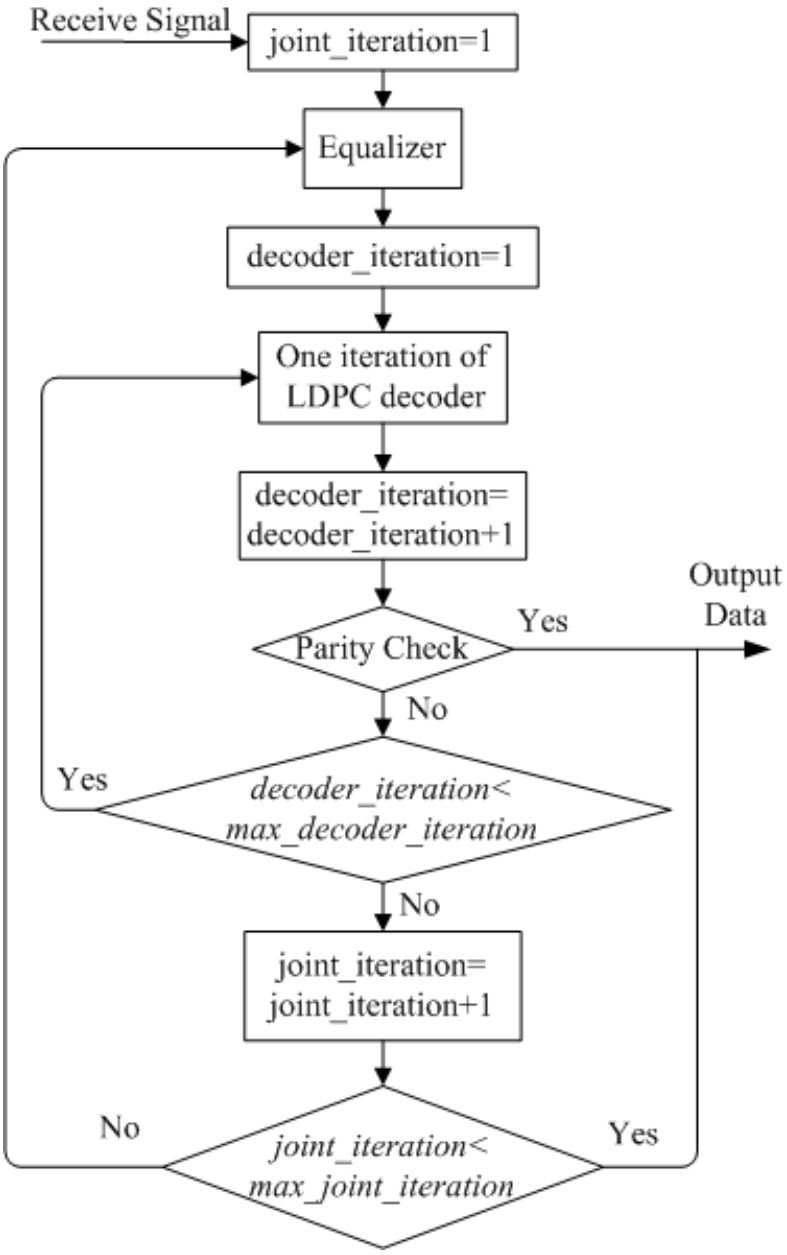

Figure 6.9: Iterative joint detection and decoding.

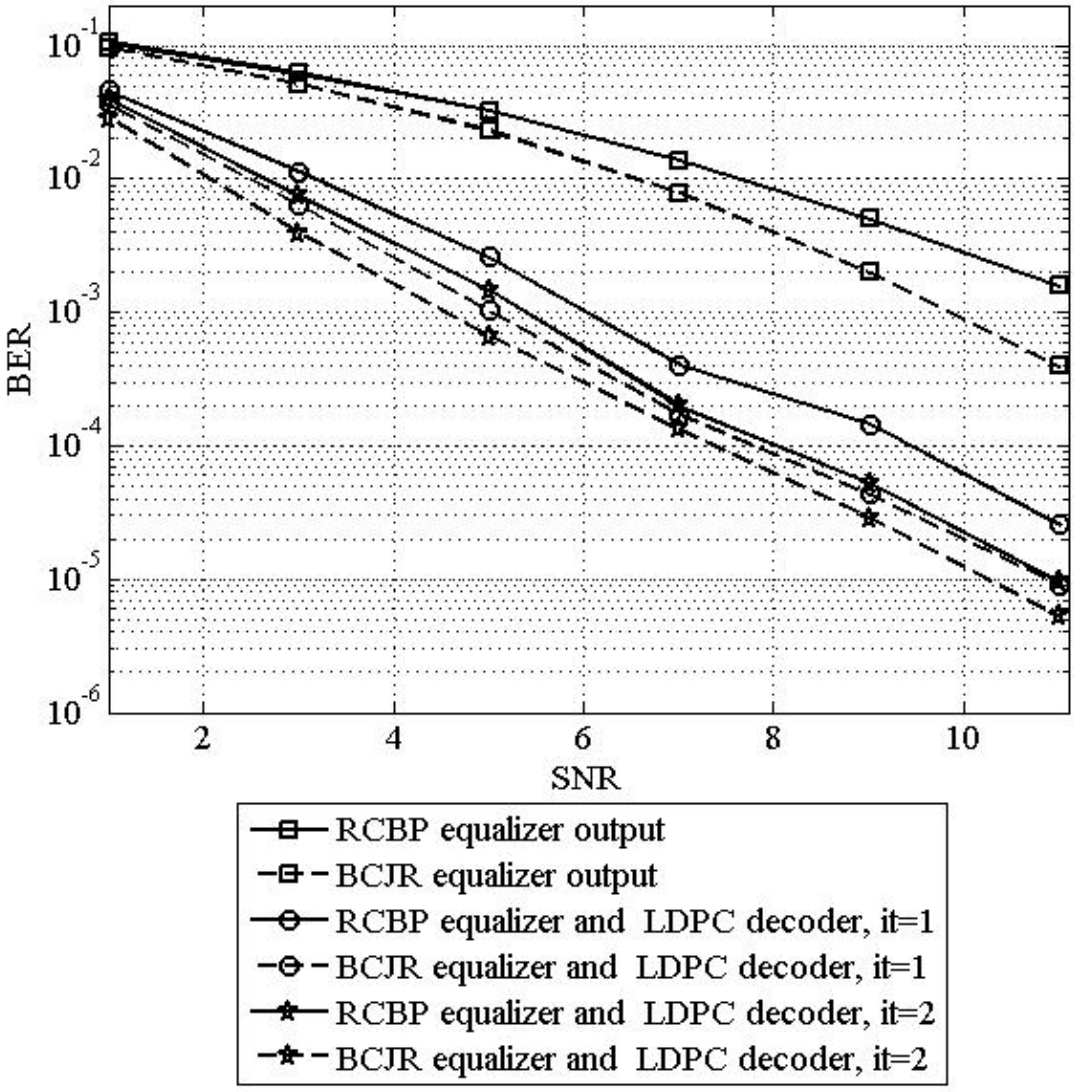

Figure 6.10: Iterative joint equalization and decoding performance, LDPC code $(N=256, M=512)$, $(w_c, w_r) = (3, 6)$, $N_u = 2$, $L = 3$, $N = 10$, and exponential power delay profile.

Here, we have considered a simple scenario where we have coded a single data stream, and divided it to N_t substreams to be transmitted. This approach is not practical in multiuser situations. It is fruitful to study and explore the coding options in multiuser scenarios, especially when the received powers are different opening up the potential for adaptive coding schemes for different users. A benefit of using LDPC codes is that we can exit the iterative process once the parity-check matrix is satisfied. It is interesting to consider and characterise the potential computational saving achieved by taking advantage of this property, especially in high SNRs.

6.5 Distributed Iterative RCBP Equalization and Cooperation

So far, in this chapter, we have primarily focused on RCBP equalization in a single BS. Here, we present the results for iterative equalization and cooperation in a simplified two-cell CBS system. Extension of RCBP equalization and information exchange between neighbouring BSs to large multicell systems with ISI and MUI is conceptually straightforward. Exploring different schemes for practical implementation of distributed iterative RCBP equalization and cooperation in multicell systems with random mobility and realistic channel model is seen as a fruitful area for future investigation.

We consider a simple one-dimensional cellular system such as a highway with two BSs, depicted in Figure 6.11. We assume there is a randomly located MS in each cell. We consider path loss and multipath frequency selective fading in this investigation. We ignore shadowing so that the BS of the cell in which a MS is located, always receives its signal power stronger than the other BS. Γ_{ij} and d_{ij} denote the received SNR per

antenna and the distance from MS i to BS j, respectively. Consequently, the closest BS always controls a MS's received SNR.

$$\Gamma_{11} = \Gamma_{22} = \Gamma \quad , \tag{6.13}$$

$$\Gamma_{ij} \neq \Gamma \left(\frac{d_{ii}}{d_{ij}} \right)^{\gamma} , i \neq j \tag{6.14}$$

We assume BPSK uncoded signals, $N_r = 2$ antennas at each BS, path loss exponent $\gamma = 3.5$, and all the wireless links to be frequency selective fading channels with memory length $L = 3$: $[0.6652 \quad 0.2447 \quad 0.0901]$. Though not accurate, this simple model provides insight into the process and performance of iterative equalization and cooperation in cellular system.

Both BSs receive and detect the signals from both MSs. The detection process includes iterative distributed equalization and cooperative information exchange between the BSs. The distributed equalization follows the same routine as the RCBP MIMO equalization with $N_t = 2$ that we have discussed in detail in previous sections. The only difference is that the received SNR per antenna is not the same for different users.

Each iteration in this scheme consists of two steps. The first step is the individual equalization at each BS. The second step is sharing the extrinsic information through BS cooperation. Figure 6.12 compares the performance of iterative equalization and BS cooperation with the performance of a global optimal equalizer using BCJR algorithm in this system. We observe that after only 2 iterations the iterative scheme is less than 0.8 dB away from optimal results at $BER = 10^{-3}$.

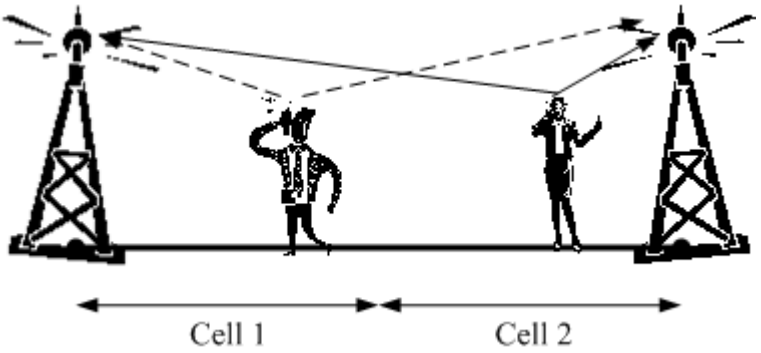

Figure 6.11: Simplified two-cell model.

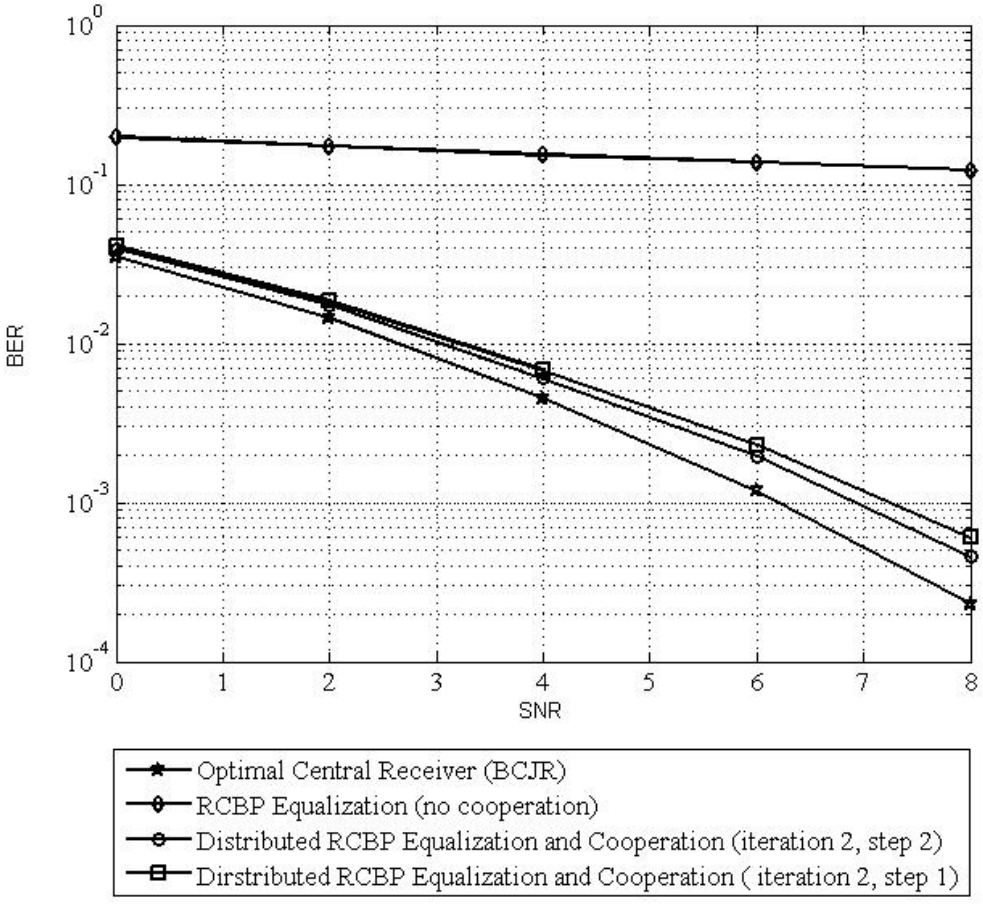

Figure 6.12: BER performance of iterative RCBP equalization and cooperation.

6.6 Conclusions

Based on BP principles, we introduced a new, symbol-by-symbol, SISO RCBP equalizer. Because of the symbol-by-symbol detection process, RCBP computational complexity is linear in the number of symbols, so it is able to process long or infinite streams of data, in contrast to block-oriented SD and PDA. Its soft output makes it suitable for iterative turbo equalization systems. We achieved excellent performance by iterative RCBP equalization and decoding of LDPC codes. Our investigation highlights the characteristics and flexibility of the RCBP algorithm to deal with high levels of multidimensional interference in future wireless communication systems.

CHAPTER 7

POWER CONTROL IN CBS SYSTEMS

In Chapter 5, we saw that CBS processing can all but eliminate the effects of mutual interference among users in neighboring cells. However, the unmodelled interference from users in more distant cells remains as a disturbing effect and places a floor on the error probability even at very large SNR values. We now turn our attention to the problem of lowering that floor. In this chapter, we introduce a novel power control strategy based on the total received power to reduce unmodelled interference in the uplink of CBS systems.

Power control via channel inversion maintains constant received signal power at the controlling BS, regardless of the position of the MS and it is common practice in the uplink of cellular systems. As we have seen throughout this thesis, unlike the conventional cellular system, CBSs share information in detecting the MSs, in effect converting the signal energy seen as interference in one cell, into a macrodiversity benefit for the originating user. We therefore propose a power control approach based on sustaining the *total* received power in CBSs. We investigate the performance of this

method through simulations and show that it has the ability to reduce the intercell interference in the CBS systems, save power or improve the BER performance in both coded and uncoded scenarios. The contents of this Chapter also appear in [13][*].

7.1 Introduction

As we discussed earlier, the traditional method to reduce intercell interference is further separating co-channel users in space or through spreading, at the cost of losing capacity. Another approach is using directional antennas in the system to reduce the number of interfering transmissions a BS receives. Power control policy is an important aspect of wireless system design and is vital in controlling the co-channel interference. Downlink power control is less influential than uplink in reducing the interference levels since downlink signals all originate from the centrally located BSs, whereas uplink signals come from MSs roaming randomly throughout the cells. In this work, therefore, we focus on a more efficient power control strategy for the uplink of a CBS system.

The power control strategy used in Section 5.6 and Section 6.5 , is based on maintaining a constant received power at the antennas of a controlling BS. Therefore the transmit power in this scheme changes according to the inverse channel gain. This channel inversion strategy is the conventional method used in the uplink of cellular systems. It ensures the same SNR for all the users regardless of their position within the cell and eliminating the near-far effect in CDMA systems. However, as we see in Figure 7.1, in this system, the boundary users transmit at very high power and have an adverse effect on intercell interference levels throughout the system. As we mentioned in Section

[*] ©2009 IEEE. Reprinted, with permission, from [13].

3.3 , *soft handoff* in CDMA systems is designed to improve the quality of service for these boundary users through selection diversity. Yet, in order to ensure that power received in the controlling BS remains constant, soft handoff does not reduce the transmit power and is not a solution for intercell interference.

Power control strategies found in linear multiuser detection structures where large and balanced signal to interference plus noise ratio (SINR) is the goal [58, 59] are not very effective, as it is not guaranteed that feasible power allocations can be found in cellular systems. Therefore, the distributed iterative algorithms based on these principles may result in all the users transmitting at their maximum power, yet failing to reach their SINR requirement [15].

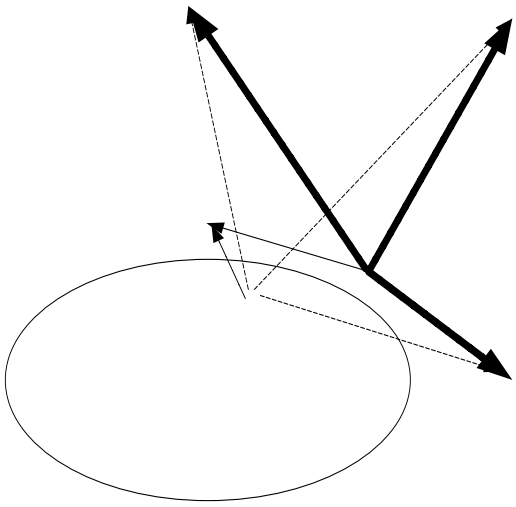

Because of the advanced MUD techniques applied in CBS systems, performance is largely determined by the total power contributed by macrodiversity combination. An efficient power control policy for CBSs uplink has to take advantage of this quality in order to reduce intercell interference. Here, we propose that the sum of powers received from a given user at all cooperating BSs is considered in power control, rather than the received power only at the controlling BS. We investigate this new method and illustrate through simulations that it leads to a significant reduction in intercell interference and saves power in MS, resulting in longer battery life. We also show that the BER performance improves both in coded and uncoded scenarios.

7.2 System Model

For this investigation, we assume a hexagonally shaped cellular system with N_e cells on the edge as we see in Figure 7.2 and d is the distance between neighbouring cell centers. N_{BS} denotes the number of hexagonal cells in this system. Each BS is in the center of its cell and has N_r omnidirectional antennas. There is one co-channel MS randomly moving in each cell, and each MS has one transmit antenna.

To model the large scale propagation effects, path loss and shadowing, we use the simplified formula from Chapter 2.

$$P_{rt}^{ikj} = K_{\mathrm{dB}} - 10\log_{10}\frac{d^{ik}}{d_0} + \psi_{\mathrm{dB}}, \qquad (7.1)$$

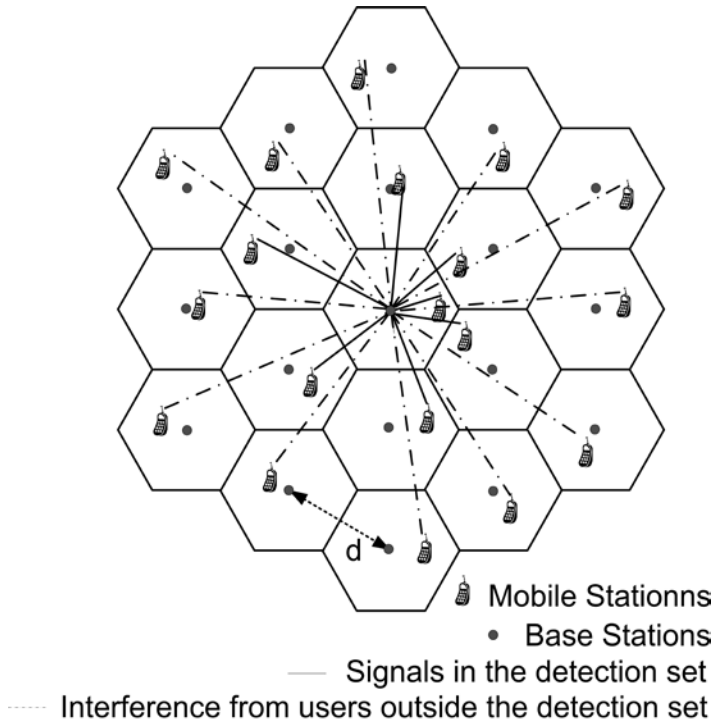

Figure 7.2: Cellular system model.

where P_r^{ik} denotes the received signal from MS i in BS k, P_t^i is the user i transmit power, d^{ik} is the distance between MS i and BS k, γ is the path loss exponent, and ψ_{dB} is a Gaussian random variable with zero mean and variance $\sigma^2_{\psi_{\text{dB}}}$ expressing the shadowing effect. K is the unshadowed path gain at reference distance d_0.

The received signal at BS k at time t, $\mathbf{y}_k^t$ is equal to

$$\mathbf{y}_k^t = \mathbf{h}_{ik}^t b_i^t + \sum_{i=1}^{N_{BS}} \mathbf{h}_{ik}^t b_i^t + \mathbf{n}_k^t, \quad (7.2)$$

where b_i^t is the transmit symbol from user i at time t, $\mathbf{h}_{ik}^t = [h_{i1}^t \; h_{i2}^t \; \ldots \; h_{iN_r}^t]^T$ is $N_r \times 1$ vector of channel gains h_{ijk} from user i to the j^{th} receive antenna of BS k. The

channel gain h_{ijk} illustrates the small scale propagation effect or fading and is a zero mean complex Gaussian random variables with variance P_r^{ik} .

$$P_{rijk}^{ik} h = \left| \right|^2 . \tag{7.3}$$

Although the total power control policy is not limited by the speed of channel variations, in order to simplify the simulation we assume a block-fading channel where the channel gains are constant over a frame of symbols and change randomly in the next frame. This block fading channel model is realistic in high data rate systems and is frequently used in literature. The components of noise vector $\mathbf{v}_{kk}^{ttt}$ are i.i.d. zero mean complex Gaussian random variables with variance σ_v^2 . Without loss of generality we can assume $\sigma_v^2 = 1$. The code rate is denoted by R_c and the SNR of user i in BS k Γ_{ik} , is then equal to

$$\Gamma_{ik} = \frac{P_r^{ik}}{R_c \sigma^2} \quad \frac{}{R_c}. \tag{7.4}$$

At the k^{th} BS, the modelled users are those interferers for which the BS obtains CSI and which it includes in the joint marginalization. As mentioned before, a user causes significant interference primarily in nearby cells, so we define the detection set of BSs that neighbour BS k ,

$$\mathcal{N}_g(k) = \{j : j \text{ and } k \text{ are neighboring cells}\}.$$

Although it is hardly accurate in cellular systems, we assume symbol-synchronous reception for simplicity. In our previous Chapter, we have shown how MUD based on the

RCBP algorithm can handle dispersive channels or asynchronous signal detection. The vector of sufficient statistics at BS k is

$$\mathbf{y}_{k}^{t} = \underbrace{\sum_{i \in \mathcal{N}_g(k)} \sum_{l=1}^{L} \mathbf{h}_{ikl}^{t} b_{il}^{t}}_{\text{Signals in the Detection Set}} + \underbrace{\mathbf{I}_{k}^{t}}_{\text{Unmodeled Interference}} + \mathbf{n}_{k}^{t} = \sum_{i \in \mathcal{N}_g(k)} \mathbf{h}_{ikl}^{t} b_{il}^{t} + \mathbf{I}_{k}^{t} + \mathbf{n}_{k}^{t} \quad . \tag{7.5}$$

The signals from other MSs in non-adjacent cells cause the unmodelled interference.

$$\mathbf{I}_{k}^{t} = \sum_{i \notin \mathcal{N}_g(k)} \mathbf{h}_{ikl}^{t} b_{il}^{t} \quad . \tag{7.6}$$

$\mathbf{I}_k^t$ is the sum of a large number of independent zero mean random variables, so it can be approximated by a Gaussian random variable according to central limit theorem and it is treated like the noise in the detection process. We should note that the term ”unmodelled interference,” as these interfering signals are not modelled in belief propagation factor graph, however, we model this unmodelled interference using the Gaussian assumption. This Gaussian approximation is regarding the interference in BS *k* at time *t*, assuming a static snapshot of the network. In 7.4.1 , however, we consider mobility in the system and model the power of $\mathbf{I}_k^t$ with a lognormal distribution.

Another simplifying assumption is perfect CSI; that is each BS has access to the values of the gain arrays in its detection set though not the gains of unmodelled users. We also assume BPSK modulation $b_l^t = \pm 1$. Table 7.1 lists other parameters used in our simulations.

Table 7.1: Simulation Parameters

γ	**3.5**
$\sigma_{\psi_{\mathrm{dB}}}$	4 dB
d_0	1m
d	1000m
N_e	15
N_{BS}	631
K dB	-31.53 dB
Block Length N	256 bits

7.3 Total Power Control

Conventional power control is based on regulating the transmit power of MSs in order to maintain a constant received signal power at the controlling BS

$$\max_k \left(P_i^{jk} \right) = Const \tag{7.7}$$

This policy is not designed for CBS systems where the controlling BS is not the only BS contributing to the detection of a MS. As we have discussed in this work, system-wide MUD allows MSs in CBS networks to benefit from macrodiversity and more dimensionality. These strong MUD techniques deal very well with modelled interferers, those for which CSI is tracked and which are included in the joint detection. The result is performance very close to the single-user limit when the modelled interferers are the only interferers. The remaining interferers, which are untracked, out of the detection set and usually weaker, are termed unmodeled interferers, and they limit the performance in more realistic propagation conditions. We propose a total power control strategy where the total received power in the detection set remains constant.

$$\sum_{i,k \in \mathcal{N}_g(0)} P_i^{ik} = Const \quad . \tag{7.8}$$

When a user is close to the local BS, it transmits at a lower power. It is also relatively far from the neighbouring BSs, so path loss even further attenuates the received signal powers in other BSs. The total power control in this scenario is close to the conventional channel inversion.

$$\sum_{i,k \in \mathcal{N}_g(0)} P_i^{ik} \approx \max_k \left(\quad \right) . \tag{7.9}$$

However, the high power boundary users that are the major cause of most of the intercell interference in cellular systems will transmit at lower powers under the total power control policy. The reduction in transmit power will lead to increased SIR in the system.

In practice, only two or three of the received signals are significant so we chose to consider the sum of three strongest received signals in regulating the transmit power. Through simulation (not presented in this work), we observed that adding more complexity by considering more than three signals is ineffective. Next, we investigate the performance of this new method through simulations and show that it not only reduces the intercell interference but also saves power and improves the BER performance of MSs.

7.4 Simulations

Simulating randomly placed MSs, their signal transmission and CBS detection in this massive system is computationally challenging. We devised a method to save some

computations without impairing the results. The first step is to study the influence of total power control policy on co-channel intercell interference. This investigation provides us with the statistics used in the BER simulations as well as some insights to the advantage of the proposed methods. We first model the average interference power with a normal distribution in order to simulate the BER performance of MSs in both coded and uncoded cases.

7.4.1 Intercell Interference

As we mentioned before, I_k^t , the intercell interference in BS k at time t , is a zero mean, complex Gaussian random variable in a static network (I_k^t is the interference in a snapshot of the network at time t). Assuming mobility of the user over time the variance of I_k^t is in itself a random variable P_{I_k} . Provided the transmitted signal $E\left\{\left|b_i^t\right|^2\right\}=1$, P_{I_k} can be easily calculated

$$P_{I_k} = \sum_{i \neq k, i \in \mathcal{N}_g(0)} r_{ik}^{-\gamma} . \tag{7.10}$$

We simulated the hexagonal system described in Section 7.2 and calculated P_{I_k} in the central BS of the system using both conventional and total power control policy. Figure 7.3 shows the histogram of P_{I_k} (in dB) in the case where the power control constant is set to 8 dB. We see that total power control strategy improves the average P_{I_k} by 2.14 dB. In other simulations (not shown here), we also observed that this 2.14 dB improvement is independent from the power control constant in (7.8) and that MSs saved

an average 1.4 dB in transmit power. Because of the new policy, MSs are using less power and there is less unmodeled co-channel interference in the BSs.

Figure 7.3 reveals that P_{I_k} histogram in logarithmic domain is close to a normal distribution. That means that probability distribution function (pdf) of P_{I_k} is close to a log-normal distribution. In order to simplify the BER, we approximate the pdf of P_{I_k} (expressed in dB) with a normal distribution and randomly generate P_{I_k} . I_k^t is then easily simulated by a zero mean, complex Gaussian random variable with variance P_{I_k} . This process is similar to the Gaussian forcing used in PDA [28] and IMUD [4].

7.4.2 BER Performance

In our hexagonal systems, each BS (in the interior cells of the system), has 7 MSs in its detection set (immediate neighbours). We apply RCBP (4,3) in the BER simulations. The iterative groupwise RCBP algorithm was shown to be an efficient MUD technique for CBS systems in Chapter 5. The numbers (4,3) mean that the 7 users in the detection set are divided into two groups of 4 and 3 users that are detected iteratively. We randomly generate the intercell interference and treat it as noise in our detection process. As before, we discard the results from the MSs that are located on the edge of the system because they enjoy less dimensionality.

Uncoded

Figure 7.4 shows the BER performance of MSs in the uncoded scenario for $N_r = 3$ and $N_r = 4$, where N_r is the number of antennas at the BS. We observe great

improvement in BER performance under the new total power control policy. For $N_r = 4$ the SNR gain is more than 2 dB when BER of 10^{-3} or less is desired. As we explained, the reason for this performance improvement is the reduction in unmodelled co-channel interference.

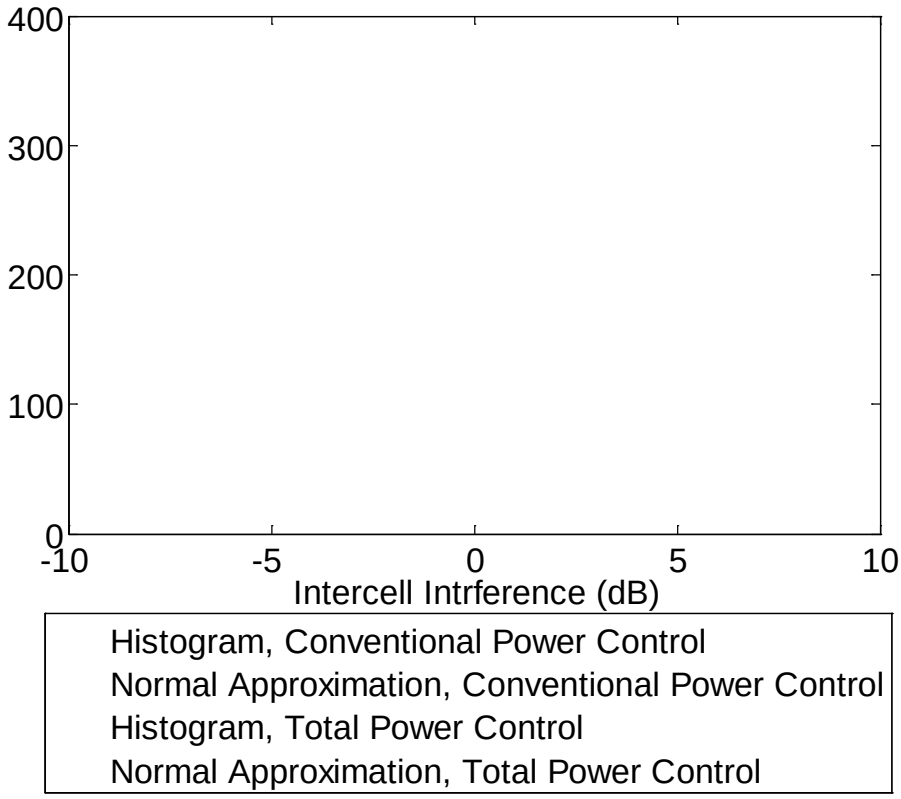

Figure 7.3: Interference in the central cell, hexagonal system, $SNR = 8$ dB **.**

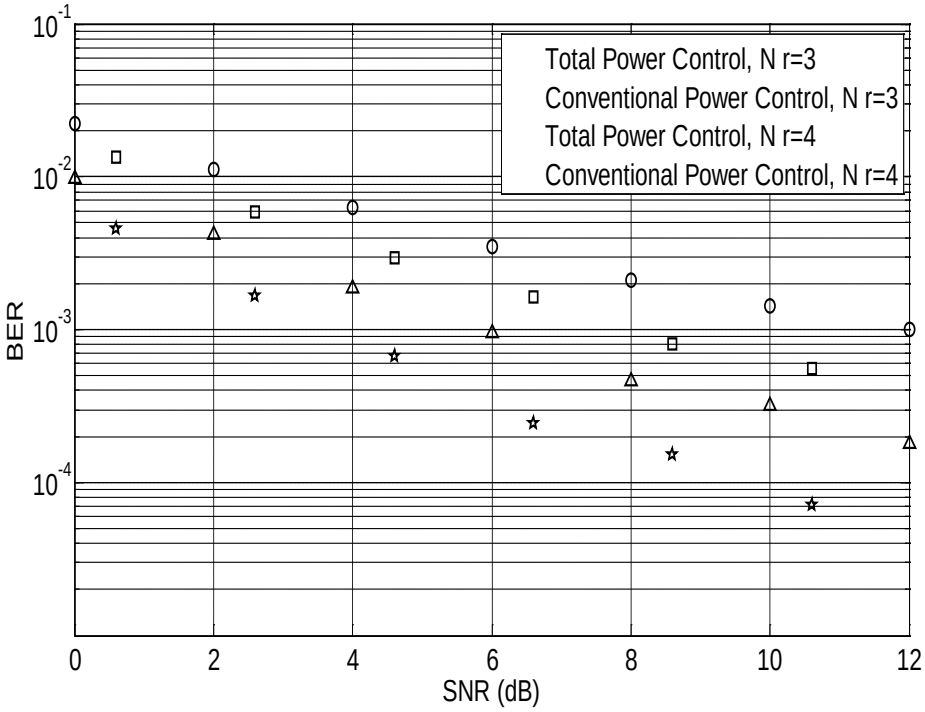

Figure 7.4: Comparison of BER performance, uncoded scenario.

Iterative Decoding and Detection

Similar to our previous investigations, we also look at the performance of RCBP in a coded system. In Chapter 5, we illustrated that distributed iterative detection and decoding using LDPC codes provides excellent performance. Here we compare the performance of such iterative system under both conventional and total power control strategies.

Figure 7.5 shows our proposed architecture for iterative detection and decoding in CBS networks. This structure is iterative on three levels. Both RCBP detector and BP-

based LDPC decoder have internal iterations. In addition, there is external iteration between the detectors and decoders. For our simulations, we have used randomly generated LDPC codes with rate $R_c = 1/2$, length $(M,N) = (128,256)$, and $(w_c, w_r) = (3,6)$, where M is the number of parity checks, N is the block length, w_c and w_r are the number of ones per column and rows of parity check matrix respectively. We remove 4-edge cycles in order to improve the code performance and allow only 10 internal iterations at the decoder. Figure 7.6 shows that after two external iterations, MSs can achieve BER of 10^{-4} , at SNR of 5.5 dB using the total power control policy which is 2 dB better than the standard power inversion scheme. The improvement introduced by the new total power control scheme is magnified by coding. In particular, the error floors that left the value of uncoded CBS systems with conventional power control in some doubt are no longer a problem.This study proves that using the techniques we provided in this work, we could successfully handle co-channel interference in CBS systems.

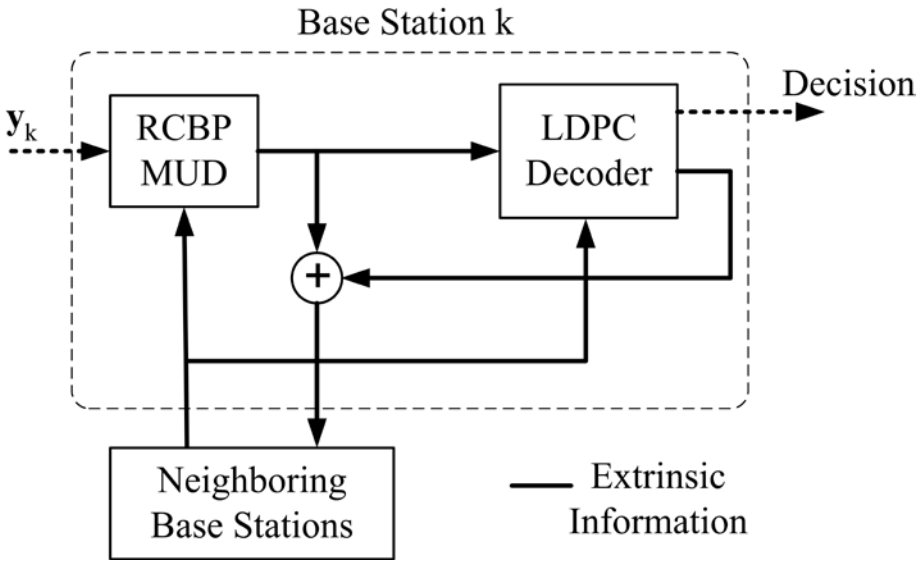

Figure 7.5: Iterative detection and decoding architecture.

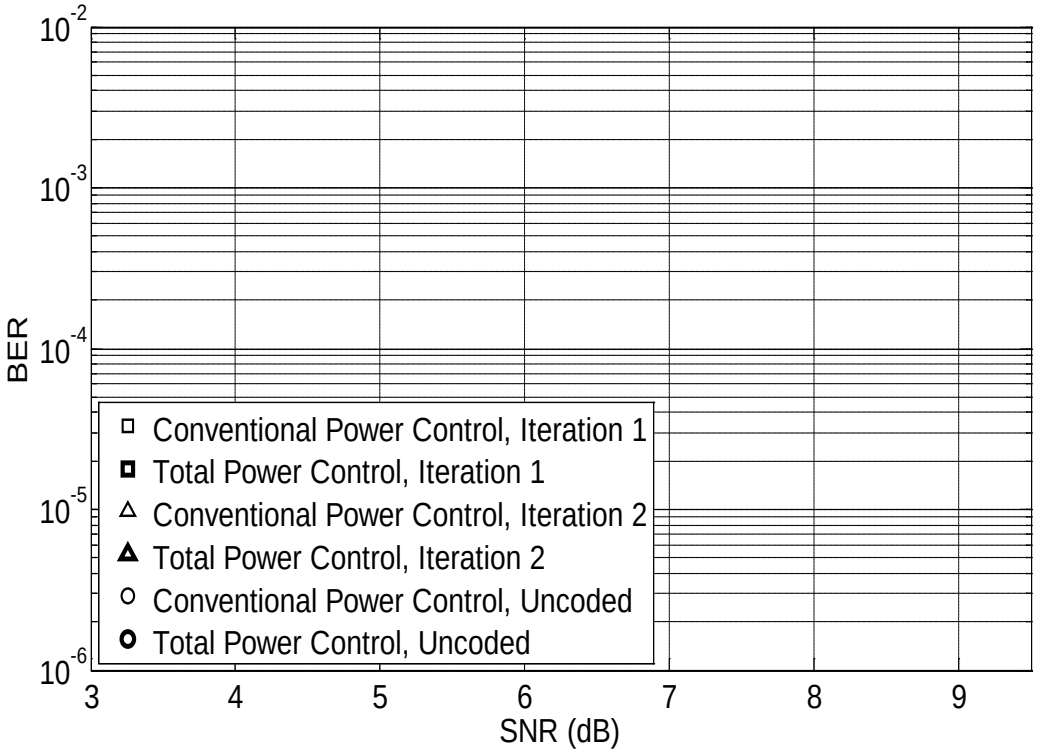

Figure 7.6: BER performance in iterative detection and decoding $N_r = 3$.

CHAPTER 8

CONCLUSIONS

Cooperative base stations (CBSs) have the potential to increase the capacity of cellular networks, largely through the achievement of full frequency reuse and taking advantage of increased dimensionality through macrodiversity. Managing the resulting high levels of interference is the fundamental problem facing the practical implementation of CBS systems. In this work, we offered several solutions to manage with and reduce the negative effects of co-channel interference in CBSs uplink. Multiuser detection (MUD) has been well investigated to cope with interference for single cell systems. We have examined system-wide approach to MUD based on CBS systems.

We introduced the reduced complexity belief propagation (RCBP) algorithm as an efficient MUD framework to handle the multidimensional interference. We successfully applied RCBP for distributed system-wide MUD in CBS systems and demonstrated its excellent capability in iterative cooperative detection and decoding scheme. We also showed that a narrowband CBS system can support more than one user per slot per cell, in addition to the reuse of that slot in every cell, thereby providing a major capacity

increase. We examined the application of distributed RCBP receivers in a realistic system model considering random mobility, path loss, shadowing, power control, and where the interference is not limited to immediately adjacent cells. We noticed that the residual unmodelled interference from users in cells outside the immediate neighbourhood produced a BER floor at high SNR. Nevertheless, the cooperative BS approach, as implemented by RCBP, showed a significant improvement compared with multi-user detectors implemented at BSs individually.

We extended the RCBP approach to ISI as well as MUI through MIMO equalization, and demonstrated very good to near-optimal performance via simulations in a variety of scenarios. Our primary focus was on individual BSs with multiple receive antennas detecting multiple users in frequency selective channels. We illustrated through simulations that the RCBP equalizer could achieve excellent performance by applying iterative equalization in combination with LDPC codes. Although the primary focus was the organization of computation for combined ISI and MUI, Chapter 6 also presented results for a simplified two-cell CBS system with realistic propagation.

In order to reduce the negative effect of unmodelled interference in the uplink of CBS systems, we proposed a new power control approach based on sustaining the total received power in CBSs. We investigated the performance of this method through simulations and showed that it has the ability to reduce the intercell interference in the CBS systems, save power or improve the BER performance in both coded and uncoded scenarios.

Many interesting research questions are opened by the apparent success of CBS design. It seems we are only scratching the surface of the CBS approach to cell system design. Below, we outline a few promising research issues to be addressed in future.

8.1 Road Ahead

As mentioned in Chapter 6, extension of RCBP equalization and information exchange between neighbouring BSs to large multicell with random mobility and realistic channel model is seen as a fruitful area for future investigation. Analytic study of power control in CBS systems is an interesting topic that has the potential to initiate more advanced power control policies based on macrodiversity and distributed interference. Another attractive subject is looking into advanced coding schemes for CBS systems.

As we discussed in Section 3.2 , examining the nature of information exchanged between bases, traffic analysis and control mechanisms are subjects of concern in CBS design. Practical implementation also requires learning about and mitigating the effect of imperfect CSI. On that note, a promising approach is to research BP-based adaptive channel estimation as well as joint iterative detection and estimation structures, opening up the potential for hardware or DSP code economies.

Forming smart detection sets is another important design issue. The goal is to find a criterion for determining which users should be in the detection set at a function node. Application of directional antennas in reducing co-channel interference and cooperation between segments in such systems is an additional rewarding research area. Likewise, downlink design offers a completely diverse range of challenges in efficient and practical

implementation of CBS systems. Joint detection and decoding of LDPC codes on a combined factor graph is another intriguing research subject.

We could also apply the approaches developed here in other aspects of communications design. Our proposed RCBP algorithm can be used in many other high interference applications such as MUD in CDMA systems. We also propose designing clustered LDPC codes with high density and many short cycles in a cluster of consecutive bits, and low-density sparse dependency outside the clusters. These clustered LDPC codes have the potential to improve performance in shorter block lengths. RCBP algorithm can be used for efficient decoding of such scheme. There are many issues to explore such as convergence analysis using method such as density evolution.

REFERENCES

[1] F.H.P. Fitzek and M. Katz, Cooperation in Wireless Networks: Principles and Applications, Dordrecht, The Netherlands: Springer, 2006, pp. 641.

[2] S. Bavarian and J.K. Cavers, "Reduced Complexity Belief Propagation Algorithm Based on Iterative Groupwise Multiuser Detection," in *Electrical and Computer Engineering, Canadian Conference on (CCECE 2007)*, pp. 466-468, 2007.

[3] J. Pearl, Probabilistic Reasoning in Intelligent Systems: Networks of Plausible Inference, San Mate, CA: Morgan Kaufmann, 1988 .

[4] B.W. Zarikoff, J.K. Cavers and S. Bavarian, "An iterative groupwise multiuser detector for overloaded MIMO applications," *Wireless Communications, IEEE Transactions on*, vol. 6, pp. 443-447, 2007.

[5] B.W. Zarikoff and J.K. Cavers, "An iterative groupwise multiuser detector with soft output," in *Personal, Indoor and Mobile Radio Communications, 15th IEEE International Symposium on (PIMRC 2004)*, pp. 2920-2924, September 2004.

[6] H. Vikalo, B. Hassibi and T. Kailath, "Iterative decoding for MIMO channels via modified sphere decoding," *Wireless Communications, IEEE Transactions on*, vol. 3, pp. 2299-2311, 2004.

[7] S. Bavarian and J.K. Cavers, "Reduced Complexity Distributed Base Station Processing in the Uplink of Cellular Networks," in *Global Telecommunications Conference, IEEE (GLOBECOM '07)*, pp. 4500-4504, November 2007.

[8] S. Bavarian and J.K. Cavers, "Reduced-Complexity Belief Propagation for System-Wide MUD in the Uplink of Cellular Networks," *Selected Areas in Communications, IEEE Journal on*, vol. 26, pp. 541-549, 2008.

[9] E. Aktas, J. Evans and S. Hanly, "Distributed Base Station Processing in the Uplink of Cellular Networks," *Communications, IEEE International Conference on (ICC '06.)*, vol. 4, pp. 1641-1646, 2006.

[10] E. Aktas, J. Evans and S. Hanly, "Distributed Decoding in a Cellular Multiple-Access Channel," *Wireless Communications, IEEE Transactions on*, vol. 7, pp. 241-250, 2008.

[11] S. Bavarian and J.K. Cavers, "A new framework for soft decision equalization in frequency selective MIMO channels," *Communications, IEEE Transactions on*, vol. 57, pp. 415-422, 2009.

[12] S. Bavarian and J.K. Cavers, "Symbol by symbol soft-input soft-output multiuser detection for frequency selective MIMO channels," *Wireless Communications and Networking Conference, IEEE*, vol. 1, pp. 515-520 Vol. 1, 2005.

[13] S. Bavarian and J.K. Cavers, "Total Power Control for Cooperative Base Stations Uplink," in Accepted for presentation in *IEEE Vehicular Technology Conference Spring 2009 (VTC-spring09)*, April 2009.

[14] J.K. Cavers, Mobile channel characteristics, Boston, MA: Kluwer Academic, 2000, pp. 226.

[15] A. Goldsmith, Wireless Communications, Cambridge University Press, 2005, pp. 644.

[16] R. Vaughan and J.B. Andersen, Channels, propagation and antennas for mobile communications, London: Institution of Electrical Engineers, 2003, pp. 753.

[17] J. Winters, "On the Capacity of Radio Communication Systems with Diversity in a Rayleigh Fading Environment," *Selected Areas in Communications, IEEE Journal on*, vol. 5, pp. 871-878, 1987.

[18] G.J. Foschini and M. Gans, "On limits of wireless communications in fading environment when using multiple antennas," *Wireless Personal Communications*, pp. 311-335, March 1998.

[19] L. Bahl, J. Cocke, F. Jelinek and J. Raviv, "Optimal decoding of linear codes for minimizing symbol error rate (Corresp.)," *Information Theory, IEEE Transactions on*, vol. 20, pp. 284-287, 1974.

[20] A. Duel-Hallen and C. Heegard, "Delayed decision-feedback sequence estimation," *Communications, IEEE Transactions on*, vol. 37, pp. 428-436, 1989.

[21] M.V. Eyuboglu and S.U.H. Qureshi, "Reduced-state sequence estimation with set partitioning and decision feedback," *Communications, IEEE Transactions o*n, vol. 36, pp. 13-20, 1988.

[22] C. Fragouli, N. Al-Dhahir, S.N. Diggavi and W. Turin, "Prefiltered space-time M-BCJR equalizer for frequency-selective channels," *Communications, IEEE Transactions on*, vol. 50, pp. 742-753, 2002.

[23] V. Franz and J.B. Anderson, "Concatenated decoding with a reduced-search BCJR algorithm," *Selected Areas in Communications, IEEE Journal on*, vol. 16, pp. 186-195, 1998.

[24] G. Bauch and N. Al-Dhahir, "Reduced-complexity space-time turbo-equalization for frequency-selective MIMO channels," *Wireless Communications, IEEE Transactions on*, vol. 1, pp. 819-828, 2002.

[25] M. Tuchler, R. Koetter and A.C. Singer, "Turbo equalization: principles and new results," *Communications, IEEE Transactions on*, vol. 50, pp. 754-767, 2002.

[26] U. Fincke and M. Pohst, "Improved methods for calculating vectors of short length in a lattice, including a complexity analysis," *Mathematics of Computation*, vol. 44, pp. 463-471, April 1985.

[27] B. Hassibi and H. Vikalo, "On the sphere-decoding algorithm I. Expected complexity," *Signal Processing, IEEE Transactions on*, vol. 53, pp. 2806-2818, 2005.

[28] J. Luo, K.R. Pattipati, P.K. Willett and F. Hasegawa, "Near-optimal multiuser detection in synchronous CDMA using probabilistic data association," *Communications Letters, IEEE*, vol. 5, pp. 361-363, 2001.

[29] Peng Hui Tan and L.K. Rasmussen, "The application of semidefinite programming for detection in CDMA," *Selected Areas in Communications, IEEE Journal on*, vol. 19, pp. 1442-1449, 2001.

[30] F.R. Kschischang, B.J. Frey and H.-. Loeliger, "Factor graphs and the sum-product algorithm," *Information Theory, IEEE Transactions on*, vol. 47, pp. 498-519, 2001.

[31] T.J. Richardson, M.A. Shokrollahi and R.L. Urbanke, "Design of capacity-approaching irregular low-density parity-check codes," *Information Theory, IEEE Transactions on*, vol. 47, pp. 619-637, 2001.

[32] R. Gallager, "Low-density parity-check codes," *Information Theory, IEEE Transactions on*, vol. 8, pp. 21-28, 1962.

[33] D.J.C. MacKay, "Good error-correcting codes based on very sparse matrices," *Information Theory, IEEE Transactions on*, vol. 45, pp. 399-431, 1999.

[34] S.V. Hanly and P. Whiting, "Information-theoretic capacity of multi-receiver networks," *Telecommunications Systems*, vol. 1, pp. 1-42, 1993.

[35] A.D. Wyner, "Shannon-theoretic approach to a Gaussian cellular multiple-access channel," *Information Theory, IEEE Transactions on*, vol. 40, pp. 1713-1727, 1994.

[36] O. Somekh and S. Shamai, "Shannon-theoretic approach to a Gaussian cellular multiple-access channel with fading," *Information Theory, IEEE Transactions on*, vol. 46, pp. 1401-1425, 2000.

[37] O. Simeone, O. Somekh, H.V. Poor and S. Shamai, "Local Base Station Cooperation Via Finite-Capacity Links for the Uplink of Linear Cellular Networks," *Information Theory, IEEE Transactions on*, vol. 55, pp. 190-204, 2009.

[38] S. Verdu, Multiuser Detection, Cambridge, UK ; New York: Cambridge University Press, 1998, .

[39] Yu-Shuan Yeh, J.C. Wilson and S.C. Schwartz, "Outage probability in mobile telephony with directive antennas and macrodiversity," *Vehicular Technology, IEEE Transactions on*, vol. 33, pp. 123-127, 1984.

[40] L.F. Chang and J.C.-. Chuang, "Diversity selection using coding in a portable radio communications channel with frequency-selective fading," *Selected Areas in Communications, IEEE Journal on*, vol. 7, pp. 89-98, 1989.

[41] A.J. Viterbi, Principles of Spread Spectrum Communication, New York: Addison-Wesley Publishing Company, 1995, .

[42] Z.J. Haas and Chih-Peng Li, "The multiply-detected macrodiversity scheme for wireless cellular systems," *Vehicular Technology, IEEE Transactions on*, vol. 47, pp. 506-530, 1998.

[43] S.V. Hanly, "Capacity and power control in spread spectrum macrodiversity radio networks," *Communications, IEEE Transactions on*, vol. 44, pp. 247-256, 1996.

[44] L. Welburn, J.K. Cavers and K.W. Sowerby, "A computational paradigm for space-time multiuser detection," *Communications, IEEE Transactions on*, vol. 52, pp. 1595-1604, 2004.

[45] M.C. Valenti and B.D. Woerner, "Iterative multiuser detection, macrodiversity combining, and decoding for the TDMA cellular uplink," *Selected Areas in Communications*, IEEE Journal on, vol. 19, pp. 1570-1583, 2001.

[46] O. Shental, A.J. Weiss, N. Shental and Y. Weiss, "Generalized belief propagation receiver for near-optimal detection of two-dimensional channels with memory," *Information Theory Workshop, IEEE*, pp. 225-229, 2004.

[47] G. Colavolpe and G. Germi, "On the application of factor graphs and the sum-product algorithm to ISI channels," *Communications, IEEE Transactions on*, vol. 53, pp. 818-825, 2005.

[48] R.J. McEliece, D.J.C. MacKay and Jung-Fu Cheng, "Turbo decoding as an instance of Pearl's “belief propagation” algorithm," *Selected Areas in Communications, IEEE Journal on*, vol. 16, pp. 140-152, 1998.

[49] Y. Yin, Y. Huang and J. Zhang, "Turbo equalization using probabilistic data association," *Global Telecommunications Conference, IEEE (GLOBECOM '04)*, vol. 4, pp. 2535-2539 Vol.4, 2004.

[50] S. Liu and Z. Tian, "Near-optimum soft decision equalization for frequency selective MIMO channels," *Signal Processing, IEEE Transactions on*, vol. 52, pp. 721-733, 2004.

[51] S. Liu and Z. Tian, "Sliding-window based soft decision equalization for frequency selective MIMO channels," *Sensor Array and Multichannel Signal Processing Workshop Proceedings*, pp. 158-162, 2004.

[52] S. Liu and Z. Tian, "A Kalman-PDA approach to soft-decision equalization for frequency selective MIMO channels," *Signal Processing Advances in Wireless Communications, IEEE 5th Workshop on*, pp. 223-227, 2004.

[53] Subhadeep Roy and Tolga M. Duman, "Soft input soft output Kalman equalizer for MIMO frequency selective fading channels," *Wireless Communications, IEEE Transactions on*, vol. 6, pp. 506-514, 2007.

[54] M.N. Kaynak, T.M. Duman and E.M. Kurtas, "Belief Propagation over SISO/MIMO Frequency Selective Fading Channels," *Wireless Communications, IEEE Transactions on*, vol. 6, pp. 2001-2005, 2007.

[55] X.W.B. Lu, G. Yue and M. Madihian, "Factor-graph-based soft self-iterative equalizer for multipath channels," *Eurasip Journal on Wireless Communications and Netwroking*, Special Issue on Advanced Signal Processing Algorithms for Wireless Communications, pp. 187-198, April 2005.

[56] R. Visoz, A.O. Berthet and S. Chtourou, "A new class of iterative equalizers for space-time BICM over MIMO block fading multipath AWGN channel," *Communications, IEEE Transactions on*, vol. 53, pp. 2076-2091, 2005.

[57] Renqiu Wang and G.B. Giannakis, "Approaching MIMO channel capacity with soft detection based on hard sphere decoding," *Communications, IEEE Transactions on*, vol. 54, pp. 587-590, 2006.

[58] G.J. Foschini and Z. Miljanic, "A simple distributed autonomous power control algorithm and its convergence," *Vehicular Technology, IEEE Transactions on*, vol. 42, pp. 641-646, 1993.

[59] S.A. Grandhi, R. Vijayan and D.J. Goodman, "Distributed power control in cellular radio systems," *Communications, IEEE Transactions on*, vol. 42, pp. 226-228, 1994.